

Differentiation and characterization of human induced pluripotent stem cell derived astrocytes

Inaugural-Dissertation

zur Erlangung des Doktorgrades
der Mathematisch-Naturwissenschaftlichen Fakultät
der Heinrich-Heine-Universität Düsseldorf

vorgelegt von

Pretty Garg
aus Panipat

Düsseldorf, Dezember 2015

aus dem Institut für Neuro- und Sinnesphysiologie
der Heinrich-Heine-Universität Düsseldorf

Gedruckt mit der Genehmigung der
Mathematisch-Naturwissenschaftlichen Fakultät der
Heinrich-Heine-Universität Düsseldorf

Referent: Prof. Dr. Kurt Gottmann

Koreferent: Prof. Dr. Christine R. Rose

Tag der mündlichen Prüfung:

"I have not failed. I have just found 10,000 things that do not work."

- *Thomas Edison*

To my family...

Summary

Previously, several studies have reported differentiation of astrocyte from human induced pluripotent stem cells using serum or CNTF or BMP and LIF in a time span of about six months due to the long culture time required for NSCs to attain gliogenic potential. Most of these studies focused on producing high GFAP expressing astrocytes, thereby leading to underappreciation of astrocyte heterogeneity.

In this study, NSCs were first characterized for their gliogenic potential by evaluating the expression of astrocyte restricted progenitor markers like CD44, NF1A, NF1B, NF1C, NF1X, EGFR and STAT3 at mRNA and protein level at different passages and culture conditions. Exposure to a high dose of the growth factors FGF or EGF was employed to render early NSCs gliogenic in a time span of only two months. Based on these results, NSCs of intermediate passage with high gliogenic potential were used for further differentiation. PD0325901, a small molecule inhibitor of the MEK pathway, previously used as a replacement for BMP and LIF to maintain mouse ES cultures, was employed as an innovative approach for astrocyte differentiation. The differentiation towards astrocytes after 14 days of PD treatment was assessed by analyzing the expression of astrocyte markers like S100 β , GFAP, ALDH1L1, EAAT1, Acsbg1, GS, Cx43, ApoE and EAAT2 by quantitative PCR, western blotting or immunocytochemistry (ICC). Although, ICC revealed only a low percentage of high GFAP expressing cells, all other markers were found to be expressed, suggesting astrocyte identity of the low GFAP cells. Notably, high GFAP expressing cells could be differentiated from high passage NSCs using the same small molecule, which was probably due to the previously described epigenetic repression of the GFAP promotor in young NSCs. The cortical lineage of NSCs and differentiated astrocytes was confirmed by ICC using forebrain and hindbrain markers.

Owing to the short differentiation time using the small molecule, it was important to investigate the functional maturity of the generated astrocytes. The low GFAP expressing cells elicited calcium transients in response to glutamate and ATP and were also able to take up glutamate. Exposure to the inflammatory agents TNF α and bacterial endotoxin LPS and to acidic pH turned these astrocytes reactive as shown by upregulation of reactivity markers like Serpina3n, Lcn2 and GFAP. The signaling pathway underlying PD mediated astrocyte differentiation was identified as PI3K dependent Akt1 phosphorylation, which on one hand lead to the upregulation and phosphorylation of STAT1/3 and on the other hand to the translocation of the astrocytic

transcriptional repressor Olig2 from the nucleus to the cytoplasm. These data establish the use of a small molecule for MEK inhibition as a highly effective approach to generate distinct types of human astrocytes, which provide a platform to explore the role of astrocyte subtypes in brain physiology and pathology.

Zusammenfassung

Frühere Arbeiten haben die Differenzierung von Astrozyten aus menschlichen pluripotenten Stammzellen in einer Zeitspanne von etwa 6 Monaten unter der Verwendung von Serum, CNTF oder BMP und LIF gezeigt. Dem liegt vor allem der lang andauernde Prozess des Erwerbens von gliogenen Eigenschaften in neuronalen Stammzellen (NSZ) zu Grunde. Die meisten dieser Studien fokussieren außerdem auf die Erzeugung von stark GFAP exprimierenden Astrozyten und führen dadurch zu einer Vernachlässigung der Astrozytenheterogenität.

In der vorliegenden Arbeit wurden zunächst NSZ auf ihre gliogenen Eigenschaften untersucht. Dazu wurde die Expression von Astrozyten-Vorläufer-Markern wie NF1A, NF1B, NF1C, NF1X, EGFR, STAT3 und CD44 auf mRNA- und Protein-Ebene zu unterschiedlichen Kultivierungszeitpunkten und unter verschiedenen Kulturbedingungen analysiert. Die Behandlung von frühen NSZ mit hohen Konzentrationen der Wachstumsfaktoren FGF-2 oder EGF führte innerhalb von 2 Monaten zu einer Induktion von gliogenen Eigenschaften. Basierend auf diesen Ergebnissen wurden gliogene NSZ mittlerer Passagenzahl für die weitere Differenzierung verwendet. PD0325901 (PD), ein niedermolekularer Inhibitor des MEK Signalwegs, der bereits an Stelle von BMP und LIF bei der Kultivierung von embryonalen Stammzellen der Maus erfolgreich eingesetzt worden ist, wurde hier als innovativer Ansatz für die Astrozytendifferenzierung eingeführt. Die Differenzierung zu Astrozyten nach einer 14 tägigen PD Behandlung wurde anhand von Astrozyten-Markern wie S100 β , GFAP, ALDH1L1, EAAT1, Acsbg1, GS, Cx43, ApoE und EAAT2 validiert. Deren Expression wurde mittels quantitativer PCR, Western Blot und Immunozytochemie (IZC) untersucht. Obwohl die IZC nur wenige stark GFAP exprimierende Zellen zeigte, konnte die Expression der anderen Marker bestätigt werden, was auf eine astrozytäre Identität der niedrig GFAP exprimierenden Zellen schließen lässt. Bemerkenswert ist auch die Beobachtung, dass derselbe MEK Inhibitor in höher passagierten NSZ zur Differenzierung von stark GFAP positiven Astrozyten führt. Dies lässt sich durch die bereits beschriebene epigenetische Repression des GFAP Promotors in jungen NSZ erklären. Die kortikale Identität der NSZ und differenzierten Astrozyten ließ sich durch IZC mittels Vorderhirn- und Hirnstamm-Markern feststellen.

Aufgrund der kurzen Differenzierungszeit mit dem niedermolekularen Inhibitor, war es wichtig, die funktionelle Ausreifung der Astrozyten zu untersuchen. Die niedrig GFAP exprimierenden Zellen reagierten auf Glutamat und ATP mit einer Erhöhung der intrazellulären Kalzium-Konzentration und waren ebenfalls dazu in der Lage Glutamat aufzunehmen.

Entzündungsauslösende Substanzen wie $\text{TNF}\alpha$ und das bakterielle Endotoxin LPS, wie auch eine Azidifizierung des extrazellulären Milieus führten zur Reaktivität der Astrozyten. Dies konnte durch eine Hochregulation der Reaktivitätsmarker *Serpina3n*, *Lcn2* und GFAP gezeigt werden. Als Signalweg der PD induzierten Astrozytendifferenzierung konnte die PI3K vermittelte Phosphorylierung von Akt1 identifiziert werden. Diese führte sowohl zu einer Hochregulation und Phosphorylierung von STAT1/3 also auch zur Translokation des Astrozyten-Repressors Olig2 vom Zellkern ins Zytoplasma.

Die Ergebnisse dieser Arbeit etablieren die Verwendung eines niedermolekularen MEK Inhibitors als hoch effektiven Ansatz zur Generierung von verschiedenen Typen menschlicher Astrozyten, welche als Plattform zur Untersuchung der Rolle von Astrozyten in der Physiologie und Pathologie des Gehirns dienen können.

Table of contents

1. Introduction.....	1
1.1 From neuroepithelium to astrocytes.....	1
1.2 Signaling pathways required for differentiation towards astrocytes.....	7
1.3 Characteristic markers, functions and heterogeneity of astrocytes.....	10
1.3.1 Markers described to identify and classify astrocytes.....	10
1.3.2 Functional properties attributed to astrocytes.....	16
1.3.3 Heterogeneity of astrocytes.....	20
1.4 Induced pluripotent stem cells- disease modeling and therapy.....	22
1.4.1 iPSCs - development and applications.....	22
1.4.2 iPSCs - a way towards astrocytes.....	24
1.5 Aims of the study.....	25
2. Materials and methods.....	27
2.1 Buffers and reagents.....	27
2.1.1 Cell culture medium formulations.....	27
2.1.2 Cell culture medium supplements.....	28
2.1.3 Buffers and reagents for immunocytochemistry.....	29
2.1.4 Buffers and reagents for calcein staining.....	31
2.1.5 Buffers and reagents for FACS.....	31
2.1.6 Buffers and reagents for quantitative PCR.....	32
2.1.7 Buffers and reagents for protein isolation and western blot.....	33
2.1.8 Buffers and reagents for calcium imaging.....	36
2.1.9 Buffers and reagents for glutamate uptake assay.....	36
2.1.10 Buffers and reagents for reactive astrocyte assay.....	37
2.2 Cell culture.....	38
2.2.1 Maintenance of human iPSCs.....	38
2.2.2 Neural induction of human iPSCs.....	39
2.2.3 Generating NSCs from iPSCs.....	40
2.2.4 Differentiation of NSCs towards astrocytes.....	40
2.3 Immunocytochemistry.....	41
2.4 Calcein staining.....	42
2.5 FACS.....	42
2.6 Quantitative PCR.....	43
2.6.1 mRNA isolation.....	43
2.6.2 cDNA synthesis.....	43
2.6.3 qPCR.....	43
2.7 Western blot.....	44
2.7.1 Protein isolation.....	44
2.7.2 Protein estimation.....	45
2.7.3 Blotting and developing.....	45
2.8 Calcium imaging.....	46
2.9 Glutamate uptake assay.....	47
2.10 Reactive astrocyte assay.....	49
2.11 Statistics.....	49

3. Results	50
3.1 Characterization of iPSCs derived human neural stem cells	50
3.1.1 Determination of gliogenic potential of different NSC lines	50
3.1.2 Validation of glial restriction in NSCs over prolonged culture time	52
3.1.3 Validation of culture conditions supporting glial restriction	54
3.2 The gliogenic switch and astrocyte differentiation	56
3.2.1 Differentiation of NSCs into high GFAP expressing astrocytes increases with passaging	56
3.2.2 Triggering the gliogenic switch in early NSCs	59
3.3 Small molecule mediated differentiation of iPSCs derived NSCs into low GFAP expressing astrocytes	62
3.3.1 Exit from NSC stage in the presence of PD	62
3.3.2 PD treated NSCs differentiated into low GFAP expressing astrocytes of cortical lineage	65
3.4 Signaling pathways involved in PD mediated astrocyte differentiation	71
3.4.1 PD mediates late onset of STAT1/3 phosphorylation during differentiation into low GFAP expressing astrocytes	71
3.4.2 PD mediates differentiation into low GFAP astrocytes via Akt1 dependent pathway	75
3.5 Functional aspects of small molecule differentiated low GFAP astrocytes	79
3.5.1 Low GFAP astrocytes exhibit calcium transients typical of astrocytes	79
3.5.2 Low GFAP astrocytes exhibit sodium dependent glutamate uptake	82
3.5.3 Low GFAP astrocytes respond to reactive stimuli	83
4. Discussion	86
4.1 Derivation of neural stem cells from iPSCs and characterization of their gliogenic potential	86
4.2 Differentiation of NSCs towards high GFAP expressing astrocytes	89
4.3 Induction of the gliogenic switch	91
4.4 Differentiation of NSCs towards low GFAP expressing astrocytes in the presence of PD	93
4.5 Signaling cascade for PD mediated astrocyte differentiation	97
4.6 Functional activity of PD derived low GFAP expressing astrocytes	100
5. References	105
6. Appendix	118
6.1 Abbreviations	118
6.2 Units and prefixes	121
6.3 List of plastic ware	122
6.4 List of primary antibodies	124
6.5 List of secondary antibodies	126
6.6 List of primers for quantitative PCR	127
6.7 Reaction mixture and conditions for cDNA synthesis	129
6.8 Reaction mixture and conditions for quantitative PCR	130
6.9 Calculations for quantitative PCR	131
6.9.1 Determination of amplification efficiency	131
6.9.2 Relative quantification of qPCR data	132

6.10	Calculations for protein estimation.....	133
6.11	Calculations for glutamate uptake assay.....	134
6.12	List of figures.....	136
6.13	Curriculum vitae.....	138
6.14	Publications and conferences.....	138
6.14.1	Publications.....	138
6.14.2	Meetings and poster presentations.....	138
7.	Acknowledgements.....	139
8.	Eidesstattliche Erklärung.....	140

1. Introduction

The central nervous system is composed of neurons and glial cells (macroglia and microglia). Microglia originates from the hematopoietic system, whereas macroglia is derived from the neural tube. The later includes a small population of ependymal cells, oligodendrocytes and astrocytes. The human brain has been shown to constitute 86 billion neurons and the ratio of glia to neuron is known to be highly variable (ranging from 0.23 to 11.35) depending on the brain region (*Azevedo et al., 2009*). In addition, the astrocyte to neuron ratio also varies between species from 1:6 in worms to, 1:3 in rodents and 1.4:1 in humans. The importance of human astrocytes is emphasized by the findings that they are ~2.0 fold larger and possess 10 fold more GFAP positive processes than their rodent counterparts. These reports suggest that in evolution, astrocyte to neuron ratio and astrocyte complexity increase with cognitive skills (*Oberheim et al., 2012*). Recently, it has been shown that human astrocytes grafted into mice provide these animals with improved learning capability (*Han et al., 2013*), suggesting an essential role of astrocytes, especially human astrocytes in learning and information processing in the brain. Astrocytes have also been shown to be severely affected in diverse neurological diseases (*Molofsky et al., 2012; Liddel and Barres, 2015*). The invention of patient specific induced pluripotent stem cells (iPSCs) opens future prospects for disease modeling, given that physiologically functional, cellular model systems can be generated from these cells. Despite the plethora of protocols for the generation of neuronal subtypes, the defined differentiation of distinct types of astrocytes is still in its infancy.

1.1 From neuroepithelium to astrocytes

The complex process of rodent brain development has been extensively studied. It starts at around the third gestational week and is believed to continue throughout life in terms of synaptic plasticity. A series of dynamic and adaptive processes, cued by both intrinsic signaling cascades and environmental factors promote the emergence and differentiation of neural structures and functions. Both neurons and macroglia in the central nervous system arise from neuroepithelial cells some of which directly differentiate into neurons. With thickening of the epithelium in the developing brain and under the influence of Notch signaling in the ventricular zone (VZ), neuroepithelial cells transform into radial glia cells (RGCs), characterized by the presence of a small process attached to ventricular surface (apical) and a fine radial process extending to the pial surface (basal) on the outer region of the brain (*Gaiano et al., 2000*). In the early phase of neurogenesis, radial glial cells undergo self renewal by symmetric cell division thereby expanding the proliferative population. Gradually, the formation of neurons is marked by the

beginning of asymmetrical division of RGCs, the majority of them resulting in the formation of a neuron and an intermediate progenitor cell (nIPC). The nIPC generated in the asymmetric neurogenic division, migrates to the subventricular zone (SVZ) where it undergoes another round of symmetric division. ~90% of this symmetric division is terminal; resulting in the generation of neurons migrating towards the cortex and 10% of the divisions results in self replenishment of the IPC pool (*Figure 1A*). Recent studies show that during development of highly gyrated human neocortex both ventricular RGCs and a new type of outer RGCs generate IPCs, which undergo multiple rounds of amplification, thereby forming an outer SVZ before producing neurons (*Liu et al., 2011; Florio and Huttner, 2014*). The generation of cortical neurons continues till embryonic day 108 (*Clancy et al., 2001*). The radial, short distance migration of the early born neurons from VZ to developing neocortex occurs by somal translocation in which they inherit the pial fiber of the parent radial glial cell (*LaMonica et al., 2012*). Gradually with an increase in brain size, the distance to be migrated also increases. Thereafter, besides generating new neurons, RGCs also serves as the migration guides for their neuronal progeny to form functional cortical columns (*Nadarajah et al. 2002*). The migration of neurons into the developing neocortex finally results in the formation of an orderly 6-layered structure with an inside out pattern of formation, the inner layers being the first to be formed and the outer ones being the last.

Once the RGCs undergo a gliogenic switch, neurogenesis is taken over by gliogenesis. Different studies propose diverse mechanisms for generation of astrocytes and oligodendrocytes. *Noctor et al., 2004* have shown that towards the end of neurogenesis, RGCs in the VZ give rise to one multipolar daughter cell and one translocating daughter cell which inherits the pial fiber of the parent radial glial cell and translocates over relatively long distances from the ventricular surface toward the cortical plate where it is transformed into GFAP expressing astrocytes. The other multipolar daughter cell also migrates away from VZ towards the cortical plate. Besides this, there is also evidence that supports the existence of astrocyte only and oligodendrocyte only progenitor clones at the embryonic stages (*Rowitch and Kriegstein, 2010*). However, it is still not clear whether the glial cells originate from direct progenitor or through an intermediate progenitor stage as observed for neurons. Interestingly, astrocytes also mirror the inside out pattern of laminar organization (*Ichikawa et al., 1983*). Parallel to this intricate process of generating diverse neural cell types; the regional specificity along anterior-posterior (AP), dorso-ventral (DV) and medial-lateral (ML) axes is guided by a temporarily available morphogen gradient; comprising FGF8, Retinoic acid (RA) along the AP axis, and SHH, BMP and WNT along DV axis as the key players for patterning (*O'Leary et al., 2007; Niederreither and Dolle, 2008*) (*Figure 1B*).

In addition to embryonic stages, neurogenesis and gliogenesis also persist in the adult brain at specific locations, namely the SVZ and the subgranular zone (SGZ) of the dentate gyrus in hippocampus. In SVZ, adult neurogenesis is mediated by quiescent NSCs more commonly referred to as type B cells, which also express the astrocytic markers: GFAP and GLAST, thereby sometimes described as SVZ astrocytes. B cells give rise to C cells with the ability to proliferate. C cells in turn produce A cells (immature neuroblasts) which then migrates to the olfactory bulb to replenish the pool of interneurons. The SGZ is dominated by the presence of radial astrocytes (also known as type I progenitors) which acts as precursors for newly formed neurons in adult dentate gyrus (*Kriegstein and Alvarez-Buylla, 2009*).

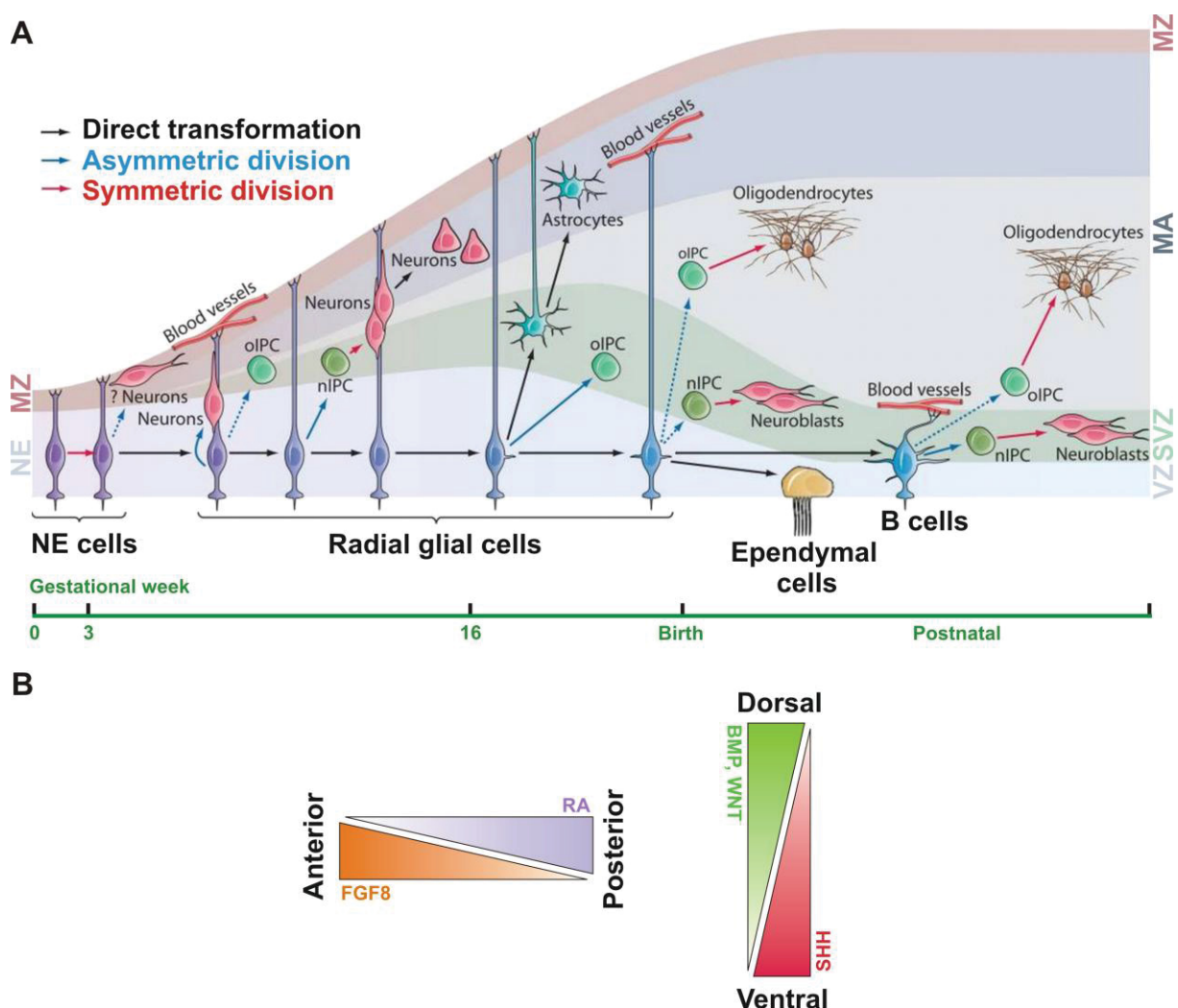


Figure 1: Generation of neural cell types during development.

Adapted from *Kriegstein and Alvarez-Buylla, 2009*. **A**) Early neuroepithelial cells (NE cells) give rise to radial glial cells (RGCs) which in turn generates neurons, astrocytes and oligodendrocytes. Later in the adult stage RGCs persists and forms neurons. Solid arrows are evidence based and dashed arrows are hypothetical. nIPC= neurogenic intermediate progenitor cell, oIPC= oligodendrocytic intermediate progenitor cell, NE= neuroepithelium, MZ= marginal zone, MA= mantle, SVZ=

subventricular zone, VZ= ventricular zone. **B)** Morphogen gradient along AP and DV axes during early development.

As mentioned before, during embryonic development, early RGCs resist the potential to give rise to glial cells. This is because, during the neurogenic phase, astrocytic genes (GFAP, S100 β , AldoC and Kir4.1) are hypermethylated, rendering them insensitive to cytokines like CNTF, BMP2 and LIF (*Hatada et al., 2008*). Overall, downregulation of proneural genes and several events resulting in epigenetic changes are required to induce the gliogenic switch. Based on chick and rodent spinal cord developmental studies, epigenetic modifications are known to depend on multiple factors: *a)* notch signaling, *b)* oxygen concentration, *c)* Coup-tfI/II and *d)* the presence of FGF2. The first three of these factors control gene transcription, whereas long term exposure to FGF2 brings about changes at the chromatin level. From *in vitro* studies on mouse embryonic stem (ES) cells derived NSCs, it is known that in neurogenic stem cells, histone 3 (H3) at the GFAP promoter is methylated at lys9 (H3K9) and acetylated at lys4 (H3K4). Exposure to high amount of FGF mediates demethylation of H3K9, deacetylation and methylation of H3K4 (*Figure 2A*). This renders the promoter site available for binding to STAT3 complex and allows GFAP transcription in the presence of growth factors (*Song and Ghosh, 2004*). In addition, there occurs a feedback signal from the Notch ligand delta, expressed on the committed neuronal progenitors towards notch expressing RGCs, which activates NF1A, allowing its binding to several astrocyte gene promoters. This encourages demethylation of astrocyte genes by inhibiting their interaction with DNA methyltransferase I (DNMTI), thereby triggering the glial switch (*Namihira et al., 2009*). Activation of NF1A has also been shown by another independent mechanism mediated by Sox9 via enhancer123, followed by formation of Sox9/NF1A complex which induces glial specific genes (*Kang et al., 2012*). The expression of NF1A is considered to be enough to turn on the gliogenic switch at least in the rodent models of spinal cord development. In addition, other NF1 transcription factors like NF1B, C and X are also considered to play a similar role in gliogenesis. NF1B has been shown to regulate expression of FGFR and GLAST during early neural development and GFAP at late stages (*Mason et al., 2009*). Furthermore, hypoxia inducible factor (HIF1 α) has been shown to promote Notch signaling which is supported by the fact that the environment surrounding the embryonic tissues is hypoxic (*Figure 2B*). Besides this, chicken ovalbumin upstream promoter transcription factors I and II (COUP-TFI/II) also contribute to demethylation of the GFAP promoter by an undefined mechanism (*Namihira et al., 2013*). Another study has reported that Erk1/2 plays a critical role in gliogenesis via a Erm/Etv5 dependent pathway. In this study, MEK deletion was able to

completely block glial specification in mutant animals (*Li et al., 2012*); confirming the *in vitro* findings that demonstrate the ability of FGF to trigger the gliogenic switch (*Song and Ghosh, 2004*).

In early development, the presence of proneural genes impedes gliogenesis (*Nieto et al., 2001; Sun et al., 2001*). Neurogenin 1/2 (*ngn*), a bHLH transcription factor, sequesters p300 and CBP-Smad1 away from STAT1/STAT3, thereby inhibiting the activation of the key pathways for astrocyte differentiation. Instead, CBP/p300 and Smad1 associates with *ngn* at neural specific gene promoters like *NeuroD* (*Sun et al., 2001*). Initially, the expression of *ngn* is also enhanced by the presence of low concentration of BMP (*Ota and Ito, 2006*). Depending on the stage of development, BMP plays a dual role by participating in both the neuronal and astrocytic differentiation. BMP and LIF only act as astrocyte inducing signals during late embryonic cortical development, when NSCs increase the expression of EGF receptors (*Viti et al., 2003*). During the neurogenic phase, stem cells exhibit low levels of EGFR. At this stage, by binding to its receptor, BMP inhibits both direct and FGF mediated up regulation of EGFR (*Figure 2C*). During mid gestation, there is a reduction in the expression of BMP receptor. Also, the level of FGF2 increases which then augments the expression of EGFR, making NSCs responsive to EGF and also gliogenic (*Lillien et al., 2000*). Also, with the expression of notch ligand, embryonic neurons start to secrete cardiotrophin1 (CT1), facilitating the activation of gliogenic genes via gp130-JAK-STAT pathway (*Barnabé et al., 2005*).

Besides this, the role of extracellular matrix protein Reelin has been shown to be important in maintaining the balance between neurogenesis and gliogenesis in the adult hippocampus. This was supported by a reduction in NeuN positive granule cells and augmentation of GFAP expressing astrocytes in reeler mutant mice (*Zhao et al., 2007*). Another report has suggested the inhibition of gliogenesis by Myc which is counteracted upon the expression of p19^{ARF} in a p53 dependent manner. Based on GFAP expression, the astrocytic lineage was shown to be delayed or attenuated in postnatal stages in p19^{ARF} mutants (*Nagao et al., 2008*). Recently, the role of non coding micro RNAs (miR) have come up as another essential gliogenic signal in embryonic spinal cord. miR153 is reported to have an inhibitory effect on the expression of NF1 genes which is a prerequisite for transition from the neuronal lineage. Furthermore, the same study shows that the inhibition of miR153 in early NSCs induces gliogenesis (*Figure 2B*). miR124 has also been shown to favor the neurogenic phase by impeding the expression of Sox9 and other early gliogenic genes (*Tsuyama et al., 2015*). Another study demonstrated a downregulation of

Coup-tfII-p38 MAPK mediated gliogenesis by overexpression of miR-17/106 (*Naka-Kaneda et al., 2014*).

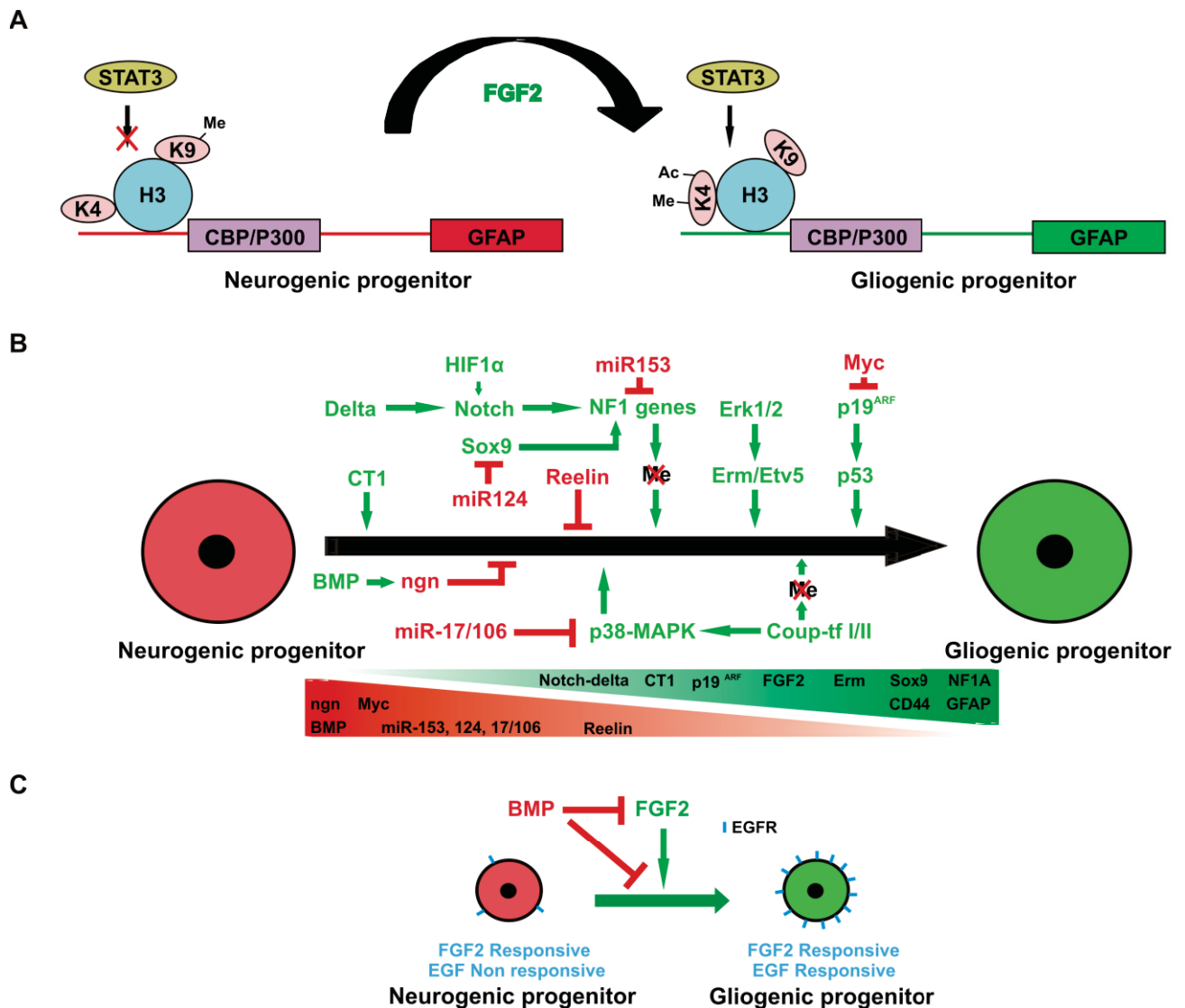


Figure 2: Transition from neurogenic to gliogenic state.

A) Increased concentration or long term exposure to FGF2 mediates histone 3 modification required to for binding of STAT3 to the promoter region of GFAP. **B)** Several other described mechanisms responsible for the gliogenic switch. **C)** Inhibitory effect of BMP and the stimulating effect of FGF2 on the expression of EGFR. Ac= acetylation, H3= histone 3, K4= lysine4, K9= lysine 9, Ngn= neurogenin, Me= methylation.

Despite these multiple signals which have been shown to be important for gliogenic switch, the exact mechanism remains largely unknown. A major limitation of all these studies investigating the gliogenic switch is that, they all converge at the expression of GFAP as ‘the’ marker to understand the commitment towards astrocytic lineage. Collectively, these studies suggest an increase in the expression of Sox9 and NF1 genes in early gliogenic precursors. Further investigation is required to study the relation between these different ways of initiating astrocytic

differentiation in order to build a better temporal model for the exit from neurogenesis, especially with respect to the generation of different types of astrocytes.

1.2 Signaling pathways required for differentiation towards astrocytes

Once the transition from neurogenesis to gliogenesis has taken place, the astrocyte restricted precursors are available to be acted upon by cytokines CNTF, LIF and growth factors like BMPs (BMP2, 4 and 7) which act either independently or synergistically to activate signaling cascades required for the final differentiation step. One of the key signaling pathways involved is signal transducer and activators of transcription 1/3 (STAT1/3) mediated activation of the GFAP promoter (*Bonni et al., 1997*). Several studies have contributed to our current understanding of the JAK-STAT model of astrocyte differentiation. It has been shown that mutant mice for gp130 or LIF receptor (LIFR) display obstructed astrocytic differentiation in terms of GFAP expression (*Koblar et al., 1998*). Only late cortical progenitors have been found to be responsive to the presence of LIF or CNTF. In addition, increased STAT1/3 activity has been reported in late cortices as compared to the earlier ones (*Kessaris et al., 2008*). CNTF and LIF binds to cell surface coreceptor gp130, resulting in its dimerization with LIFR. This in turn activates Janus kinase (JAK) a tyrosine kinase in the cytoplasm. This is responsible for the phosphorylation and dimerization of STAT1/3. The activated STAT protein translocates from cytoplasm to the nucleus and binds at the putative sites of the GFAP promoter region (-1512 to -1504 being the strongest for STAT, -1292 to -1284 and 277 to 285, *Rajan et al., 1998*). Also, it forms a complex with p300 by binding at its amino terminus, relaxing the chromatin structure and triggering transcription of GFAP (*Figure 3A*). Unwinding of the chromatin is aided by the histone deacetylase property of p300 protein. The STAT signaling generates a self activating autoregulatory loop thereby strengthening and stabilizing the astrocytic differentiation (*He et al., 2005*). Blood vessels have also been proposed to play a significant role in astrocyte differentiation by secretion of LIF from the endothelial cells (*Mi et al., 2001*). Another known pathway for astrocyte differentiation is BMP mediated SMAD signaling. Dimers of BMP bind and tetramerize BMP receptor I, and II. The serine-threonine kinase activity of BMPR-II phosphorylates BMPR I, which then brings about phosphorylation of SMAD1. Activated SMAD1 forms a complex with SMAD4 and translocates to the nucleus where it binds to the carboxy terminus of p300. p300 acts as a bridge between STAT and SMAD signaling thereby allowing the synergistic activity of BMP and LIF towards differentiation into astrocytes as assessed by increase in the expression of GFAP (*Yanagisawa et al., 2001*).

In addition to the canonical STAT/SMAD pathway for astrocyte differentiation, PI3K-Akt signaling has also been shown to be another major player in the expression of GFAP. This is mediated by CNTF dependent activation of PI3K which in turn phosphorylates Akt1 (protein kinase B) in the plasma membrane. This activates astrocyte differentiation in two plausible ways mediated by NCoR and Olig2. Activated Akt1 either directly or upon subsequent phosphorylation of glycogen synthase kinase 3- β (GSK-3 β), brings about phosphorylation of nuclear receptor corepressor (NCoR), resulting in its translocation from nucleus to cytoplasm. In the nucleus, NCoR is believed to form a complex with HDAC thereby repressing GFAP expression (*Figure 3B*). This mechanism was proposed by the study where embryonic cortical progenitors from NCoR mutant mice were reported to have impaired self renewal and precocious differentiation into astrocytes (*Hermanson et al., 2002*). Also, in another study, brain specific inactivation of PTEN (an endogenous inhibitor of PI3K) displayed increased astrogliosis brought about by over activation of Akt1 (*Morrison, 2002*). These reports suggest a role of NCoR as repressor for astrocyte specific genes. This hypothesis was further strengthened by another study showing the formation of a complex between neuregulin receptor Erb4 and NCoR which then translocates to the nucleus, binds to the promoter region of astrocytic genes, thereby blocking their expression (*Sardi et al., 2006*). Another mechanism of action of activated Akt1 involves basic helix-loop-helix transcription factor Olig2 in the VZ of new born and SVZ of the adult mouse brain. Like NCoR, Olig2 is also phosphorylated and translocated out of the nucleus to allow NSCs to be responsive to CNTF or BMP, implying that nuclear accumulation of Olig2 inhibits astrocyte differentiation (*Setoguchi et al., 2004*). However, it is not yet clear whether the release of astrocytic gene repression upon cytoplasmic migration of both NCoR and Olig2 is necessary to permit astrocyte differentiation.

Furthermore, Notch has been long considered to play a very important role in activating differentiation towards astrocytes in retina in a number of ways. Upon binding to its ligand, Notch undergoes proteolytic cleavage resulting in the formation of notch intracellular domain (NICD) which translocates to the nucleus. In the nucleus, it mediates activation of *hes* genes in a CSL-SKIP dependent manner which directly or indirectly act on the GFAP promoter. Also, NICD is known to directly induce GFAP expression (*Ge et al., 2002; Rodriguez-Rivera et al., 2009*). Besides this, it has been proposed that Notch interacts with STAT3 to activate GFAP as deletion of STAT3 inhibits induction of GFAP by Notch. Despite these findings, it is not yet clear whether or not Notch activation is an absolute or a temporal requirement for differentiation into astrocytes (*Kessaris et al., 2008*).

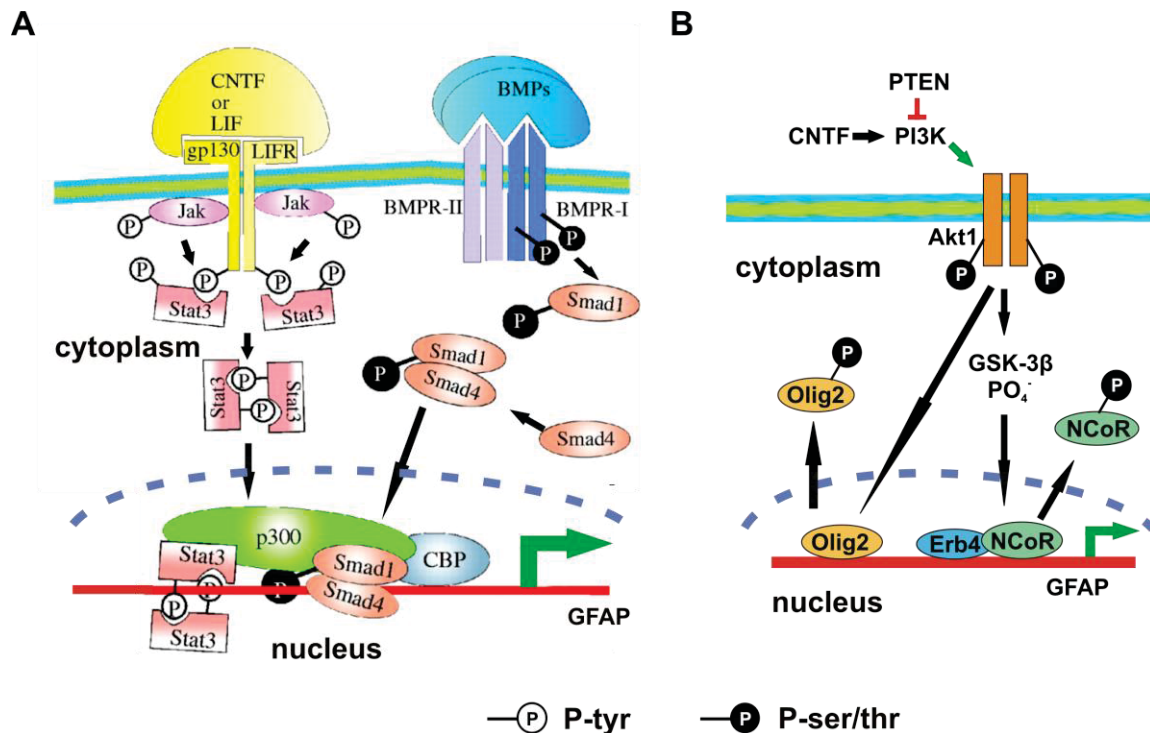


Figure 3: Regulatory pathways for differentiation towards astrocytes.

A) Adapted from Kessaris *et al.*, 2008. CNTF/LIF and BMP mediated activation of canonical JAK-STAT and SMAD pathway leading to expression of GFAP. **B)** Involvement of pAkt1 in phosphorylation of NCoR and Olig2 and their translocation into cytoplasm resulting in GFAP expression and differentiation into astrocytes.

Other possible pathways crucial for astrocyte generation are being explored. In 2008, Cebolla *et al.*, has shown that the neurotrophic peptide pituitary adenylate cyclase-activating polypeptide (PACAP), enhances astrocyte differentiation of cortical precursors via activation of a cAMP-dependent pathway as examined by GFAP expression. This is mediated by transcriptional repressor downstream regulatory element antagonist modulator (DREAM), which is bound to the GFAP promoter at specific sites. In an additional study, cAMP was reported to activate Notch cleavage by γ -secretase thereby inducing NICD dependent expression of GFAP (Angulo-Rojo *et al.*, 2013). Recently, another study have highlighted the role of presence of let-7 and miR 125 non coding RNAs, which share common targets and act in parallel to JAK/STAT signaling to promote GFAP based astrocyte differentiation. Also, it has been shown that both of these non coding RNAs are present in high amount in astrocyte restricted precursors as well as astrocytes. (Shenoy *et al.*, 2015). As mentioned before, most of these reports rely on the expression of GFAP as the astrocytic marker and therefore further studies are required to relate the expression of other important astrocytic markers like ALDH1L1 and glutamine synthetase (GS). Also, it remains to be elucidated whether or not these pathways are working in parallel or one pathway can compensate for the lack of the other or whether they exhibit a temporal pattern.

1.3 Characteristic markers, functions and heterogeneity of astrocytes

1.3.1 Markers described to identify and classify astrocytes

As seen until now, most of the studies for defining astrocytes and their development depend largely on the expression of GFAP. But with more detailed studies of astrocytes, it is becoming clear that not all astrocytes are labeled uniformly with GFAP. Also, the type B stem cells in adult SVZ stains positive for GFAP. In addition, GFAP expression is augmented in reactive astrocytes as well as serum derived cultured astrocytes. These findings suggest that the use of GFAP as ‘the prototypical’ astrocytic marker is highly disputable. Depending on our current understanding of the astrocyte differentiation from different brain regions, the temporal order of expression of astrocyte specific markers can be depicted as shown in *Figure 4A*.

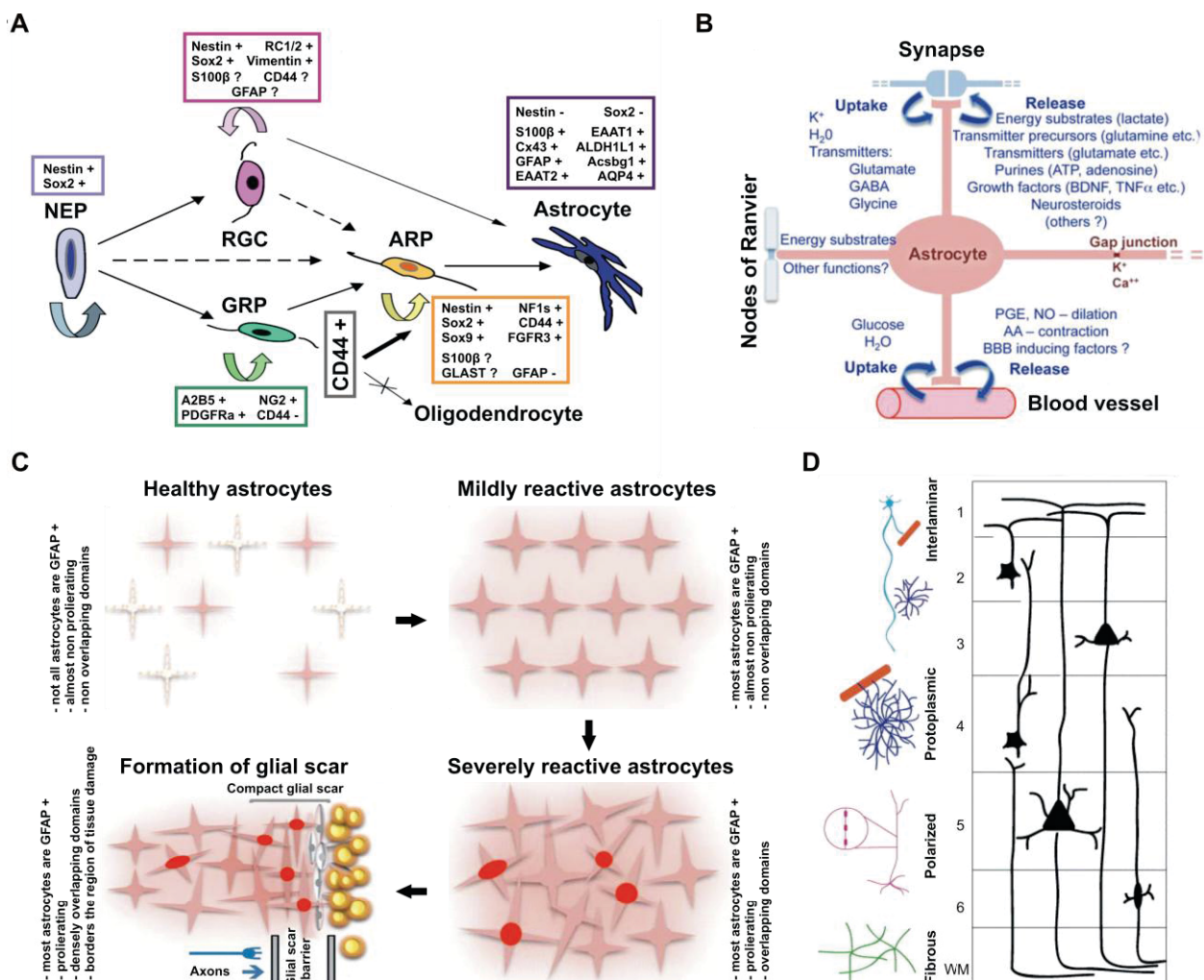


Figure 4: Astrocytic markers, their function and heterogeneity.

A) Adapted from *Liu et al., 2004*. Markers for different stages, starting from neuroepithelial cells to astrocytes. **B)** Adapted from *Sofroniew et al., 2010*. Functional properties of astrocytes in a healthy brain. **C)** Adapted from *Sofroniew et al., 2010*. Alterations in astrocytes in case of injury and disease.

White stars represent non GFAP expressing and pink stars represent GFAP expressing astrocytes. Red circles signify proliferating cells. Grey cells symbolize other infiltrating cells like fibromeningeal cells and extracellular matrix. **D)** Adapted from *Oberheim et al., 2006*. Heterogeneity of astrocytes in the human brain. 1-6 represents cortical layers, WM = white matter.

The detailed description of the markers is as follows:

a) **Sox9**: Sox9 belongs to the high mobility group box (HMG-box) family of transcription factors, and starts to be expressed in mouse spinal cord at embryonic day (E) 9.5 to 10. As stated before, Sox9 is pivotal for the induction of NF1A and forms a complex with it, subsequently activating a subset of genes at E11.5. These induced genes include *Apccdd1* and *Mmd2* which perform key migratory and metabolic roles respectively, during further differentiation in the astrocytic lineage (*Kang et al., 2012*). Also, a specific nestin-cre based deletion of Sox9 in spinal cord NSCs has shown to cause failure in glial specification with a dramatically depleted number of astrocytes even at later stages. Possibly, Sox9 might be important for astrocyte diversification specifically for gray matter astrocytes, as shown by staining for GLAST and GS (*Stolt et al., 2003*). However, in a recent study, it has been described that regional disparity might exist for the function of Sox9 as its ablation in cerebellum did not significantly affected gliogenesis, but promoted increase in number of neurons (*Vong et al., 2015*).

b) **FGFR3**: Fibroblast growth factor receptor 3 (FGFR3) is responsive to both FGF1 and 2 and appears in glial progenitors at around E10. In spinal cord development studies, it was shown that FGFR3 null mice upregulate the expression of GFAP in gray matter astrocytes, thereby implying its role in maintaining the quiescent state in these cells. Also, it is considered to be a marker for astrocyte specific progenitors as FGFR null mice continues to generate oligodendrocytes without any effect on their PDGFR positive precursors (*Pringle et al., 2003*).

c) **NF1 genes**: The Nuclear factor1 (NF1) family of transcription factors bind to CAATT boxes and have been illustrated to be indispensable for the initiation of gliogenesis in rodent spinal cord. The expression of NF1A follows that of Sox9, usually reported to be expressed at E11.5. In addition to instructing the gliogenic fate, NF1A also inhibits neurogenesis, mediated via Hes genes dependent regulation of Notch signaling (*Deneen et al., 2006; Kang et al., 2012*). In addition, NF1A regulates the DNA methylation by inhibiting interaction of astrocytic genes with DNMT1 (*Namihara et al., 2009*). Other NF1 genes: NF1B, C and X are also described to be crucial for glial specification and differentiation. Knockdown studies of NF1B have shown a drastic reduction in astrocyte differentiation in the embryonic brain as well as spinal cord, as

exhibited by a 5-10 fold decrease in the expression of GFAP (*Steele-Perkins et al., 2005*). Unlike NF1A, the expression of NF1X was found to be induced at later stages of development. Together with NF1C, it has been implicated in the expression of late astrocytic genes: GFAP and SPARCL1 (*Wilczynska et al., 2009*).

d) **CD44**: The expression of cluster of differentiation 44 (CD44) starts at around E13.5 in developing mouse spinal cord. BMP and LIF are considered to be responsible for inducing its expression in the which seem already to belong to the astrocytic lineage as CD44 positive cells fails to generate oligodendrocytes or neurons *in vivo*. Also, the overexpression of CD44 at E12.5 has been reported to result in doubling the number of GFAP positive cells accompanied by a decrease in oligodendrocytes. Furthermore, the same study has described the presence of CD44 in human fetal tissue at 18-22 gestational weeks, co labeled with another immature astrocyte marker S100 β . These CD44 expressing cells exhibited astrocyte restricted lineage as was demonstrated by the lack of neuronal and oligodendrocytic lineage markers (β -III tubulin and Olig2/GalC respectively) and their ability to differentiate into GFAP positive astrocytes upon exposure to serum (*Liu et al., 2004*). Another study has reported the presence of CD44 expressing cells in the developing mouse cerebellum, where again these cells are committed towards astrocytic lineage and depend on the presence of FGF2 and BMP4 for their proliferation and survival respectively (*Cai et al., 2012*).

e) **S100 β** : S100 β belongs to the family of Ca²⁺, Zn²⁺, Cu²⁺ binding proteins, and is highly expressed in the brain. It has been reported that the initiation of S100 β expression (at around E13 in mouse) in astrocytes marks the loss of their NSC potential, thereby stabilizing their commitment towards the astrocytic lineage (*Raponi et al., 2007*). Expression of S100 β in astrocytes is seen in all regions of the brain, occupying both cytoplasmic and nuclear location. The specificity of its expression to astrocytes alone is highly disputed as there are some findings suggesting its presence in radial glia, oligodendrocytes as well as in mature neurons in adult mice. Although the exact physiological function of S100 β is unknown, it has been attributed to play a crucial role in cytoskeleton organization and scavenging of toxic substances at the brain-CSF interface (*Vives et al., 2003*). Also, intracellular S100 β is considered to stimulate cell proliferation, migration along with inhibition of apoptosis and differentiation. In astrocytes, S100 β is also known to regulate their response to inflammation in a receptor for advanced glycation end products (RAGE) dependent manner (*Donato et al., 2009*).

f) **EAAT1/GLAST**: The activation of excitatory amino acid transporter 1 (EAAT1 or sodium dependent glutamate-aspartate transporter GLAST) promoter overlaps with the beginning of migration of neurons and follows a dorso-ventral temporal pattern in spinal cord, with initial expression at E11 in ventral and at E13 in dorsal horn. In early development, EAAT1 is postulated to be involved in regulating neuronal migration probably through reverse transporter operation, controlling glutamate concentration and activation of non synaptic NMDAR (*Shibata et al., 1997*). Although the cell specific pathways involved for EAAT1 induction are unknown, it is considered that neurons provide important cues for increasing its expression (*Regan et al., 2007*). In rat forebrain, expression of GLAST has been reported to start at the second embryonic week and reaches a maximum level by postnatal week 5 and has been shown to be present in only glial cells in both young and adult animals (*Ullensvang et al., 1997*). Along with other glutamate transporter, EAAT1 acts as a low affinity transporter and is involved in clearing glutamate from the extracellular space, thereby protecting neurons from excitotoxicity.

g) **Connexin43 (Cx43)**: Connexin acts as a building block for hemichannels by forming an assembly of 6 homo or hetero connexins. Two homo- or hetero-hemichannels from adjacent cells opposing each other form the gap junctional channel (GJC). Hemichannels and GJC serves as a means of exchange between cells and extracellular medium or intercellular communication respectively, by permitting passive diffusion of small molecules like glutamate, glutathione, glucose, ATP, cAMP, IP₃, and ions (Ca²⁺, Na⁺, K⁺) (*Alexander et al., 2003; Langer et al., 2012*). Astrocytes have been shown to express Cx30 and 43, the latter being the most dominant one (numerical values correspond to their molecular weight). The expression of Cx43 is reported to persist throughout development in radial glia and increases postnatally, prominently in astrocytes. During development, connexins are important for maintaining a proliferative stage as well as guiding neuronal migration. In astrocytes, the expression of connexins at their endfeet helps in regulating microvascular function by sensing the changes in neuronal microenvironment and also aids in maintaining the integrity of the blood brain barrier (BBB). Alteration in the expression of astrocytic Cx43 has been described in various neurological disorders (for e.g. Alzheimer's (AD) and Parkinson's (PD) disease), usually resulting in enhanced coupling and thereby modulating cellular homeostasis in a detrimental way (*Freitas-Andrade et al., 2015*).

h) **ALDH1L1**: Aldehyde dehydrogenase 1 light chain 1 (ALDH1L1, as known as 10-formyltetrahydrofolate dehydrogenase (FDH)) is a folate metabolizing enzyme, first shown to be expressed in rodent astrocytes, making them an important site for folate metabolism (*Neymeyer et al., 1997*). Later, using P0 mouse, it was reported that ALDH1L1 labels all astrocytes throughout

the brain, whereas GFAP was predominantly expressed in the white matter. Also, it does not co-stain with neuronal or oligodendrocyte markers, thereby promoting the use of ALDH1L1 as a highly specific, ‘pan’ astrocytic marker which could be employed for preparation of pure astrocytic cultures by performing FACS (Cahoy *et al.*, 2008). By means of GLT1⁺, ALDH1L1⁺ reporter mice; another study have reported a decrease in the expression of ALDH1L1 with maturation of spinal cord astrocytes and its up regulation upon their reactivity as usually seen for GFAP (Yang *et al.*, 2011).

i) **Glutamine synthetase (GS):** GS has been popularly accepted as a classical astrocyte marker, labeling both high and low GFAP expressing astrocytes. By performing in situ hybridization, mRNA for GS was reported to be present at E14 in rodents and peaks after birth at around P15 (Mearow *et al.*, 1989). The enzyme restricted solely to astrocytes, functions as a glutamate catabolizing enzyme, using ammonium and glutamate to synthesize glutamine. By taking part in the Glutamate-Glutamine shuttle between astrocytes and neurons, GS plays an important role in preventing excitotoxicity. Also, its levels are down regulated in the presence of pro-inflammatory cytokines like TNF α and in neurological disorders like epilepsy, resulting in increased extracellular glutamate concentration (Zou *et al.*, 2010; Eid *et al.*, 2013).

j) **GFAP:** Glial fibrillary acidic protein (GFAP) has been widely used as ‘the’ mature astrocytic marker to identify them both *in vivo* and *in vitro* and also to elucidate the signaling cascade for their differentiation. However as mentioned before, a deeper analysis of the expression of GFAP has revealed that not all the astrocytes express GFAP, its level being higher in white matter, fibrous astrocytes and almost insignificant in gray matter, protoplasmic ones. Protoplasmic astrocytes can however be identified by the presence of other pan astrocyte markers like ALDH1L1, GS and functional marker like EAAT2. In addition, glia limitans (astrocyte foot processes) and another subtype of astrocytes called interlaminar astrocytes also express GFAP. Its expression has been observed to start at E16 in mouse and at 23 gestational weeks in humans and peaks till E18 and 41 post conceptional week in mouse and humans respectively (DeSilva *et al.*, 2012; Roybon *et al.*, 2013). Protoplasmic astrocytes when turned reactive upon inflammatory insult, retain the ability to exhibit GFAP expression. GFAP ICC does not sufficiently reveal astrocyte morphology. Using dye filling experiments it has been illustrated that *in vivo* astrocytes possess far more processes than those observed with GFAP immunostaining, and GFAP represents only 15% of the total cell volume (Oberheim *et al.*, 2006).

k) **Acsbg1:** Acyl CoA synthetase bubblegum family member 1 (Acsbg1 or Lipidosin) has been shown to be highly enriched in astrocytic cytoplasm (*Cahoy et al., 2008*). A couple of reports have described Acsbg1 to exhibit higher expression in gray matter protoplasmic astrocytes as compared to those in white matter. Its expression has been shown to begin at E19 and increase after birth, reaching a plateau at P28 in rodents. Due to increased expression of Acsbg1 around the areas of remyelination, it is considered to be crucial for brain lipid metabolism and myelin formation (*Song et al., 2007; Li et al., 2012*).

l) **EAAT2/GLT1:** Excitatory amino acid transporter 2 (EAAT2 or Glutamate transporter 1 (GLT1 in rodents) is the second most dominant glutamate transporter expressed by astrocytes performing a similar function in glutamate clearance as described for EAAT1. EAAT2 expression begins late in development, reported to be seen at 33 gestational weeks in humans and after P0 in rodents. In humans, EAAT2 expression has been reported to increase in a region based manner till 8 postnatal weeks. Interestingly, neurons have been shown to express EAAT2 earlier in development from 23 human gestational weeks until 8 postnatal weeks. This has been correlated to proper migration and maturation of neurons. Also, by performing western blots, it is postulated that EAAT2 undergoes glycosylation with increasing developmental age, which is considered to be important for enhancing its transporter function (*DeSilva et al., 2012*).

There are numerous other reported markers for astrocytes. Aldolase C (AldoC) which is considered to be a pan astrocytic marker, acts a brain specific form of fructose-1, 6-bisphosphate aldolase and is reportedly expressed in rodent brain from E14 (*Walther et al., 1998*). Another protein called Apolipoprotein E (ApoE) helps in uptake of cholesterol containing lipoproteins and has been shown to be secreted by astrocytes, aiding neurite outgrowth, dendritic remodeling and synaptogenesis (*Mauch et al., 2001*). Neurons have also been shown to start expressing ApoE in response to excitotoxic injury (*Xu et al., 2006*). Besides this, ApoE aids in clearance of amyloid- β (A β) and therefore has been linked to AD. Aquaporin 4 (AQP4), an intergral channel protein responsible for transport of water, is another important marker for astrocytes. It is highly enriched at astrocyte endfeet where it regulates water transport across the blood brain barrier and clearance of extracellular K⁺. In the recent years, AQP4 has been described to play a vital role in the brain glymphatic system as animal models lacking AQP4 exhibits about 70% decrease in clearance of interstitial fluids and extracellular proteins like A β (*Iloff et al., 2012*). It must be noted that most of the above mentioned markers still remain to be studied in detail in context to human brain tissue which would promise a better understanding of astrocytes, their subtypes, markers and regional identity.

1.3.2 Functional properties attributed to astrocytes

Once named as glia referring to their only recognized function as brain glue, astrocytes have now been described to be one of the major cell types in the brain playing a very important role in metabolism as well as neurodegenerative diseases. Astrocytes are non excitable cells, which were earlier considered to be only structural support and metabolic supplier for neurons. Electrophysiological studies usually describes two extreme subtypes of astrocytes with a resting membrane potential of ranging from -25mV to -85mV depending on the expression of inward rectifying potassium channels (Kir channels), the expression of which is regulated by cAMP and protein kinase A (PKA). This finding was supported by depolarization of the membrane from -80 mV to -30 mV upon blockade of Kir channels with BaCl₂ (*Bolton et al., 2006*). Based on the studies in hippocampus and hypothalamus, several groups have suggested the role of astrocytes in information processing and synaptic plasticity. A large number of G protein coupled receptors are known to be present on astrocytes, rendering them responsive to all neurotransmitters and neuromodulators in terms of changes in cytosolic Ca²⁺ or cAMP. The changes in intracellular Ca²⁺ concentration are now considered to provide an intra and intercellular mode of communication via propagation of calcium waves through gap junctions or purinergic receptors. It is followed by release of gliotransmitters like glutamate, ATP and D-serine, thereby modulating neuronal activity (*Araque et al., 2014; Sahlender et al., 2014*). This hypothesis gave rise to widely accepted concept of tripartite synapse where astrocytes actively participate and exchange information with neurons (*Araque et al., 1999*). It also challenged the concept of considering astrocytes as non excitable cells. The existence of a tripartite synapse is supported by other reports in hippocampus studies, where astrocytes secrete glutamate in response to endocannabinoids released from pyramidal cells. The released glutamate in turn stimulates adjacent neurons (*Navarrete et al., 2008*). These findings strengthen the concept of neuron-glia communication. In addition to the metabotropic receptors, Bergmann glia in cerebellum expresses a limited number of ionotropic receptors for GABA and glutamate (*Iino et al., 2001*). Overall, astrocytes are important players of brain function responsible for providing nutrition, buffering extracellular environment, regulating synapse maturation as well as synaptic transmission via glutamine-glutamate exchange (*Figure 4B*).

Developmental role of astrocytes: During late development, astrocytes regulate neuronal migration and synapse maturation by providing guidance cues in the form of membrane bound or cytoplasmic or secreted proteins. Early studies from the retinal ganglion cells have demonstrated an increased number of synapses in the presence of astrocytes independent of direct or indirect

contact. Till now, several astrocytic molecules like Thrombospondins (TSP), Integrins, Ephrins, Sparc, Hevin, and Glypicans (*Pfriege*, 2009; *Kucukdereli et al.*, 2011; *Allen et al.*, 2012) have been proved to be responsible for mediating the synaptogenic effect. In addition, the presence of astrocytes and other glial cells elevates the secretion of complement cascade initiating protein C₁q, which in turn contributes to synapse pruning during development (*Stevens et al.*, 2007).

Also, in adult brain, astrocytic endfeet are a crucial component of blood brain barrier (BBB), and are responsible for determining its permeability and regulating cerebral blood flow (*Zonta et al.*, 2003; *Takano et al.*, 2006). Another important phenomenon during neurodevelopment is myelination. Although astrocytes are not direct mediators of myelination, *in vitro* studies suggest their role in alignment of oligodendrocytic processes along axons and increasing the rate of myelin wrapping through ATP and LIF dependent mechanism (*Meyer-Franke et al.*, 1999; *Ishibashi et al.*, 2006).

Metabolic role of astrocytes: When it comes to brain function and energy needs, astrocytes and neurons exhibit a wisely planned division of labor, where neurons rely on astrocytes for fuel, meeting their high energy demand for the execution of synaptic signaling and information processing. Supported mainly by glycolysis, astrocytes continuously synthesize and feed neurons with lactate as the major fuel. Several messengers like glutamate, K⁺, NO, H₂O₂, and ammonia signals the metabolic demands of neurons to astrocytes (*Magestretti et al.*, 1994). In addition, astrocytes serves as the store house for glycogen which is later released in the form of glucose or lactate in the extracellular space to be taken up by neurons (*Gruetter*, 2003). One more specialized function of astrocytes is glutamate clearance from the extracellular space to protect neurons from excitotoxicity. Once taken up, glutamate and ammonia are acted upon by glutamine synthetase in astrocytes which is supplied back to neurons to maintain their reserves for glutamate (*Berl et al.*, 1961). Another crucial function of astrocytes is the flux of water, and gasses like O₂, CO₂, NO mediated via expression of AQP4 (*Verkman et al.*, 2009). Knockout studies of AQP4 have suggested it to be a powerful therapeutic target in neurodegenerative disorders. Besides this, astrocytes exhibit spatial buffering for potassium within seconds of neuronal activity, thereby maintaining its extracellular concentration constantly low (*Walz et al.*, 1984). However, the exact mechanism underlying this remains incompletely understood *in vivo*, due to limitations of studying a single cell type with currently available pharmacological approaches. Astrocytes are also accountable for fighting against ROS to which neurons are highly susceptible. This is attributed to the presence of the antioxidant system glutathione disulfide-glutathione (GSSG-GSH) in astrocytes (*Aschner*, 2000).

Besides their role in brain physiology, astrocytes also respond to neurological disorders by turning reactive, which in turn can be detrimental or helpful to the neurons. Several factors have been reported to turn the astrocytes reactive, for e.g. Cytokines and growth factors (IL1, IL6, IL10, IFN γ , TNF α , TGF β), neurotransmitters (like noradrenaline, glutamate), reactive oxygen species, reactive nitrogen species, bacterial endotoxin LPS, conditions like glucose deprivation, hypoxia, presence of toxic substances like ammonium ions, amyloid- β etc. Reactive astrocytes are characterized by the following changes:

a) **Morphological alterations:** Changes in the morphology of reactive astrocytes can vary strikingly from hypertrophy of their process with increased thickness and number of primary process to glial scar formation depending on the intensity of the insult. The former is characterized by augmented expression of intermediate filament proteins: GFAP, Vimentin and Nestin (*Wilhelmsson et al., 2006*). However, the reactive astrocytes maintain their individual domain exhibiting only a limited overlap with the domains of the neighboring astrocytes. Thereby the total volume occupied by reactive astrocytes does not differ considerably from the non reactive ones (*Figure 4C*). Also, it is believed that this moderate form of reactive gliosis may undergo self-resolution over time, regaining the healthy appearance and function. The formation of glial scar is seen in more severe cases of CNS injury associated with the disruption of BBB. Astrocytes proliferate at the site of injury and invade the neighbouring tissue. The glial scar constitutes of astrocytes with overlapping domains, activated macrophages, endothelial cells and extracellular matrix as the main components. The scar persists for long time and may act as a mechanism of the brain to confine lesions and prevent spread of inflammation, but at the same time it is also known to block axonal regeneration. Conditional knock out of STAT3 has been shown to attenuate hypertrophy, scar formation and GFAP overexpression. On the contrary, deletion of NF-KB signaling decreased inflammation and size of the lesion after spinal cord injury, suggesting the participation of different signaling cascades in reactive gliosis (*Khakh and Sofroniew, 2015*).

b) **Increased proliferation:** Increased proliferation is another hallmark of reactive astrocytes. Depending on the type of injury from invasive or non invasive, *in vitro* cultures of such reactive, proliferating astrocytes sometimes exhibits ‘stem cells like properties’, resulting in the formation of self renewing, multipotent neurospheres (*Buffo et al., 2008*). Also, this study has shown that the source of these proliferating astrocytes is not the adult NSCs and therefore may be attributed to de-differentiation of mature astrocytes. The signaling mechanisms involved in increased astrocytic proliferation remains poorly understood. Several studies have shown the morphogens

and molecules like SHH, BMPs, EGF, FGF, ATP and Endothelin-1 dependent JNK/c-Jun to be the important players (*Levison et al., 2000; Gadea et al., 2008; Neary et al., 2009*).

c) **Changes in gene expression:** With the aid of gene arrays and proteomic studies on the cultured astrocytes, alterations in the expression of a wide variety of molecules have been reported. It includes the molecules involved in maintaining cell structure (GFAP, Nestin, Vimentin), extracellular matrix proteins (CSPGs, Laminin, Metalloproteases, Ephrins), metabolites (Lactate), and other vital astrocytic proteins (Cx43, glutamate transporters, GS, aquaporin-4, TSP etc). Depending on the neurological disease, sometimes these molecules were upregulated and sometimes downregulated. Reduction in EAAT2 and GS has been most commonly reported and is considered to be responsible for glutamate mediated excitotoxicity of neurons in several neurodegenerative disorders (*Yang et al., 2013*). Currently, using two different injury models of ischemia and LPS induced neuroinflammation in mouse, studies with Affymetrix GeneChip arrays revealed Lipocalin 2 (Lcn2, a secreted lipophilic protein) and Serpina3n (a secreted peptidase inhibitor) as the new markers for reactive astrocytes. Also this study has highlighted that at least 50% of the altered genes were specific to the type of injury, which may also suggests the occurrence of different subtypes of reactive astrocytes (*Zamanian et al., 2012*).

d) **Release of cytokines:** Several cell types in the brain (astrocytes, neurons, microglia and endothelial cells) possess the ability of secreting cytokines and expressing their receptors with a basic function of aiding cellular migration and proliferation during development. Besides this constitutive expression, cytokines have been known to be elevated in several inflammatory and pathological conditions like AD, multiple sclerosis (MS), AIDS, ischemia and tumors. A stable and long lasting increase in a pool of chemoattractant cytokines: CXCL1, CXCL2, and CXCL10 and a transient increase in CCL2 have been reported post injury in MCAO model. They in turn recruit immune cells to the site of injury. In pathological conditions, the secreted chemokines may either promote neuronal survival or result in inflammatory reaction, thereby making them a potential candidate in diagnosis and treatment (*Bajetto et al., 2002; Zamanian et al., 2012*).

The importance of the reactive astrocytes in neurodevelopmental, psychiatric and pathological disorders has only recently begun to be explored. Reactive astrogliosis, illustrated by upregulated GFAP levels has been described in wide range of disorders like: AD, PD, batten disease (BD), amyotrophic lateral sclerosis (ALS), CNS infections, ischemia and epilepsy. Also, in ALS and huntington's disease (HD), abnormal astrocytes result in non cell autonomous effects on the surrounding tissues (*Pekny et al., 2014*). In epilepsy, astrocytic dysfunction in terms of elevated

cytosolic calcium concentration has been shown to result in generation of focal seizure like discharge. Also, astrocytes engage in a recurrent excitatory loop with neurons, promoting the initiation of seizures (*Gómez-Gonzalo et al., 2010*). A series of neurodevelopmental disorders, Rett syndrome, Alexander's disease, Niemann-Pick type C disease, Fragile X syndrome also exhibit astrocytic anomalies. This is supported by developmental defects in neurons upon loss of astrocytic MeCP2 in Rett syndrome, effect on synapse formation in astrocytic FMR1 deficient mouse in fragile X syndrome, mutations in GFAP in alexander's disease and presence of NPC1 in astrocytic processes, resulting in neurodegeneration in Niemann-Pick type C disease (*Molofsky et al., 2012*). Mutations in the astrocytic genes *EAAT1* and *Kir4.1* have been implicated in autism, characterized by an imbalance of excitatory and inhibitory synapses (*Yang et al., 2013*). A spectrum of neurological disorders referred to as Rasopathies neurofibromatosis type-1 and Costello, Noonan, Leopard syndromes (due to the involvement of Ras pathway) have also been shown to involve abnormalities in astrocytes. It is characterized by intellectual disabilities which have been partially attributed to the premature formation of perineuronal nets due to early development of astrocytes. This inhibits experience dependent maturation and therefore cause cognitive decline (*Krencik et al., 2015*). Together, these studies emphasize the importance of astrocytes as a potential therapeutic target in neurological disorders. Also, the *in vitro* disease models can aid in better understanding of molecular mechanisms underlying these diseases.

1.3.3 Heterogeneity of astrocytes

The term astrocyte was coined in 1895 by Lenhossek referring to the star shaped appearance of the cells. However, currently, it is very clear that not all astrocytes are star like and their shape may range from a star or a bushy shrub to an elongated neuron like appearance. Based on several studies, human astrocytes are now considered to consist of a highly heterogeneous and complex population with at least 4 different morphological variants known till date (*Figure 4D*). Besides this, using modern dye filling techniques, it has been illustrated that each individual astrocyte exists in a non overlapping domain with the adjacent one, exhibiting only 4.6% overlap of the total cell volume (*Oberheim et al., 2012*). The subtypes of astrocytes known so far are discussed as follows:

a) **Protoplasmic astrocytes:** Protoplasmic astrocytes are the most abundant astrocyte subtype, residing mostly in deeper cortical layers (layer 2-6), constituting the majority of gray matter glia. They have been reported to be highly coupled via gap junctions resulting in long distance propagation of calcium waves reaching up to 200-250 μm far (*Haas et al., 2006*). Their cell body

ranges around 10 μm in diameter whereas, they extend a complex network of processes which can be as long as 50 μm and span an area of 100-200 μm . Besides this high complexity, each cell exhibits non overlapping domain organization. Every single domain contacts around 5 blood vessels and 8 neuronal cell bodies which may suggest a link between regulation of blood flow and synaptic activity (*Oberheim et al., 2006*). The average number of synapses wrapped by protoplasmic astrocytes in humans ranges from 2.7×10^5 to 2×10^6 . However, the coordination of activity within this complicated network remains largely unexplored. These cells are generally characterized by very low or almost negligible expression of GFAP, but can be identified by the presence of other pan astrocytic markers like ALDH1L1, GS and Cx43. Also as stated before, a couple of other astrocytic markers Acsbg1 and EAAT2 have been reported to have a higher expression in this subtype.

b) Interlaminar astrocytes: This astrocytic subtype was first described in 1890 by Andrieza and Retzius. These cells uniquely evolved to be highly specific in the primate cortices. They were found to be located in layer I of the cortex, sending a long, mainly unbranched process deep in the cortical layer 3/4. Although their cell body is only 10 μm in diameter, but their processes can be upto 1 mm in length. In addition, they also possess 3-4 short fibers forming a network near the pial surface and increasing in length with development. Unlike previously described protoplasmic astrocytes, interlamiar astrocytes do not represent domain organization. They have also been shown to participate in diseased condition like Down syndrome and AD by decreasing the interlaminar processes. The developmental history as well as their function still remains to be explored. Plausibly, they serve as a way for long distance communication or columnar organization (*Oberheim et al., 2006*).

c) Polarized astrocytes: Present only sparsely, polarized astrocytes occupy a place in deeper cortical layers near the white matter. Being unipolar, they sometimes appear more like neurons. Similar to the interlaminar astrocytes, their process can be around 1 mm in length and 2-3 μm in diameter with minimum or no branches. However, they differ from interlaminar astrocytes as their processes exhibit small bead like varicosities and protrude away from the white matter towards outer cortical layers. Also their short GFAP positive processes are quite less branched and straight as compared to their protoplasmic neighbors (*Oberheim et al., 2006*). As they send long process, they might also be involved in communication between different layers or between gray and white matter. Their exact role is yet uninvestigated.

d) **Fibrous astrocytes:** Fibrous astrocytes are confined primarily to white matter. They are far less complex than the protoplasmic astrocytes and possess fewer but highly intermingled processes, thereby exhibiting overlapping domains. Adjacent cells are however, still equidistant from one another (*Oberheim et al., 2006*). These cells possess less gap junctional coupling and mediate short distance calcium waves which are mainly transmitted via purinergic receptors (*Haas et al., 2006*). They fit into the classical role of astrocytes by providing metabolic support to the neurons. These cells are stained intensely with GFAP and also show other pan astrocytic markers.

Further research needs to be done to elucidate the developmental origin and functional properties of different subtypes of astrocytes. Also, currently there is almost no available assay to distinguish these subtypes *in vitro*.

1.4 Induced pluripotent stem cells - disease modeling and therapy

1.4.1 iPSCs - development and applications

The generation of iPSCs first described in rodent somatic cells (*Takahashi et al., 2006*) opened the doors for a new era of therapy and disease modeling. Soon in 2007, the pluripotency was achieved in human cells by two independent groups (*Takahashi et al., 2007, Yu et al., 2007*). The former group employed four transcription factors, more commonly referred to as ‘Yamanaka factors’: Oct4, Sox2, Klf4 and c-myc (OSKM). The latter group replaced Klf4 and c-myc with Lin28 and Nanog. However, reprogramming efficiency with the use of these transcription factors remained as low as 0.01-0.02%. Besides low efficiency, this way of reprogramming had two main drawbacks *a)* two of the transcription factors (Klf4 and c-myc) used for reprogramming were reported to have high oncogenic potential (*Dang, 2012; Yu et al., 2011*) thereby limiting their clinical application, *b)* the mode of reprogramming using lenti/reteroviral vectors again posed a hindrance in their transplantation due to possible viral nucleic acid integration in the host DNA. Since then, a number of other non-integration reprogramming strategies have been put forward - use of adenovirus, sendaivirus, cre-lox P mediated transgene excision, synthetic mRNA and miRNA, piggyBAC and episomal plasmids some of which leave no traces of transgene in the genome of reprogrammed iPSCs. Also, some of these methods aided in improving the reprogramming efficiency by 10% (*Rao et al., 2012*) with a benefit of zero footprint.

OSKM are known to modulate chromatin regulators responsible for DNA methylation, histone methylation and acetylation or kinase signaling pathways like Wnt, MEK, GSK3, TGFβ (*Chen et*

al., 2014; *Vidal et al.*, 2014). Currently, a wide range of small molecules has been generated to block various signaling cascades and epigenetic modifiers. They have been shown to mimic the functions of OSKM with highly improved efficiency and have completely revolutionized the iPSC technology (*Lin et al.*, 2015). Usually two or more of these small molecule inhibitors are used in conjunction for a successful reprogramming (*Chambers et al.*, 2009; *Hou et al.*, 2013). In addition to reprogramming, these inhibitors also aid in pushing the iPSC in a particular lineage depending on the pathway being blocked or activated.

The increasing advances in reprogramming eased iPSC applications. Study of neurodegenerative disease is limited due to lack of proper animal models and unavailability of human samples. iPSCs have emerged as a robust system for the study of disease progression and therapy by using patient derived cells (*Dimos et al.*, 2008). It also offers a human model system for drug testing, reducing the possibility of failing clinical trials (*Inoue et al.* 2014). As it is easy to maintain and differentiate these cells *in vitro*, the continuously generated pool of differentiated cells can be utilized for a larger scale drug and toxicity screening or development of biomarkers (*Figure 5*). For success in disease modeling, it is necessary to rule out the possibility of heterogeneous population and unsynchronized cultures occurring due to incomplete reprogramming, genetic background variability, epigenetic memory or erosion of X-chromosome inactivation. This have been overcome by direct reprogramming in specific cell type like neurons, cardiomyocytes etc (*Vierbuchen et al.*, 2010). Mimicking of disease phenotype more physiologically has been achieved by inducing pathological changes in the cell type under study (e.g. application of amyloid-beta (*Nieweg et al.*, 2015)) or their interacting partners (e.g. neurons and astrocytes in ALS) or by depletion of trophic factors (*Xu et al.*, 2013). At the same time, care has to be taken for validation of the disease phenotype at multiple levels (for e.g. using other models and if possible human samples).

In addition to disease modeling, iPSCs compared to ES cells possess a great advantage for cell transplantation as it uses autologous cells thereby reducing the risks of rejection and infection. But it is still in the developing stage owing to the high costs and long time required for reprogramming and cell culture. Besides this, 3D cultures of iPSC derivatives have shown the successful generation of cerebral organoids, bone, optic vesicle-like structures, functional liver buds, cardiac muscle tissue, primitive and pancreas islet cells, thus bringing along a new generation of tissue bioengineering. Together with the range of their applications, iPSCs serve as a promising tool for the advancement of personalized medicine.

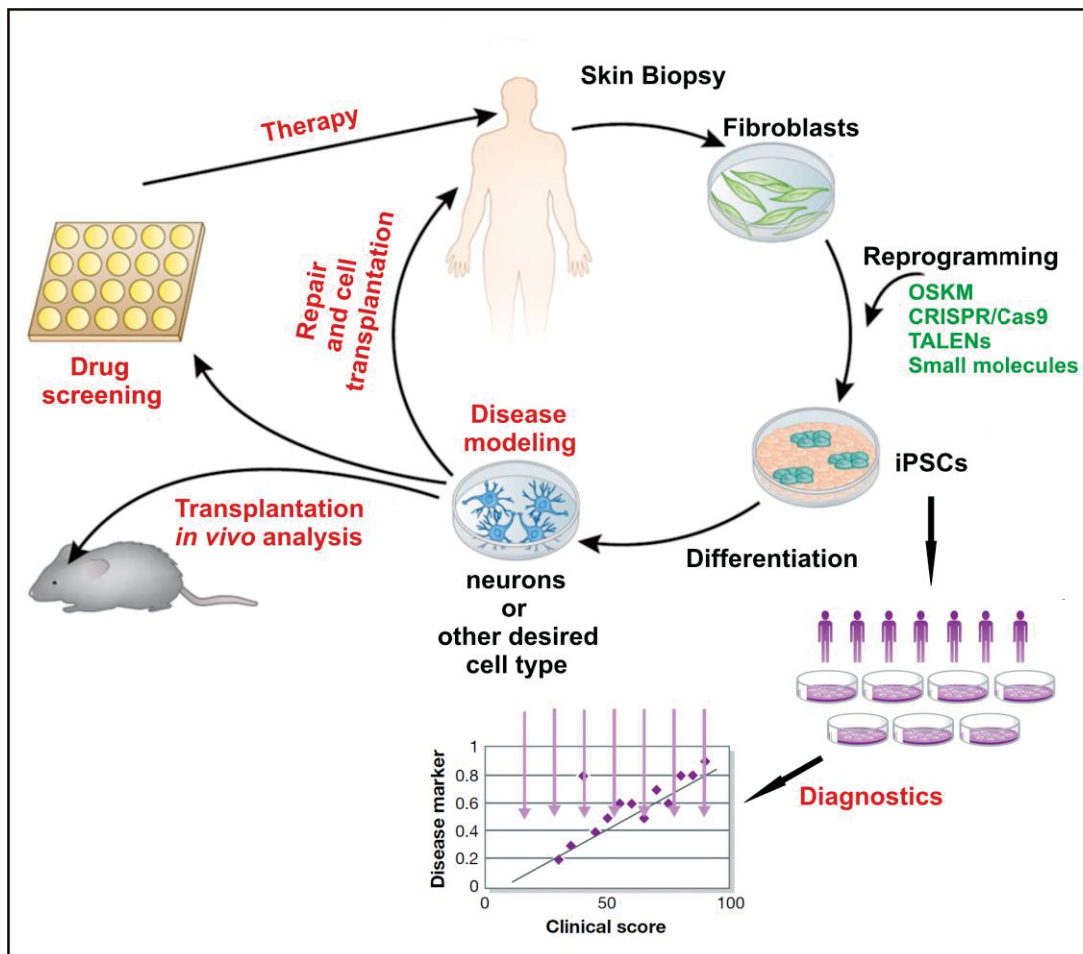


Figure 5: Development and application of iPSCs.

Adapted from *Huttner et al., 2011* and *Inoue et al., 2014*. The figure represents an overall scheme of iPSC generation and differentiation with an example of different reprogramming strategies. Once differentiated, these cells can be used for repair, therapeutics and diagnostics.

1.4.2 iPSCs – a way towards astrocytes

Neurons have been for long the major neural cell type differentiated from iPSCs for modeling neurodegenerative diseases. Hundreds of developmental pathway based protocols have been put forward to generate several functional neuronal subtypes ranging from cortical dopaminergic, cholinergic, GABAergic, glutamergic neurons, cerebellar purkinje neurons to spinal motor neurons. Small molecules have proved to be of great potential in determining the specification to a particular neuronal subtype as well as in A-P and D-V patterning (Figure 6). More recently, transcription factor mediated direct conversion of fibroblasts into inducible neurons (iNs) has even decreased the time required for the differentiation of these cells (*Pang et al., 2011*). As described before, as important players in basic brain physiology and pathology astrocytes also

require a special attention for a better understanding of disease mechanisms. The generation of subtypes of astrocytes from iPSCs has been greatly limited due to lack of our understanding about their specification and consistent markers for their precursors. Also, there are no well described markers or assays to differentiate the subtypes of astrocytes seen *in vivo*. In addition to this, most of the studies reporting the generation of astrocytes rely on the expression of GFAP which is not ubiquitously expressed in all astrocytes. A couple of other studies done for establishing differentiation of iPSCs towards astrocytes show a long culture time required at the NSC stage for their acquisition of gliogenic potential (Krencik *et al.*, 2011; Roybon *et al.*, 2013). Although, using these 6 months cultured NSCs, it has been possible to achieve regional patterning for astrocytes, but till date there is no well defined and time saving protocol for the generation of well characterized astrocytes and their subtypes.

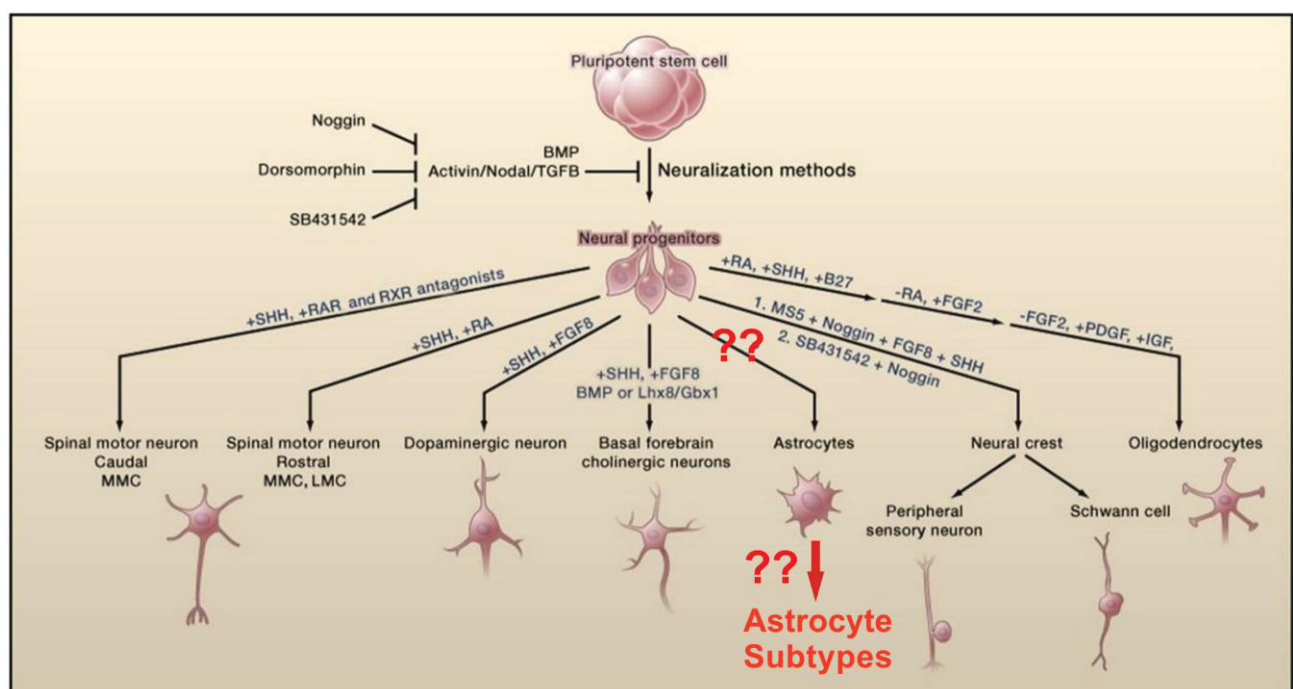


Figure 6: Generation of different neural lineage cells from iPSCs.

Adapted from Han *et al.*, 2011. iPSCs can be induced towards neural lineage by the use of BMP/TGF β inhibitors and then differentiated into neuronal subtypes using development cues. Similarly, generation of Schwann cells and Oligodendrocytes has also been reported. The protocols for the generation of astrocyte and their subtypes still remain poorly established.

1.5 Aims of the study

Pioneer studies over the last decade have enlightened the importance of astrocyte heterogeneity in the human brain. The vast differences between rodent and human astrocytes e.g. increase in cell volume, number of processes and wrapped synapses make human astrocytes preferable to investigate their basic physiology and role in neurological disorders. However, *in vivo* studies

from human samples are restricted due to ethical concerns and limited availability. Thus, *in vitro* approaches regain significance, especially regarding the potential of human induced pluripotent stem cells (hiPSCs). This young technology of generating pluripotent stem cells from adult humans has already revolutionized the field of medicine by providing new aspects of disease modeling, drug screening as well as organ transplantation (Takashaki *et al.*, 2007; Yu *et al.*, 2007; Dimos *et al.*, 2008; Inoue *et al.*, 2014). To employ *in vitro* systems for studying human disorders, it is important to mimic *in vivo* conditions in terms of presence of different cell types and distinct their subtypes. With the growing use of iPSCs, there have been several well defined protocols for their differentiation into different subtypes of neurons, but only few protocols exist for the generation of towards astrocytes and its subtypes in serum dependent or serum free conditions (Krencik *et al.*, 2011; Roybon *et al.*, 2013; Shaltouki *et al.*, 2013; Paşca *et al.*, 2015). Moreover, most of these studies are limited by the requirement of a long differentiation time to attain gliogenic cultures, use of either serum or expensive growth factors and above all, relying largely on the expression of GFAP to mark the completion of astrocyte differentiation and maturation (Gupta *et al.*, 2012; Serio *et al.*, 2013; Wang *et al.*, 2013; Williams *et al.*, 2014). This resulted in overlooking astrocyte heterogeneity while employing *in vitro* methods, thereby highlighting the need for an economical and less time consuming method for the generation of different possible subtypes of astrocytes.

Thus, the aim of the study was to establish a defined method for generating physiologically functional subtypes of astrocytes from iPSCs derived NSCs of cortical identity, which would provide a platform for understanding their distinct roles in brain physiology and neurological disorders.

2. Materials and methods

2.1 Buffers and reagents

2.1.1 Cell culture medium formulations

E8

Reagent	Supplier	Catalog no.	Concentration	Volume
DMEM/F-12	Invitrogen	31330-095	1x	49 ml
Pen Strep	Invitrogen	15140-122	100x	500 µl
NaHCO ₃	Sigma	S3817	34.3 mg/ml	500 µl
ITS	Refer 2.1.2		50x	1 ml
bFGF	Peprtech	100-18B	20 µg/ml	250 µl
TGFβ	Peprtech	100-21	2 µg/ml	50 µl
Ascorbic acid	Sigma	A8960	221mM	50 µl

N2B27

Reagent	Supplier	Catalog no.	Stock Conc.	Volume
DMEM/F-12	Biochrom	FG4815	1X	250 ml
Neurobasal	Invitrogen	21103	1X	250 ml
Pen Strep	Invitrogen	15140-122	10,000 U/ml	5 ml
Glutamax	Invitrogen	35050-038	200 mM	2.5 ml
B27 without RA	Invitrogen	17504-036	50X	5 ml
N2 supplement	Refer 2.1.2		50X	5 ml
Heparin	Sigma	H3149	10 mg/ml	150 µl
β-mercaptoethanol	Invitrogen	31350-010	50 mM	1 ml

NSC medium

Reagent	Supplier	Catalog no.	Stock Conc.	Volume
DMEM/F-12	Invitrogen	31330-095	1X	475 ml
Pen Strep	Invitrogen	15140-122	10,000 U/ml	5 ml
Glutamax	Invitrogen	35050-038	200 mM	5 ml
MEM-NEAA	Invitrogen	11140-050	100X	5 ml
B27 without RA	Invitrogen	17504-036	50X	5 ml
N2 supplement	Refer 2.1.2		50X	5 ml
Heparin	Sigma	H3149	10 mg/ml	250 µl
bFGF*	Peprtech	100-18B	20 µg/ml	500 µl
EGF*	Peprtech	AF100-15	20 µg/ml	500 µl

* Growth factors: bFGF and EGF were added after warming the medium to be used.

NSC-/- medium

Reagent	Supplier	Catalog no.	Stock Conc.	Volume
DMEM/F-12	Invitrogen	31330-095	1X	475 ml
Pen Strep	Invitrogen	15140-122	10,000 U/ml	5 ml
Glutamax	Invitrogen	35050-038	200 mM	5 ml
Minimum NEAA	Invitrogen	11140-050	100X	5 ml
B27 without RA	Invitrogen	17504-036	50X	5 ml
N2 supplement	Refer 2.1.2		50X	5 ml
Heparin	Sigma	H3149	10 mg/ml	250 µl

NBNS21S (Neuronal medium)

Reagent	Supplier	Catalog no.	Stock Conc.	Volume
Neurobasal	Invitrogen	21103	1X	47 ml
NS21*	Refer 2.1.2		50X	1 ml
Sato	Refer 2.1.2		50X	1 ml
Pen Strep	Invitrogen	15140-122	10,000 U/ml	500 µl
Glutamax	Invitrogen	35050-038	200 mM	500 µl
Sodium Pyruvate	Invitrogen	11360	100 mM	500 µl
BDNF**	Peprtech	450-02	30 µg/ml	50 µl

* NS21 was sterilized with 10 ml of neurobasal using 0.2 µm filter before adding other reagents.

** BDNF was added after warming the medium to be used.

2.1.2 Cell culture medium supplements***ITS**

Reagent	Supplier	Catalog no.	Stock Conc.	Volume
DMEM/F-12	Invitrogen	31330-095	1X	90.2 ml
Insulin	Sigma	I1882	10 mg/ml	9.99 ml
holo-Transferrin	Calbiochem	616424	20 mg/ml	2.76 ml
Sodium selenite	Sigma	S5261	1.4 mg/ml	51.5 µl

N2

Reagent	Supplier	Catalog no.	Stock Conc.	Volume
DMEM/F-12	Biochrom	FG4815	1X	79 ml
Insulin	Sigma	I1882	10 mg/ml	20 ml
holo-Transferrin	Calbiochem	616424	20 mg/ml	20 ml
Sodium selenite	Sigma	S5261	0.52 mg/ml	80 µl
BSA	Sigma	A4919	10 mg/ml	40 ml
Putrescine	Sigma	P5780	161 mg/ml	900 µl
Progesterone	Sigma	P8783	0.62 mg/ml	80 µl

NS21

NS21 was prepared as described in *Chen et al., 2008*; at a concentration of 50X.

Sato

Reagent	Supplier	Catalog no.	Stock Conc.	Volume
Neurobasal	Invitrogen	21103	1X	33.8 ml
Insulin	Sigma	I1882	10 mg/ml	10 ml
holo-Transferrin	Calbiochem	616424	20 mg/ml	10 ml
Sodium selenite	Sigma	S5261	0.4 mg/ml	400 µl
BSA	Sigma	A4919	20 mg/ml	20 ml
Putrescine	Sigma	P5780	161 mg/ml	400 µl
Progesterone	Sigma	P8783	0.62 mg/ml	400 µl

* All the medium supplements were sterilized using 0.2 µm syringe filter before aliquoting.

Additional reagents for cell culture

Reagent	Supplier	Catalog no.	Stock Conc.
Accutase	Sigma	A6964	1X
CNTF	Peptotech	450-13	10 µg/ml
DMSO	Sigma	D4540	100%
Dorsomorphine	Tocris	3093	10 mM
DPBS			1X
Gelatin	Sigma	G9391	1%
LY 294002	Tocris	1130	20mM
Matrigel	BD Bioscience	354277	9.9 mg/ml (variable)
PD 0325901	Tocris	4192	5 mM
Poly-L-Ornithine	Sigma	P3655	50 mg/ml
SB 431542	Tocris	1614	36 mM

2.1.3 Buffers and reagents for immunocytochemistry**5X PBS**

Reagent	Supplier	Catalog no.	Concentration	Amount
PBS Tablets	Invitrogen	18912-014	5X	10 tab.
ddH ₂ O				1 l

5X PBS was sterilized using 0.2 µm, bottle top filter.

1X PBS

Reagent	Supplier	Catalog no.	Concentration	Volume
PBS			5X	200 ml
ddH ₂ O				800 ml

4% Paraformaldehyde (PFA)

Reagent	Supplier	Catalog no.	Concentration	Volume
PFA	Polysciences	18814	16%	10 ml
PBS			5X	8 ml
Water	Braun	CE0123		22 ml

Permeabilization buffer

Reagent	Supplier	Catalog no.	Concentration	Volume
Glycine	Sigma	50046-1250G	1 M	600 µl
Triton-X100	Sigma	X100-100ML	10%	150 µl
PBS			1X	5.25 ml

Antibody buffer

Reagent	Supplier	Catalog no.	Concentration	Volume
BSA	Sigma	A3059	20%	600 µl
Sucrose	Merck	10176871000	50%	600 µl
PBS			1X	4.8 ml

Blocking buffer

Reagent	Supplier	Catalog no.	Concentration	Volume
Normal Goat Serum	Invitrogen	16210064	100%	1.8 ml
Antibody buffer			1X	4.2 ml

Additional reagents for immunocytochemistry

Reagent	Supplier	Catalog no.	Concentration
Fluorsave mounting medium	Calbiochem	345789	1X
Hoechst 33342	Calbiochem	382065	10 µg/ml

2.1.4 Buffers and reagents for calcein staining

Buffer for calcein loading

Reagent	Supplier	Catalog no.	Concentration
CaCl ₂	Sigma	12074	1.5 mM
Glucose	Merck	1083371000	20 mM
HEPES	Applichem	A1069.0100	15 mM
KCl	Sigma	31248	5 mM
MgCl ₂	J.T.Baker	163	0.75 mM
NaCl	Roth	9265.1	140 mM
NaH ₂ PO ₄	Sigma	S8282-500G	1.25 mM
NaOH	Sigma	22.146-5	

pH was adjusted to 7.4 using 1M NaOH and the solution was then sterilized using 0.2 µm bottle top filter. CaCl₂ and MgCl₂ were added just before use to the desired volume of buffer to obtain the working concentration.

Additional reagents for calcein staining

Reagent	Supplier	Catalog no.	Concentration
Calcein green AM	Calbiochem	206700	4 µM
DMSO	Sigma	D4540	100%

2.1.5 Buffers and reagents for FACS

Buffers for staining

Buffers used to stain for FACS were similar to those used for immunocytochemistry.

Additional reagents for FACS

Reagent	Supplier	Catalog no.	Concentration
Accutase	Sigma	A6964	1X
BSA	Sigma	A3059	1%
FACS Flow	BD Bioscience	342003	1X
Goat anti rabbit Alexa 488	Invitrogen	A11034	1:100
Rabbit anti GFAP	DAKO	Z0334	1:100
PBS Tablets	Invitrogen	18912-014	1X
Propidium iodide	Applichem	P4170	2 mg/ml

2.1.6 Buffers and reagents for quantitative PCR

Reagents for mRNA isolation and cDNA synthesis

Reagent	Supplier	Catalog no.	Concentration
Absolute Ethanol	Merck	1.00983.2511	100%
cDNA synthesis Kit	Invitrogen	4368814	
DEPC treated water	Ambion	AM9915G	
mRNA isolation kit	Roche	11828665001	
PBS	Invitrogen	18912-014	1X
RNase inhibitor	Thermo scientific	EO0381	40 U/μl

1X TAE buffer

Reagent	Supplier	Catalog no.	Concentration
EDTA	Merck	1.08418.0250	1 mM
Glacial Acetic acid	Sigma	32009.9	20 mM
NaOH	Sigma	22.146-5	
Tris (pH 7.4)	Roth	4855.2	40 mM

EDTA was dissolved using NaOH pellets. pH was set at 8.0

Reagents for agarose gel electrophoresis

Reagent	Supplier	Catalog no.	Concentration
Agarose	Sigma	A6877	2%
100 bp DNA Ladder	Invitrogen	15628-019	1 μg/μl
DNA loading dye	Invitrogen	10816-015	10X
Gel Red	Biotium	41003F	10,000X
TAE Buffer			1X

Additional reagents for quantitative PCR

Reagent	Supplier	Catalog no.	Concentration
DEPC treated water	Ambion	AM9915G	
Primers	Biolegio		100 mM
SYBR green master mix	Roche	14928100	2X

2.1.7 Buffers and reagents for protein isolation and western blot

1X Cell lysis buffer

Reagent	Supplier	Catalog no.	Stock Conc.	Volume
EDTA (pH 8.0)*	Merck	1.08418.0250	0.5 M	20 µl
EGTA (pH 8.0)*	Merck	1.08435.0025	0.1 M	100 µl
HCl	Merck	1.00316.1000	25%	
NaCl	Roth	9265.1	5 M	300 µl
NaOH	Sigma	22.146-5		
Na ₃ VO ₄ **	Sigma	450243-10G	0.5 M	20 µl
Nonidet P-40 (Igepal)	Fluka	56741	10%	200 µl
Protease inhibitor	Roche	4693159001	10X	1 ml
Tris Cl (pH 8.6)	Promega	H5123	1 M	100 µl
Triton-X-100	Sigma	X100-100ML	10%	1 ml
H ₂ O	Sigma	W3500		7.3 ml

* EDTA and EGTA were dissolved using NaOH pellets to adjust the pH to 8.0

** Na₃VO₄ was dissolved by using 1M NaOH or 25% HCl in order to set pH to 10 with repeated boiling and cooling steps until a colorless solution was obtained. pH was finally adjusted to 10.0 once more and the solution was aliquoted and frozen at -20 °C.

Reagents for protein estimation

Reagent	Supplier	Catalog no.	Concentration
BCA Kit	Thermo Scientific	23228	
BSA	Sigma	A3059	1 mg/ml
CuSO ₄	Thermo Scientific	23224	4%
H ₂ O	Sigma	W3500	

5X sample loading buffer

Reagent	Supplier	Catalog no.	Concentration	Amount
Tris Cl (pH 6.8)	Promega	H5123	1.5 M	2 ml
Bromophenol blue	Aldrich	11439-1	1%	500 µl
Glycerol	Sigma	G8773	100%	5 ml
SDS	Sigma	75746-250G		1 g
β-mercaptoethanol*	Serva	28625	100%	2.5 ml

* Loading buffer was prepared and aliquoted without adding β-mercaptoethanol. It was later added to small volumes of loading buffer (500 µl) just before use to obtain a working concentration of 5%.

4X gel resolving buffer (1.5 M Tris, pH 8.8)

36.33g of Tris Cl (Promega, H5123) was dissolved in 175 ml of ddH₂O. pH was set to 8.8 using 1M NaOH (Sigma, 22.146.5) and the volume was made up to 200ml using ddH₂O.

4X gel stacking buffer (1.5 M Tris, pH 6.8)

36.33g of Tris Cl (Promega, H5123) was dissolved in 175 ml of ddH₂O. pH was set to 6.8 using 1 M NaOH (Sigma, 22.146.5) and the volume was made up to 200ml using ddH₂O.

Additional reagents for casting the gel

Reagent	Supplier	Catalog no.	Concentration
Acrylamide/Bis Solution	Biorad	161-0154	30%
APS	Applichem	A0834.0250	10%
SDS	Sigma	75746-250G	10%
TEMED	Applichem	A1148.0100	100%

Composition for resolving gel

Reagent	8% gel (ml)	10% gel (ml)	11% gel (ml)
ddH ₂ O	2.3	2	1.83
4X Resolving buffer (pH 8.8)	1.3	1.3	1.3
30% Acrylamide/Bis Solution	1.3	1.7	1.87
10% SDS	0.05	0.05	0.05
10% APS	0.05	0.05	0.05
TEMED	0.003	0.002	0.002
Total volume	5 ml	5 ml	5 ml

Composition for stacking gel

Reagent	Volume (ml)
ddH ₂ O	3.61
4X Stacking buffer (pH 6.8)	0.42
Acrylamide/Bis Solution	0.83
SDS	0.05
APS	0.05
TEMED	0.005
Total volume	5 ml

Gel running buffer

Reagent	Supplier	Catalog no.	10X Concentration	1X Concentration
Tris base	Roth	4855.2	250 mM	25 mM
Glycine	Sigma	50046-1250G	1.92 M	190 mM
SDS	Sigma	75746-250G	1%	0.10%

pH was adjusted to 8.3 using 25% HCl (Merck, 1.00316.1000).

1X Transfer buffer

Reagent	Supplier	Catalog no.	Concentration	Amount
Tris base	Roth	4855.2	48 mM	5.814 g
Glycine	Sigma	50046-1250G	39 mM	2.928 g
SDS	Sigma	75746-250G	0.04%	0.37 g
Methanol	Merck	1.06009.2511	20%	200 ml
ddH ₂ O			80%	800 ml

Transfer buffer was cooled at 4 °C for 2 hours before use.

10X TBS

Reagent	Supplier	Catalog no.	Amount
Tris	Roth	4855.2	24.2 g
NaCl	Roth	9265.1	80 g
ddH ₂ O			1 l

pH was adjusted to 7.6 using 25% HCl (Merck, 1.00316.1000).

1X TBST

Reagent	Supplier	Catalog no.	Concentration	Volume
TBS			10X	100 ml
Tween-20	Serva	37470	10%	10 ml
ddH ₂ O				900 ml

PonceauS

Reagent	Supplier	Catalog no.	Concentration
Ponceau S	Sigma	81460-5G	0.10%
Glacial Acetic Acid	Sigma	32009.9	5%

5% Milk

5g of milk powder (Roth, T145.3) was dissolved in 100 ml of TBST.

3% BSA

3g of BSA (Sigma, A3059) was dissolved in 100 ml of TBST.

Additional reagents for western blot

Reagent	Supplier	Catalog no.
ECL	GE Healthcare	RPN 232
Nitrocellulose membrane	Biostep	01-14-101
Protein marker	Biorad	161-0374

2.1.8 Buffers and reagents for calcium imaging

Loading and imaging buffer

Reagent	Supplier	Catalog no.	Concentration
CaCl ₂	Sigma	12074	1.5 mM
Glucose	Merck	1083371000	20 mM
HEPES	Applichem	A1069.0100	15 mM
KCl	Sigma	31248	5 mM
MgCl ₂ *	J.T.Baker	163	0.75 mM
NaCl	Roth	9265.1	140 mM
NaH ₂ PO ₄	Sigma	S8282-500G	1.25 mM
NaOH	Sigma	22.146-5	

pH was adjusted to 7.4 using 1M NaOH and then the solution was sterilized using 0.2 µm bottle top filter. CaCl₂ and MgCl₂ were added just before use to the desired volume of buffer to obtain above mentioned working concentration.

Additional reagents for calcium imaging

Reagent	Supplier	Catalog no.	Concentration
ATP, pH 7.4	Sigma	A2383	100 µM
DMSO	Sigma	D4540	100%
Fluo-4 AM	Invitrogen	F-1420	5 µM
KCl	Sigma	31248	50 mM
L-Glutamate	Sigma	G6150	100 µM

2.1.9 Buffers and reagents for glutamate uptake assay

HBSS with NaCl

Reagent	Supplier	Catalog no.	Concentration
CaCl ₂	Sigma	12074	2 mM
Glucose	Merck	1083371000	23 mM
HEPES	Applichem	A1069.0100	15 mM
KCl	Sigma	31248	3 mM
MgCl ₂	J.T.Baker	163	1 mM
NaCl	Roth	9265.1	140 mM
NaOH	Sigma	22.146-5	

pH was adjusted to 7.4 using 1M NaOH and the solution was then sterilized using 0.2 µm filter.

HBSS without NaCl

Reagent	Supplier	Catalog no.	Concentration
CaCl ₂	Sigma	12074	2 mM
Glucose	Merck	1083371000	23 mM
HEPES	Applichem	A1069.0100	15 mM
KCl	Sigma	31248	143 mM
MgCl ₂	J.T.Baker	163	1 mM
NaOH	Sigma	22.146-5	

pH was adjusted to 7.4 using 1M NaOH and the solution was then sterilized using 0.2 µm filter.

Additional reagents for glutamate uptake assay

Reagent	Supplier	Catalog no.	Concentration
Glutamate determination kit	Sigma	GLN-1	
L-Glutamate	Sigma	G6150	50 µM
L-trans-2,4-PDC	Tocris	298	1 mM

2.1.10 Buffers and reagents for reactive astrocyte assay**Reagents for reactivity assay**

Reagent	Supplier	Catalog no.	Concentration
LPS	Sigma	L2880	100 ng/ml
TNFα	Peprtech	300-01A	50 ng/ml

pH 7.4 buffer

Reagent	Supplier	Catalog no.	Concentration
CaCl ₂	Sigma	12074	1.8 mM
Glucose	Merck	1083371000	5.5 mM
HEPES	Applichem	A1069.0100	10 mM
KCl	Sigma	31248	5.4 mM
MgSO ₄	Sigma	M2643	0.8 mM
NaCl	Roth	9265.1	117.9 mM
NaH ₂ PO ₄	Sigma	S8282-500G	1 mM
NaHCO ₃	Sigma	S3817	14.7 mM
NaOH	Sigma	22.146-5	
Phenol Red	Applichem	A0680.0010	10 mg/l

pH was adjusted to 7.4 using 1M NaOH. NaHCO₃ and phenol red were added after setting the pH. Solution was then sterilized using 0.2 µm filter.

pH 6.8 buffer

Reagent	Supplier	Catalog no.	Concentration
CaCl ₂	Sigma	12074	1.8 mM
Glucose	Merck	1083371000	5.5 mM
KCl	Sigma	31248	5.4 mM
MgSO ₄	Sigma	M2643	0.8 mM
NaCl	Roth	9265.1	128.9 mM
NaH ₂ PO ₄	Sigma	S8282-500G	1 mM
NaHCO ₃	Sigma	S3817	3.7 mM
NaOH	Sigma	22.146-5	
Phenol Red	Applichem	A0680.0010	10 mg/l
PIPES	Applichem	A1079.0250	10 mM

pH was adjusted to 6.8 using 1M NaOH. NaHCO₃ and phenol red were added after setting the pH. The solution was then sterilized using 0.2 µm filter.

2.2 Cell culture**2.2.1 Maintenance of human iPSCs**

Human iPSCs (8/25 iPSC line derived from human cord blood unrestricted somatic stem cells, reprogrammed with OSKM using retroviral vectors (*Zaehres et al., 2010*) and DF6-9-9T.B P23 iPSC line, Lot MCB-01, WiCell, Madison, WI, USA) were maintained under feeder free conditions, according to a modified protocol, described by *Chen et al., 2011*. They were cultured at 37 °C, 5% CO₂, on matrigel (0.5 mg/ml) coated dish in E8 medium with daily medium changes. Sporadically differentiated cells were removed using a flamed glass pasteur pipette under the microscope. Cells were split on a weekly basis once they attained ~70% confluency. For passaging, cells were once washed and then incubated with DPBS-/- for 10 min at room temperature. Treatment with DPBS-/- was stopped by adding 1 ml of spent E8 medium. Cells were then removed from the surface using a cell scraper, collected in a 15 ml tube and pelleted at 300 rpm for 1 min. The cells were then diluted in fresh E8 medium and seeded at a predefined density (1:12).

The iPSCs stocks were maintained by cryopreserving in 100% CryoStor® CS10 (STEM CELL Technologies, SARL, Cologne, Germany) and stored in liquid nitrogen (-196 °C). In order to revive the cells, the cryovials were thawed in a water bath at 37 °C for 1 min. The cells were then diluted with 10 ml of E8 medium and pelleted down at 1100 rpm for 4 min. iPSCs were used for a maximum of 60 passages.

2.2.2 Neural induction of human iPSCs

Human iPSCs were pre-treated with N2B27 medium for 3 days at 37 °C, 5% CO₂. It was followed by induction of neural lineage by using the dual SMAD inhibition approach described by *Chambers et al., 2009*. Tumor growth factor β (TGF β) and bone morphogenetic protein (BMP) signaling cascades were inhibited using two small molecules: SB431542 (6 μ M) and Dorsomorphin (10 μ M) respectively for 6 days in N2B27 medium with one time medium change and small molecule replenishment in between (*Morizane et al., 2011*). Afterwards, the small molecule treated cells were detached by washing and incubating in DPBS-/- for 5 min at room temperature. DPBS-/- treatment was discontinued by adding 1 ml of spent N2B27 medium and then the cells were scraped off and pelleted at 400 rpm for 1 min. The pelleted cell aggregates were then seeded in a T25 flask containing pre-warmed N2B27 medium and incubated at 37 °C, 5% CO₂ for next two weeks in order to generate embryoid bodies (EBs). Medium changes were done on 1, 2, 3, 5, 7, and 14 d of EB formation.

The big round EBs thus formed were seeded on a matrigel (0.167 mg/ml) coated 100 mm petridish in N2B27 medium and incubated at 37 °C, 5% CO₂ for another 2-4 weeks with weekly medium changes (*Figure 7*).

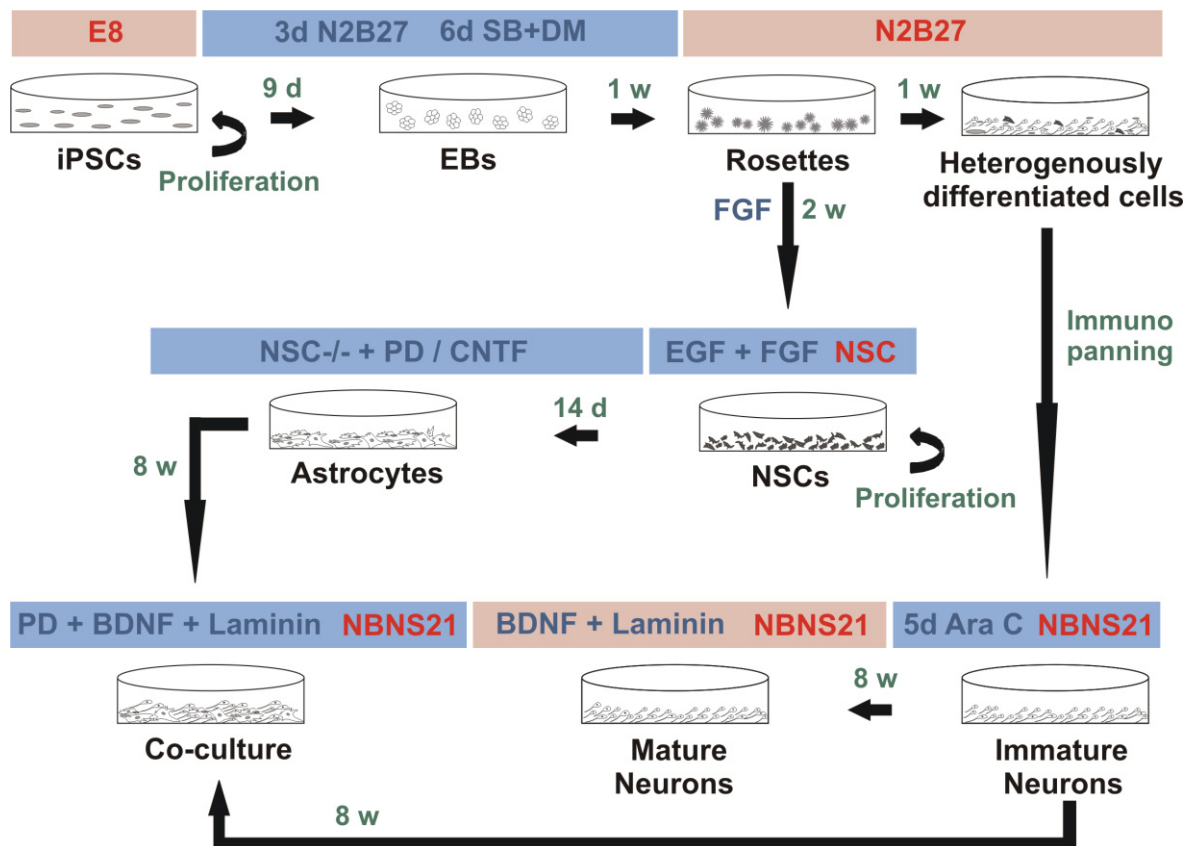


Figure 7: Schematic representation of neural differentiation. (Legend on next page)

Red color represents the medium used. Blue color symbolizes the additional factors like growth factor or small molecule added. SB = SB431542, DM = Dorsomorphin, d = days, w = weeks

2.2.3 Generating NSCs from iPSCs

1 w after EB plating, rosette structures representing the neuroepithelial stage were picked under the microscope and cultured in suspension for 2 w in the presence of FGF (5 ng/ml). To remove non neural cells with a tendency to attach to culture dish plastic, newly formed neurospheres were mechanically dissociated twice per week for 2 weeks using a P200 pipette tip and replated in a fresh culture dish (modified protocol from *Hu et al., 2009*). Neurospheres were then plated on laminin or matrigel (0.167 mg/ml) coated dish to allow the formation of a monolayer culture. Initial cultures were done in the presence of FGF alone (10 ng/ml) in order to maintain a neurogenic NSC fate and after 4-5 passages they were cultured in EGF (20 ng/ml) and FGF (20 ng/ml). The cells were cryopreserved at neurosphere stage as well as at passages 1 and 2 to maintain the early neural stem cell stock.

NSCs were cultured in NSC medium on matrigel or gelatin (0.1%). Medium was changed every 3rd day and cells were passaged once in a week using accutase upon attainment of ~80% confluency. The cells were regularly cryo-preserved with increasing passages in 10% DMSO + NSC medium to maintain the stock. The cells were revived by thawing the cryovial at 37 °C in a waterbath for 1 min, followed by neutralization in 10 ml of NSC medium. The cells were then centrifuged at 1100 rpm for 5 min and resuspended in NSC medium followed by plating in a matrigel or gelatin coated dish containing pre-warmed NSC medium.

2.2.4 Differentiation of NSCs towards astrocytes

Astrocyte differentiation was carried out by following different approaches as mentioned below.

NSC-/-: NSCs from passage 15-20 or 40-45 were cultured on a matrigel (0.167 mg/ml) or gelatin (0.1%) coated dish in growth factor free medium (NSC-/-) for a period of 14 days at 37 °C, 5% CO₂. Half medium change was done every 3rd day.

CNTF: NSCs from passage 15-20 or 40-45 were cultured on a matrigel (0.167 mg/ml) or gelatin (0.1%) coated dish in growth factor free NSC medium, supplemented with CNTF (30 ng/ml) for a period of 14 days at 37 °C, 5% CO₂. CNTF was replenished every 3rd day by performing half medium change.

PD: NSCs from passage 15-20 or 40-45 were cultured on a matrigel (0.167 mg/ml) or gelatin (0.1%) coated dish in growth factor free NSC medium, supplemented with PD (0.25 μM) for a

period of 14 days at 37 °C, 5% CO₂. Half medium change was done at 9 and 12 d with PD replenishment. The concentration of PD was standardized by exposing NSCs to an increasing dose of PD (from 0.25 µM to 1 µM) followed by investigating the expression of astrocyte specific genes as illustrated in *Figure 8*. Concentration of 0.25 µM was used as it was found to be sufficient to induce upregulation of astrocytic genes.

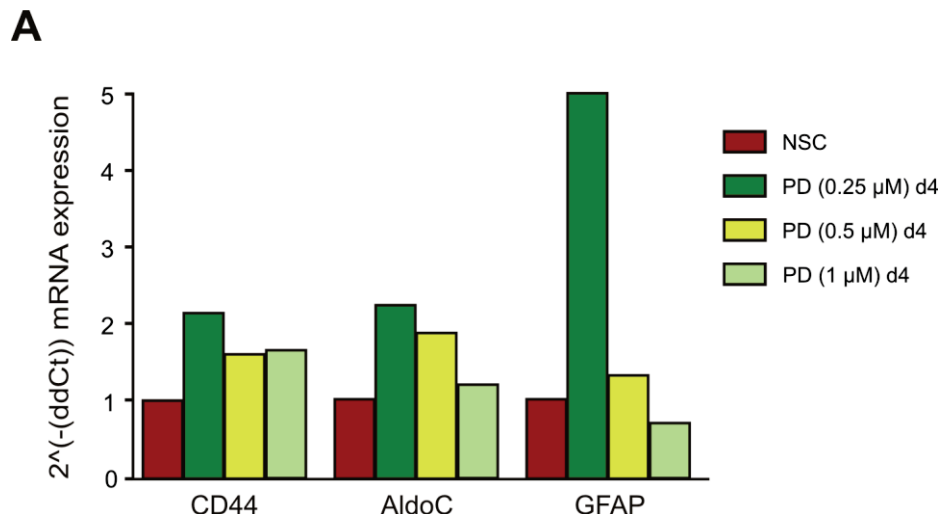


Figure 8: Standardization of optimal concentration of PD.

A) mRNA expression pattern for CD44, AldoC and GFAP in NSC control condition and cells exposed to different dose of PD for 4 d.

FGF or EGF induced astrocytic differentiation: NSCs from passage 5-7 were cultured on a matrigel (0.167 mg/ml) or gelatin (0.1%) coated dish in NSC medium supplemented with a high concentration of either FGF or EGF (100 ng/ml) with an optimal concentration of the other growth factor (20 ng/ml) for 7 d at 37 °C, 5% CO₂. It was followed by treatment of NSCs with NSC-/-, CNTF or PD for 14 d.

2.3 Immunocytochemistry

Cells were washed with 1X PBS and then fixed with 4% PFA for 13 min at room temperature. Then PFA was removed and cells were washed three times with 1X PBS. Excess formaldehyde was quenched and cells were permeabilized for 10 min in permeabilization buffer with mild shaking (permeabilization step was omitted in case of staining for membrane proteins like EAAT1). It was followed by reducing non specific binding of antibody by incubating the cells with blocking buffer for 1 hr at room temperature. Cells were then incubated with specific dilution of primary antibodies (ref. Appendix 6.4) overnight at 4 °C (incubation for ALDH1L1 was done for 48 h). Next, cells were washed 3 times with 1X PBS followed by incubation with secondary antibody (ref. Appendix 6.5) for 1 h at room temperature. After this, cells were labeled

with nuclei dye: Hoechst 33342 (1:1000) for 10 min and then washed 3 times with 1X PBS and 1 time with ddH₂O to remove any leftover salts. Fluorescence was preserved by mounting the coverslips using fluorsave mounting medium. Coverslips were stored at 4 °C in dark until imaged.

Imaging was done using 20X Objective (Zeiss-LD-A-Plan-0.30/Ph1/∞/0.1) of an epifluorescence microscope (Zeiss Axiovert 200M). Filter sets used are mentioned in Appendix 6.5. At least 4-5 different regions were imaged per coverslip. The exposure time was maintained equally for all imaging procedure.

For counting the number of cells, threshold was set at least 3 standard deviations (S.D) higher than background intensity. For counting high GFAP expressing cells, a minimum threshold of 17 S.D and maximum of 30 S.D was applied in Metavue software (MDS Analytical technologies). Counting was done using cell counter macro in Image J-1.46r (NIH, U.S.A).

2.4 Calcein staining

NSCs and 14 d, PD derived astrocytes were washed once with 1 ml of HEPES buffer and then incubated with Calcein Green AM in HEPES buffer for 30 min at 37 °C, 5% CO₂. Cells were then washed three times with HEPES buffer and imaged using 20X Objective (Zeiss-LD A Plan-0.30 Ph1/∞/0.1) of an epifluorescence microscope (Zeiss Axiovert 200M). Filter sets used are mentioned in Appendix 6.5. At least 4-5 different regions were imaged for each condition and same exposure time was maintained within the groups.

2.5 FACS

Cells were detached from the surface by incubating with accutase for 5 min at 37 °C, 5% CO₂. After neutralizing with spent medium, cells were pelleted at 1100 rpm for 5 min. The pellet was washed once with 1% BSA and again harvested by centrifugation at 1100 rpm for 5 min. It was followed by fixation with 4% PFA for 20 min. After this, all the steps were performed at 4 °C. Following fixation, cells were washed twice with 1% BSA and harvested each time by pelleting at 2000 rpm for 3 min. Cells were permeabilized and blocked using the same buffers and incubation time as used for these steps in immunostaining. After blocking, cells were incubated with primary antibody at 1:100 dilution for 2 h at 4 °C and then washed two times using 1% BSA with intermittent pelleting at 2000 rpm for 3 min. Subsequently, the cells were incubated with anti rabbit Alexafluor 488 at a dilution of 1:100 for 1 h at 4 °C and then washed twice with 1% BSA. It was followed by nuclei staining using Propidium iodide (PI) for 5 min and again washing

the cells once with 1% BSA. After harvesting the cells by centrifugation at 2000 rpm for 3 min, all the samples were resuspended in 500 µl of 1% BSA and incubated on ice until measured for fluorescence intensity. To determine the auto fluorescence of the cell, unstained control was kept for each cell type under study. In addition, secondary antibody alone was also used to take any non specific staining into account. FITC based measurement of cells was performed using BD FACS Canto II.

2.6 Quantitative PCR

2.6.1 mRNA isolation

mRNA for qPCR was isolated using High pure mRNA isolation kit (Roche) as per manufacturer's protocol. Briefly, cells were washed once with PBS, followed by lysis with 400 µl of lysis buffer and 200 µl of 1X PBS. A cell scraper was used to remove the cells from the surface and lysate was then passed through the column provided, at 8000 rcf for 30 s. In order to avoid contamination from DNA, column containing the bound nucleic acid was incubated with DNase for 15 min. The column was washed once with 500 µl of wash buffer I and II each at 8000 rcf for 30 s. Additional wash was given with 200 µl of wash buffer II at 12,000 rcf for 3 min to remove any remaining solution. mRNA was eluted from the column with 35 µl of DEPC treated water by spinning the column at 8000 rcf for 1 min. All the steps were performed at room temperature. Isolated mRNA was immediately kept at 4 °C and mRNA concentration was determined using Nanodrop 2000c (Thermo scientific, version: 1.4.1). For long term use, mRNA was stored at -80 °C.

2.6.2 cDNA synthesis

cDNA was synthesized using 500 ng of freshly isolated mRNA using High capacity cDNA synthesis kit (ABI). Reaction mixture and PCR conditions used are mentioned in Appendix 6.7. After synthesis, cDNA was stored at -20 °C until further use. As an equal amount of RNA from different treatments was used for cDNA synthesis, and because cDNA for the samples under comparison was synthesized together, therefore, cDNA was not further quantified. For qPCR, cDNA was diluted using DEPC treated water to obtain a final concentration of 2.5 ng/µl.

2.6.3 qPCR

The primers for qPCR were designed using NCBI Primer-Blast considering parameters like 80-250 bp amplicon length, 59-62 °C melting temperature and 50-60% GC content. For genes with multiple splice variants, primers were designed within the coding region common to all the

isoforms. The resulting primers were analyzed for their ability to form hairpins, self dimer and heterodimers using the Oligoanalyzer 3.1 version of integrated DNA technologies (IDT). The primer pairs exhibiting the potential to form dimers with delta G above -8.0 kcal/mole were not considered suitable. Before employing the primers for qPCR, they were optimized for the working annealing temperature and confirmed for the expected product by running a 2% agarose gel. In addition, amplification efficiency of each primer was tested by running a PCR with serial dilution of the cDNA (ref. Appendix 6.9.1). A list of primers used for this study can be found in Appendix 6.6. Housekeeping genes which were not affected by differentiation from NSCs to astrocytes were initially selected by analyzing four different housekeeping genes β -Actin, GAPDH, EEF1A1 and RPL13A for both NSCs and astrocytes. Differences in C_T values between NSCs and astrocytes was calculated (*Figure 9*). β -Actin was found to have the maximum difference between NSCs and astrocytes and therefore never used for either western or PCR as a housekeeping control. Other genes varied by a factor of less than 0.1 dC_T and were therefore considered as suitable housekeeping genes. The conditions used for PCR cycle and dissociation curve are mentioned in Appendix 6.8. Real time PCR was performed using ABI 7500 Real time PCR system (Sequence Detection Software-1.3). Comparative analysis was done using the $2^{-(\Delta\Delta C_T)}$ method (*Livak et al., 2001*) as described in Appendix 6.9.2.

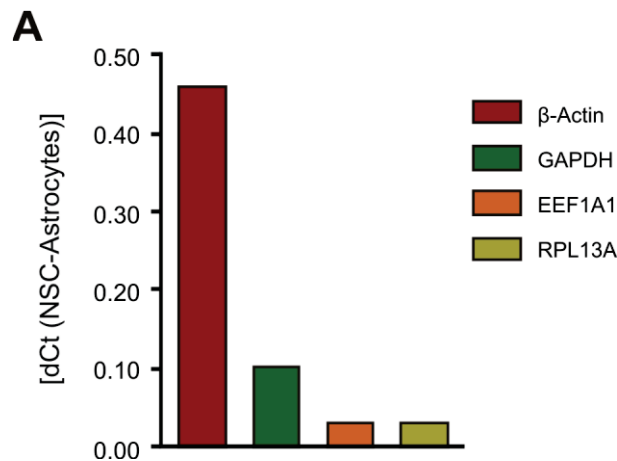


Figure 9: Standardization of optimal housekeeping gene for quantitative PCR.

A) Difference in the C_T values of β -Actin, GAPDH, EEF1A1 and RPL13A between NSCs and astrocytes to determine an appropriate housekeeping gene.

2.7 Western blot

2.7.1 Protein isolation

Culture dish with cells was kept on ice and cells were washed once with 1X PBS, followed by addition of 100 μ l of lysis buffer per 60 mm dish. Lysis buffer was spread uniformly to cover the

entire surface of the dish and left for 15 min. Cells were then gently scraped off and collected in a 1.5 ml microfuge tube. Lysate was incubated on ice for 15 min followed by centrifugation at 12,000 rcf, 4 °C for 20 min to pellet down the cell debris. Further on, supernatant was collected and used for protein estimation. Isolated protein samples were stored at -80 °C until further use.

2.7.2 Protein estimation

The concentration of protein in the samples was estimated using the BCA method (*Smith et al., 1985*) as it offers sensitivity for 0.2-1.0 mg/ml of protein and owing to its compatibility to a wide range of detergents present in the lysis buffer and easy detection in a colorimetric way. The reagent consists of *a*) a solution containing bicinchoninic acid, sodium carbonate, sodium tartrate and sodium bicarbonate in 0.1 N NaOH, pH 11.25 *b*) 4% Copper sulphate. The assay relies on the formation of a Cu^{2+} -protein complex under alkaline conditions, followed by reduction of the Cu^{2+} to Cu^{1+} . The amount of reduction is proportional to the amount of protein present. BCA forms a purple-blue complex with Cu^{1+} in alkaline environment, thus providing a basis to monitor the reduction of alkaline Cu^{2+} by proteins.

BSA was used as a standard to calculate the concentration of unknown protein samples. A serial dilution of BSA was made using ddH₂O (ref. Appendix 6.10). 23 µl of water and 2 µl of protein sample was used, giving a dilution factor of 12.5. The above mentioned reagent *a* and *b* were mixed in the ratio 50:1 and 200 µl of this mixture was added to each well being estimated. The plate was then covered and incubated at 37 °C for 30 min. The purple-blue complex formed was read spectrophotometrically at 560 nm using Infinite M200Pro plate reader (Tecan). The concentration of protein samples was determined by applying the formulae mentioned in Appendix 6.10.

2.7.3 Blotting and developing

40 µg of protein sample was mixed with 5X sample loading buffer and heated at 65 °C for 10 min to denature and linearize the proteins. SDS-PAGE was performed for size based separation of the proteins under study. The percentage of the resolving gel varied depending on the size of the protein of interest. The gel was run at 30 mA until the samples entered the resolving gel and then 40 mA was applied until the dye front reached the bottom of the gel. The proteins were then transferred on a 0.2 µm nitrocellulose membrane at 200 mA for 1:15 h. Care was taken to maintain constant cooling and stirring during both, the gel running and transfer time. Transfer was confirmed by performing Ponceau-S staining on the membrane which was then washed off using 1X TBST. Non specific binding was reduced by blocking in 5% milk for all the proteins

except phospho proteins which were blocked using 3% BSA. Primary antibodies were diluted in 5% milk or 3% BSA at a desired concentration (ref. Appendix 4) and incubated over night at 4 °C with constant shaking (Acsbg1, ALDH1L1 were incubated for 48 h). Prior to incubation with secondary antibody, the membrane was washed thrice with 1X TBST. HRP conjugated secondary antibodies were used at a pre-defined concentration (ref. Appendix 5) and the membrane was incubated for 1 h at room temperature with constant shaking. Then the membrane was washed three times with 1X TBST and once with ddH₂O. The membrane was either directly proceeded for detection or stored at 4 °C until detection.

The membrane was then exposed to enhanced luminal based detection reagents (ECL) mixed in the ratio 1:1 just prior to detection. Resulting chemiluminescence was detected using Fusion FX system (Peflab, VWR). The exposure time varied from seconds to min depending on the antibody. Several images were acquired with different exposure time. Any case of saturation was detected using the software parameters and was excluded from analysis. Analysis was done using Gel macro in Image J-1.46r (NIH, U.S.A). All the bands were subjected to background subtraction and then normalized to their corresponding house keeping control (GAPDH). Further, fold changes were calculated with respect to the control mentioned in individual graphs.

2.8 Calcium imaging

Calcium imaging was performed using Fluo-4 acetoxymethyl ester dye as it is easily taken up by the cells in the presence of Ca²⁺ and Mg²⁺ and exhibits high fluorescence with a K_d of 335 nM. Once inside the cell, the ester is hydrolysed by endogenous esterases, thereby making it fluorescent and sensitive to Ca²⁺ (Figure 10).

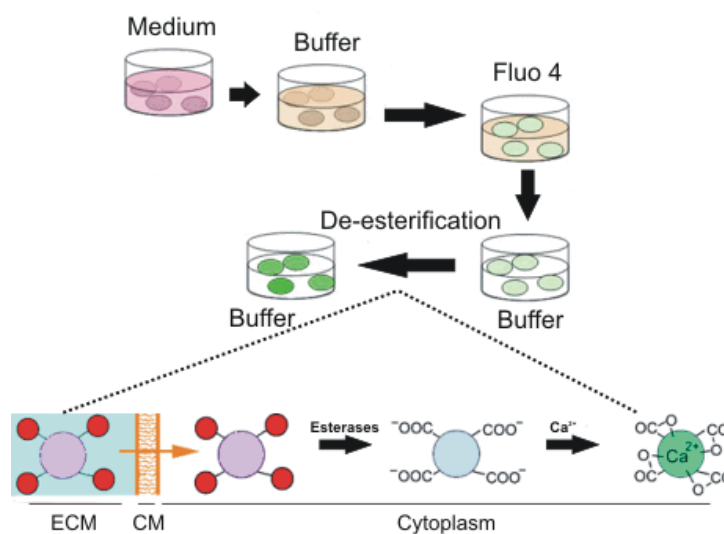


Figure 10: Dye loading and de-esterification. Legend on next page

Adapted from <http://www.embl.de/eamnet/html/calcium/dyes/fluorescentdyes3.htm>. Fluo-4 AM is taken up by the cells and hydrolysed by endogenous esterases thereby rendering the dye fluorescent and sensitive to Ca^{2+} . ECM= Extracellular medium, CM= Cell membrane

For imaging of astrocytes, stimulating agents: ATP (100 μM), L-Glutamate (100 μM) and KCl (50 mM) were applied after 2 min of baseline imaging. For analysis of calcium activity, after background subtraction, maximum projection of all the images was obtained using Image J-1.46r (NIH, U.S.A) and region of interest (ROIs) were made around the whole cell. Fluorescence intensity was measured for each image over a time of 10 min. For spontaneous activity and responses to chemical stimuli, cells were considered to be active if any increase above the baseline signal was observed over the whole duration of imaging. For measuring response to glutamate, the responses observed within the first 100 s of substance application were taken into account for counting the number of responsive cells. A typical long lasting, somatic response was observed in most cases (*Figure 11*).

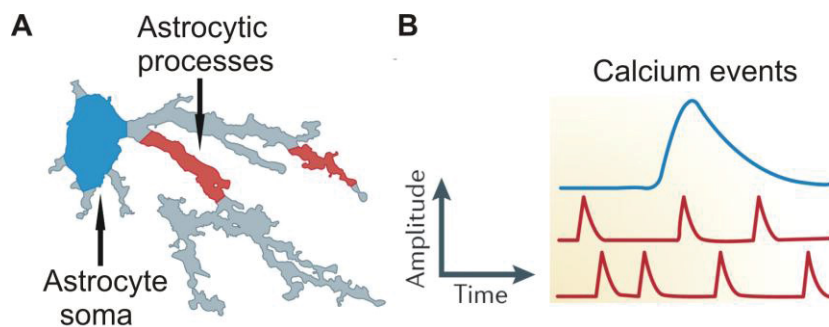


Figure 11: Diversity of Ca^{2+} signaling in astrocytes.

Adapted from *Volterra et al., 2014*. **A)** A representation of astrocytic cell body and processes based on hippocampal astrocytes *in situ*. **B)** The Ca^{2+} events typically observed in the soma (blue) are less frequent but longer and larger in amplitude compared to those occurring in the processes (red).

2.9 Glutamate uptake assay

Cells differentiated for 14 d in PD were equilibrated with HBSS for 10 min at 37 °C, 5% CO_2 . Then the cells were exposed to *a)* HBSS + L-Glutamate (50 μM), *b)* HBSS + L-Glutamate (50 μM) + L-*trans*-Pyrrolidine-2,4-dicarboxylic acid (PDC, 1 mM), *c)* HBSS (without Na^+) + L-Glutamate (50 μM) for 2 h at 37 °C, 5% CO_2 . Subsequently, the extracellular solution was collected and immediately pelleted at 1100 rpm, 4°C for 4 min to remove the cell debris and prevent any degradation of left over L-Glutamate in the solution. At the same time, cells were washed with 1X PBS and stored at -80 °C until further proceeded for protein isolation (*Figure 12*). After centrifugation, the extracellular solution was kept on ice.

The assay was performed using Glutamate determination kit (Sigma). Basically, the assay relies on the conversion of NAD^+ to NADH which is then measured spectrophotometrically and is proportional to the amount of glutamate that is oxidized to α -Ketoglutarate and ammonium ions in the presence of Glutamic dehydrogenase (GLDH) enzyme (Lund P, 1986). To perform the assay, the required amount of ddH₂O was added to a 96 well plate for standards (ref. Appendix 6.11). It was followed by addition of 100 μl of Tris-EDTA Hydrazine buffer to each well for standard and samples. Then 10 μl of NAD and 1 μl of ATP were added in every well. Next, the required amount of L-Glutamate (1 mM) was added to the wells for a standard curve (ref. Appendix 6.11) and 89 μl of sample was added to their respective wells. Immediately, the background signal was measured at 340 nm using Infinite M200Pro plate reader (Tecan). Without any delay, 2 μl of L-GLDH was added to each well and mixed properly. The plate was covered and incubated at 22 °C for 40 min and the change in signal was measured again at 340 nm. Measurements were repeated until a constant reading was obtained. All the samples were assayed in duplicates in order to account for pipetting variation.

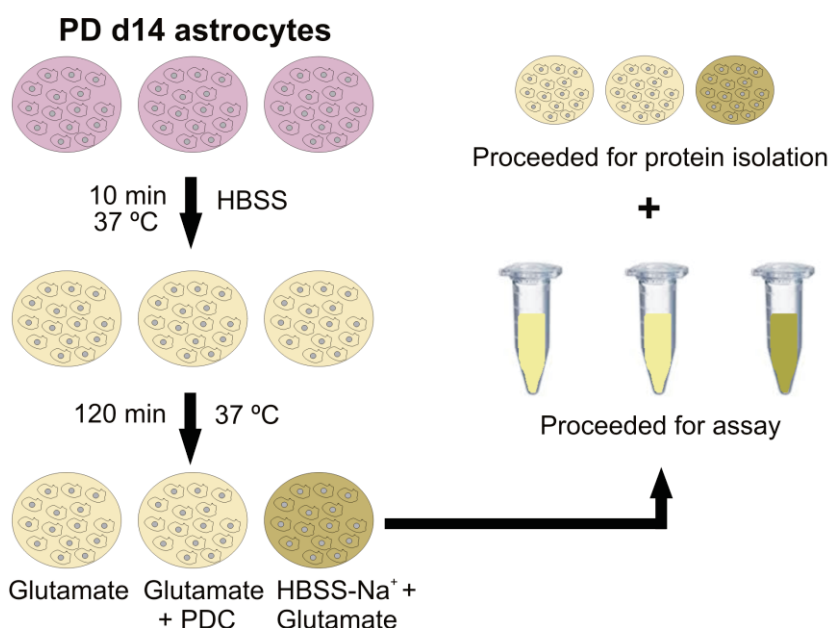


Figure 12: Experimental set up for glutamate uptake assay.

Pink color represents the culture medium, yellow color represents the HBSS buffer and green color represents HBSS without Na^+ .

Meanwhile, the cells were lysed to isolate protein and total amount of protein per sample was quantified as described before (2.7.2). $\mu\text{M}/\mu\text{g}$ of L-Glutamate uptake was calculated as described in Appendix 6.11.

2.10 Reactive astrocyte assay

NSCs and 14 d, PD derived low GFAP astrocytes were incubated with or without pro-inflammatory molecule: TNF α (50 ng/ml) and bacterial endotoxin lipopolysaccharide (LPS, 100 ng/ml) for 24 hrs at 37 °C, 5% CO₂. The samples were then processed for mRNA isolation (as described in 2.6.1) followed by cDNA synthesis and finally performing a quantitative PCR assay for reactive astrocyte markers (Serpina3, Lcn2 and GFAP). Calculations for qPCR were done following $2^{-(\Delta\Delta C_T)}$ method as described in Appendix 6.9.2.

In another setting of reactivity assay, 14 d PD treated cells were incubated in HEPES or PIPES based buffer with a) pH 7.4 and b) pH 6.8 buffer for 10 h at 37 °C, 5% CO₂. The cells were then fixed and stained for GFAP as the reactivity marker (*Giffard et al., 2000*).

2.11 Statistics

Data analysis was done in Microsoft excel and statistical tests were performed in GraphPad Prism 6. In case of two conditions, unpaired t-test was applied. Experiments with three or more conditions were tested with one way ANOVA and to determine the significance between groups, Tukey's post hoc analysis was done.

p-values less than 0.05 were considered statistically significant and represented with a single asterisk in graphs. Double and triple asterisks denote p-value smaller than 0.01 and 0.001 respectively. The plotted bars correspond to arithmetic means of the data sets (n; generated with a different passage of NSCs). Error bars signify standard errors of the mean (s.e.m) unless otherwise stated. Statistical n is mentioned along with every figure legend in the results section. Graphs were created in GraphPad Prism 6. For FACS experiments, graphs were plotted using FCS Express 5 Plus Research Edition. Figures were created using Corel Draw 12.

3. Results

3.1 Characterization of iPSCs derived human neural stem cells

3.1.1 Determination of the gliogenic potential of different NSC lines

The conditions for generating and culturing neural stem cells (NSCs) described in various publications show a high degree of variability concerning parameters like growth factor concentration and combination, splitting frequency and ratio or the type of surface substrate. All of these factors influence the developmental stage of *in vitro* maintained NSCs, making it difficult to compare the starting population used for the generation of astrocytes in the different publications. Early neural precursor cells are neurogenic and lack the potential to give rise to glial cells both *in vivo* and *in vitro*. During development, upon completion of neurogenesis, there occurs a gliogenic switch in NSCs, thereby turning them into glial restricted precursors (GRPs), which are characterized by an increase in gliogenic markers. Several markers have been previously reported to be present in GRPs for e.g. A2B5, BLBP and FGFR3 (Owada *et al.*, 1996; Pringle *et al.*, 2003). To more closely describe the astrocyte restricted precursors, markers like Sox 9, NF1 transcription factors (Deneen *et al.*, 2006; Kang *et al.*, 2012) and CD44 (Liu *et al.*, 2004) have been widely accepted.

In order to determine the gliogenic potential of iPSC derived NSCs, which were initially generated under different culture conditions (FGF alone or EGF and FGF at different concentrations (10 ng/ml or 20 ng/ml) for 2-3 passages, plated on gelatin or matrigel), the present NSC lines were characterized by performing quantitative PCR and immunocytochemical staining for well established NSCs and astrocyte restricted precursor (ARP) markers. A differential mRNA expression of the ARP markers was noted among different NSC lines, although the levels of the pan NSC markers- Nestin and Sox2 were almost consistent (Figure 13A). In addition, findings from the immunocytochemical studies of the GRPs marker- A2B5 and the ARP marker- CD44 in different NSC lines were found to be consistent with the mRNA levels (Figure 13B). The results from both mRNA and protein studies showed the presence of different stages of NSCs probably due to initial variations in our culture conditions. The lines with almost no expression of CD44 were considered to be more neurogenic (NSC E and NSC F). However, NSC line K proved to be more gliogenic at this stage owing to high expression of CD44 and A2B5.

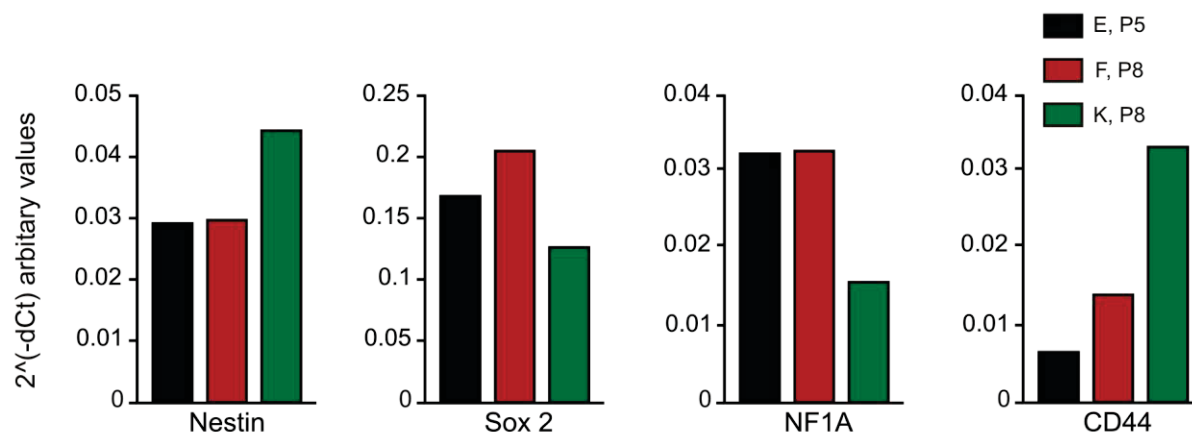
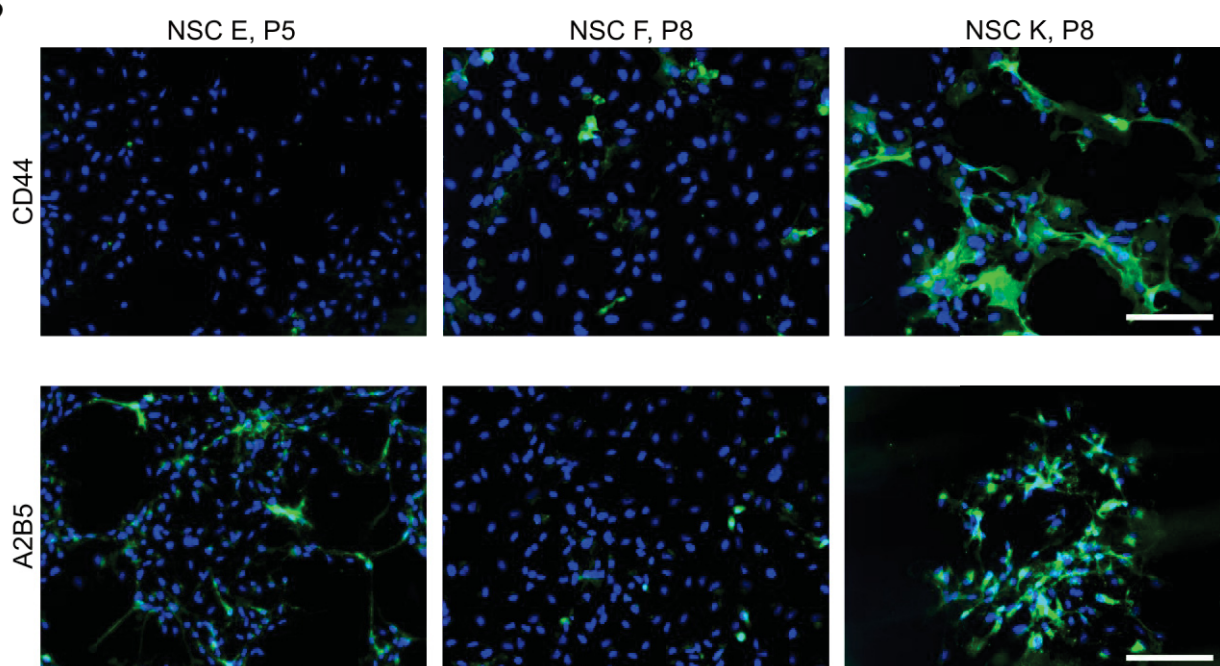
A**B**

Figure 13: Differential expression of neural stem cell and glial progenitor markers in human iPSCs derived neural stem cells.

A) Quantitative PCR to evaluate the mRNA expression level of neural stem cell markers: Nestin, Sox 2 and glial lineage markers: NF1A, CD44 in NSC lines E, F and K. **B)** Immunostaining for astrocyte and glial restricted markers: CD44 and A2B5 in above mentioned NSC lines. Blue color represents Hoechst staining to label the nuclei. Scale bar = 100 μm. (n=1).

Further characterization was done with other well established ARP markers. One neurogenic line (NSC B) and two gliogenic lines (NSC O and K) were compared for the expression of ARP markers by performing quantitative PCR for CD44, EGFR (*Lillien et al., 2000*), STAT3 (*Hong et al., 2014*), NF1B, NF1C and NF1X. A remarkable increase was observed for the first four of these ARP markers in gliogenic lines as compared to the more neurogenic line NSC B. NF1C and NF1X were almost consistent in all the lines, with a slight increase in NF1X in line O (*Figure*

144). Taking these observations into account, NSC line O and K expressing ARP specific markers were further used as NSC starting population for astrocyte differentiation in this study.

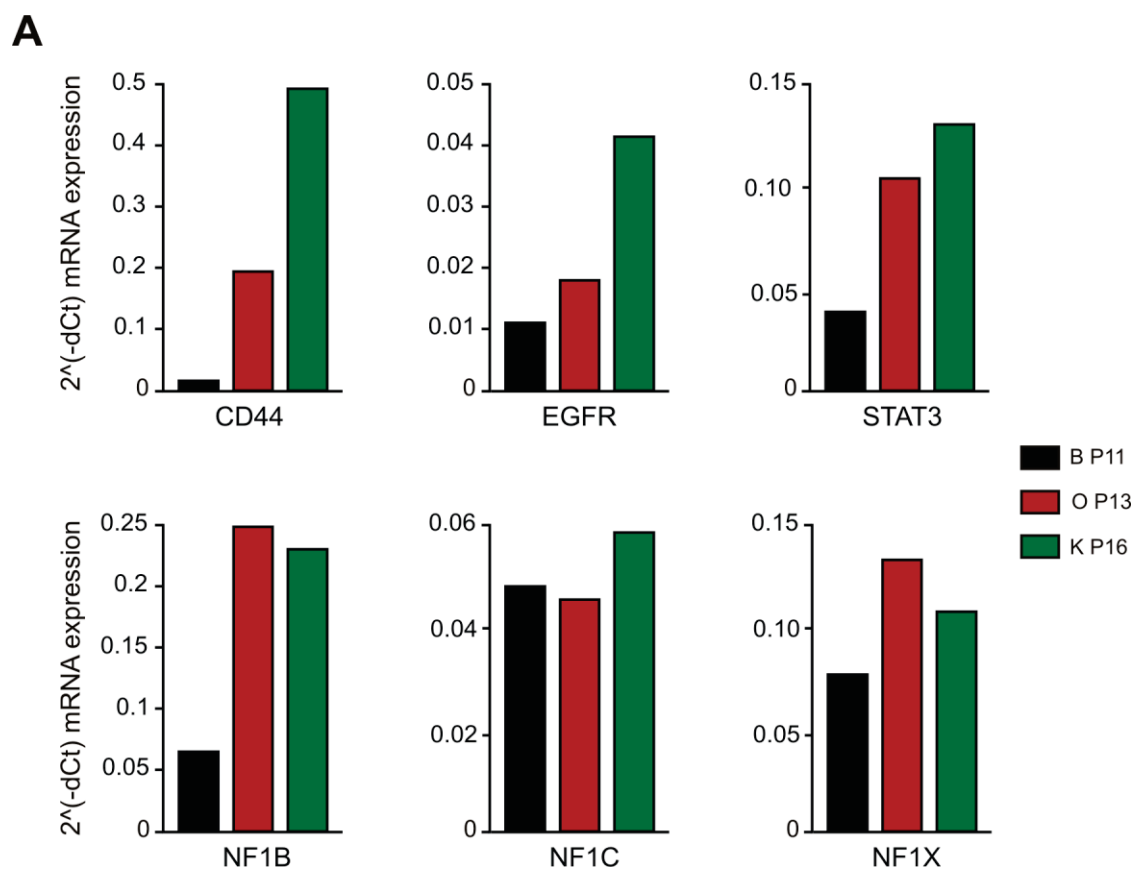


Figure 14: Determination of neurogenic and gliogenic lines based on differential expression of glial progenitor markers.

A) mRNA expression level of various glial lineage markers: CD44, EGFR, STAT3, NF1B, NF1C and NF1X in NSC lines B, K and O. n=1.

3.1.2 Validation of glial restriction in NSCs over prolonged culture time

As stated previously, the gliogenic potential of NSCs has been reported to increase over time both *in vivo* and *in vitro*. To validate these findings, new NSC lines (NSC1a, 1b and 2) were generated under defined conditions (laminin coating and 10 ng/ml FGF containing medium until P5, followed by matrigel coating and 20 ng/ml EGF and FGF containing medium). Immunocytochemistry and quantitative PCR were performed for increasing passages of NSCs to study the expression pattern of gliogenic markers. Nestin was used to confirm that the cells retained NSCs state upon increased passaging. The expression of Nestin at NSCs Passage 7 and 12 was found to be consistent at protein level, but with a slight decrease at mRNA level. A temporal increase in the expression of protein level of A2B5 and CD44 was observed with passaging of NSCs upon culture in EGF and FGF (20 ng/ml each) containing medium. Also, CD44 was found to be upregulated by 2.5 fold at mRNA level between P7 and P12 (Figure 15A,

B). As seen by ICC and PCR, it was only after at least 12 passages (approximately 2-3 months) in culture that almost 90% of the NSCs were positive for both A2B5 and CD44. In addition, more than 2 fold increase in mRNA expression of NF family of transcription factors- NF1B, NF1C and NF1X was observed upon increased passaging (*Figure 15C*).

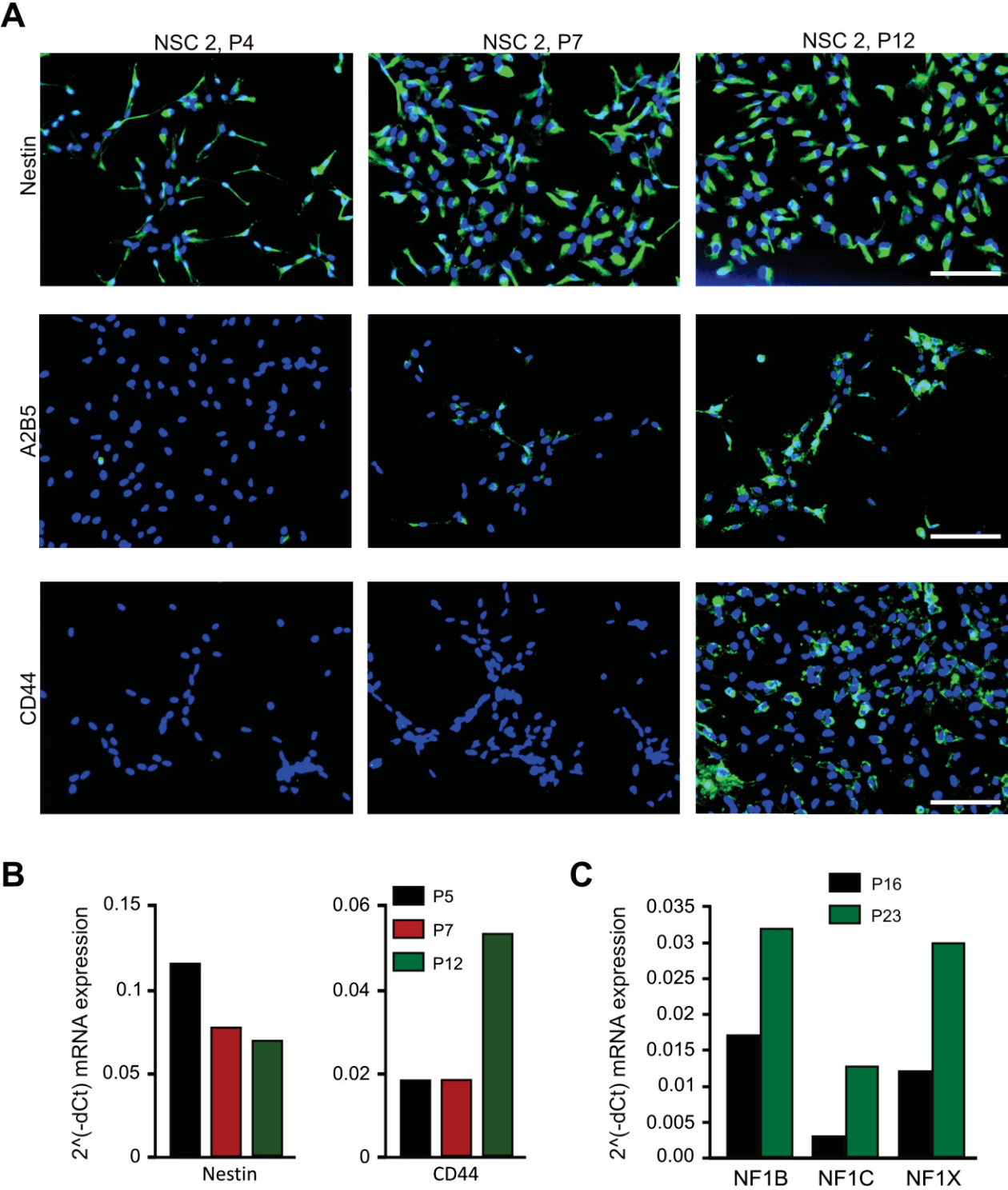


Figure 15: Temporal increase in glial restricted progenitor markers in neural stem cells over passaging in culture. Legend on next page

A) Immunostaining for neural stem cell marker- Nestin, glial restricted progenitor marker- A2B5 and astrocyte restricted precursor marker- CD44 with increase in NSC passage (P4, 7 and 12). Blue color represents Hoechst staining to label the nuclei. Scale bar = 100 μ m. **B)** Quantitative PCR for Nestin and CD44 at passage: 5, 7 and 12 of neural stem cells. **C)** mRNA expression levels of NF1B, NF1C and NF1X at NSC passage 16 and 23. (n=1).

This finding supports the role of these transcription factors at late stages of astrocyte differentiation as their expression in NSCs continue to increase even after 4-5 months in culture. Taken together, these results identify P12 as a critical passage for the generation of ARP, which could be employed for differentiation towards astrocytes.

3.1.3 Validation of culture conditions supporting glial restriction

In vivo, the gliogenic switch is regulated by changes in gene expression and epigenetic changes, mediated by the growth factors secreted by NSCs themselves (Song and Ghosh, 2004). To address the importance of FGF or EGF in turning on this switch, early passages (P5-10) of NSCs (NSC1a, 1b and 2) were cultured in medium containing either FGF alone or EGF plus FGF at low concentrations (10 ng/ml each). The expression level of astrocyte lineage markers- NF1A and CD44 was investigated under these culture conditions. An increase in the expression of NF1A as well as CD44 was observed with prolonged passaging in FGF alone condition, confirming the effect of culture duration observed before. However, the presence of EGF significantly augmented the expression of CD44 and NF1A at early passages (Figure 16A). These results were further confirmed by performing quantitative PCR and comparing the mRNA expression of different gliogenic genes. A significant 2.4 (\pm 0.392) fold rise in CD44 and 1.7(\pm 0.111) fold increase in NF1A were detected with EGF + FGF condition as compared to FGF alone. Also, other NF1 transcription factors (NF1B, NF1C and NF1X) were found to be upregulated in the presence of EGF at an early passage (Figure 16B). This suggests the need for further exploration of a less studied role of EGF in aiding gliogenesis.

Overall, these data provided the information for selecting gliogenic lines and a suitable passage number, which could potentially allow a successful differentiation into the astrocytic lineage. Based on these results, most of the experiments performed later for this study were carried out using NSC lines O and K between passages 15-20. Also, all the cultures for NSCs were maintained in EGF and FGF (20 ng/ml each) medium to promote self regulatory induction of gliogenesis over time.

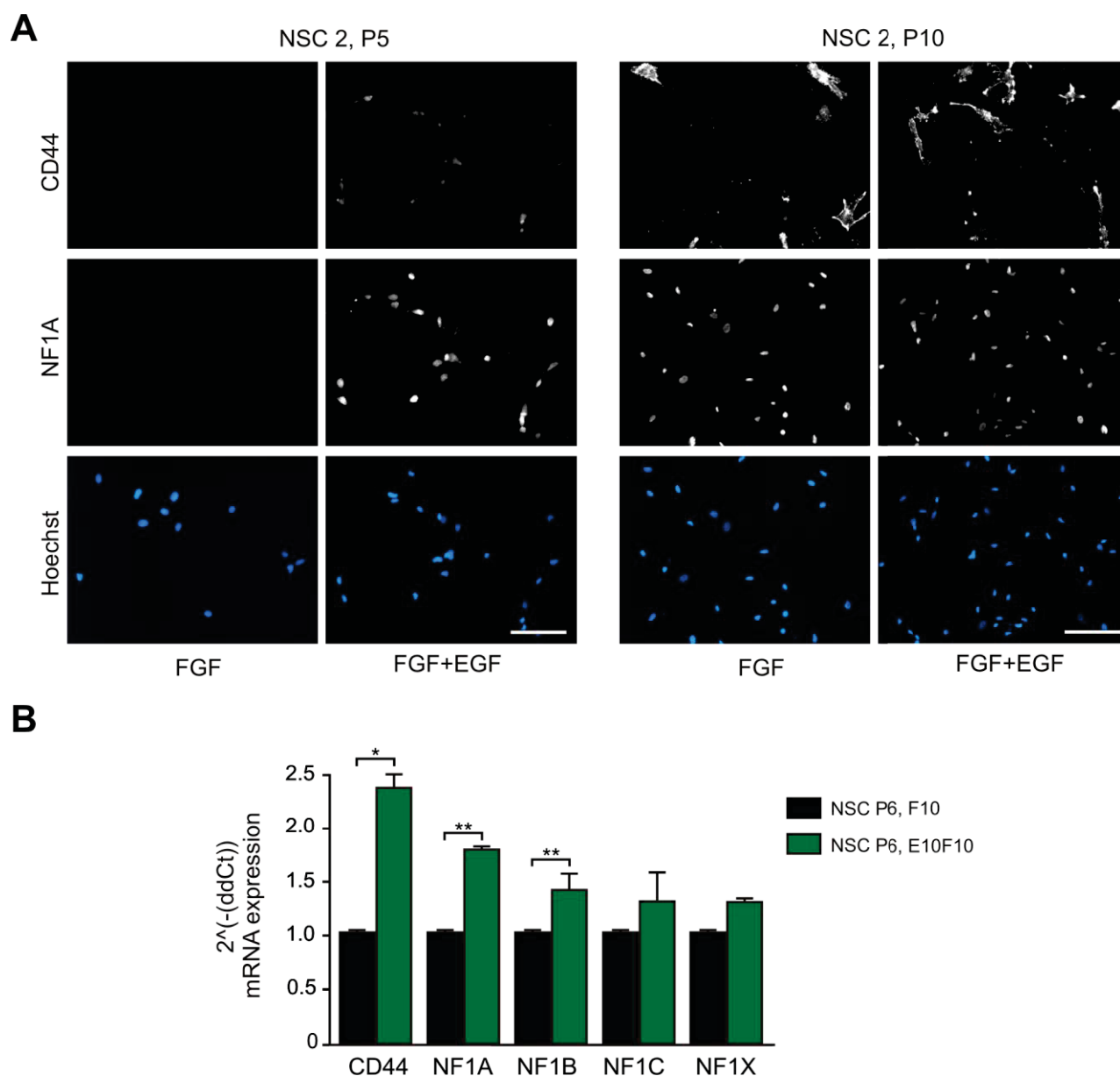


Figure 16: EGF dependent increase in astrocyte restricted precursor markers in early neural stem cells.

A) Immunostaining for CD44 and NF1A in F10 and E10F10 medium at NSC passage 5 and 10. Blue color represents Hoechst staining to label the nuclei. Scale bar = 100 μ m. **B)** mRNA expression pattern of CD44, NF1A, NF1B, NF1C and NF1X in F10 and E10F10 medium at NSC passage 6. F10= FGF (10 ng/ml), E10F10= EGF and FGF (10 ng/ml each). Data are represented as mean \pm s.e.m (n=3 for CD44, NF1A and NF1B, n=2 for NF1C and NF1X; * p < 0.05, ** p < 0.01, unpaired t-test).

3.2 The gliogenic switch and astrocyte differentiation

3.2.1 Differentiation of NSCs into high GFAP expressing astrocytes increases with passaging

As shown above, NSCs higher than passage 8-10 express CD44 and therefore should be suitable for differentiation into astrocytes. Taking this into consideration, at first NSCs from passage 15-20 (3-4 months) were used to differentiate them into astrocytes. For this, previously illustrated approaches of differentiation were undertaken: growth factor removal (NSC-/-) (Zhang *et al.*, 2001) and the use of CNTF (Krencik *et al.*, 2011, Shaltouki *et al.* 2012). Along with this, a small molecule inhibitor of MEK pathway- PD0325901 was employed to antagonize growth factor induced self renewal of NSCs and to mediate astrocytic differentiation. The use of serum was excluded, as its batch to batch variations promote inconsistent results and more importantly, use of serum has previously been addressed to result in non physiological changes in astrocytes rendering them in a reactive state (Zamanian *et al.*, 2012). After 14 days of differentiation, cells were stained for GFAP, an astrocytic marker, which until recently represented the gold standard for astrocyte identification. Not all the cells exhibit an equal staining for GFAP. The images shown may not be representative for filamentous structure of GFAP staining as the intensity was increased evenly in all the treatment conditions to enable visualization of all the positive cells. An example image with a lower intensity, displaying the filamentous staining of GFAP is also shown (Figure 17A, white inset). The analysis of cells expressing high levels of GFAP was performed after setting the threshold at minimum 17 and maximum 30 SD from the background. Undifferentiated NSCs were used as a negative control as less than 1% of these cells expressed high GFAP levels. Following these protocols, a maximum of 30% (± 9.07 , n=3) high GFAP expressing cells were obtained (Figure 17B). This was attained with the growth factor removal approach (NSC-/-), but it was observed to be highly variable as represented by individual data sets in Figure 17B. Inhibition of MEK with PD, did not lead to a significant increase in the number of cells expressing high levels of GFAP at this passage (Figure 17B). These results are in line with the observations by Krencik *et al.*, 2011. They found, that only 12% of 3-4 months old NSCs differentiated into high GFAP astrocytes in the presence of CNTF.

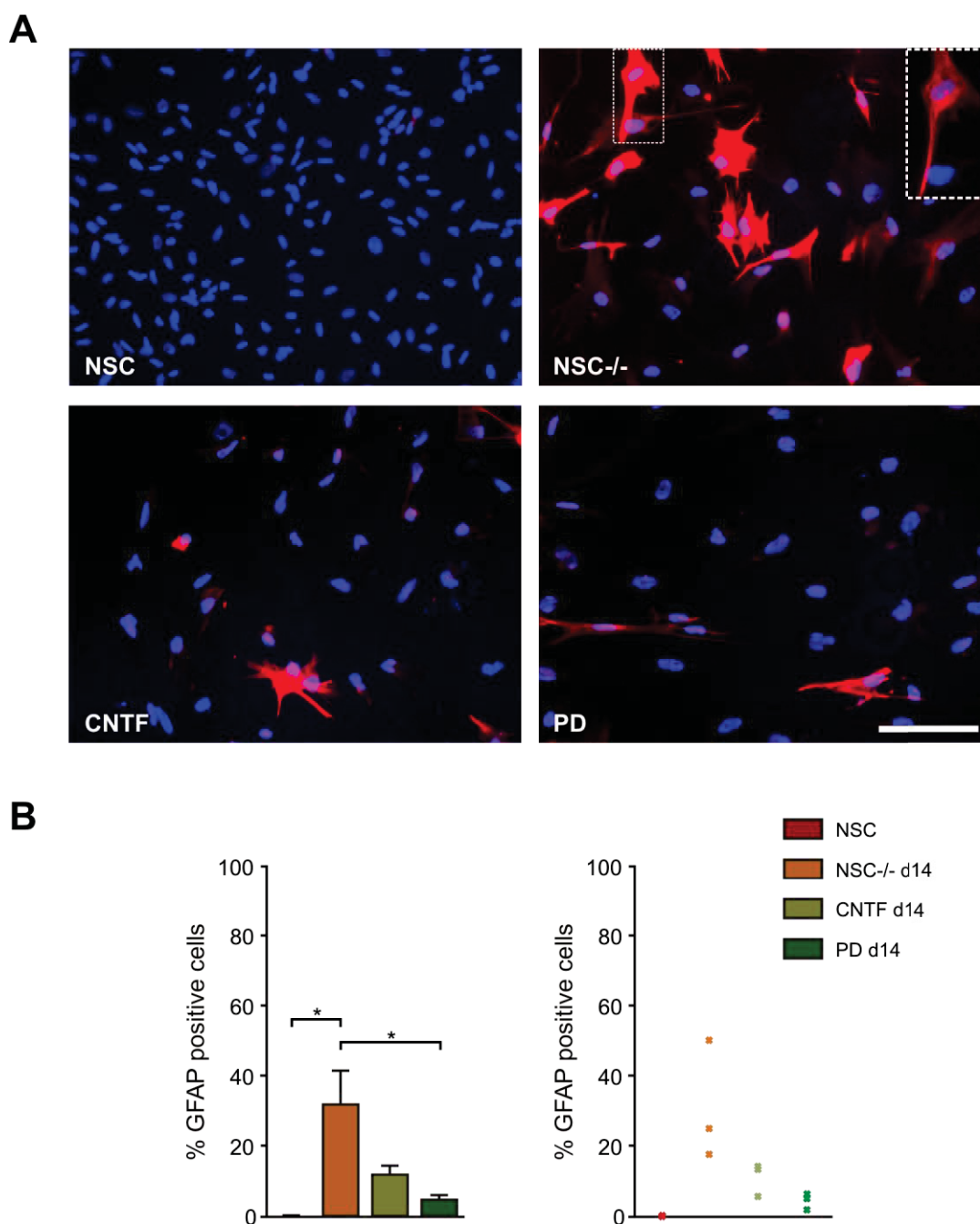


Figure 17: Inefficient differentiation of NSCs into high GFAP expressing cells.

A) Immunostaining for GFAP (red) for NSCs at passage 15-20, NSCs after 14 d of growth factor deprivation (NSC-/-), CNTF, or PD. White inset represents a low intensity image for GFAP to visualize its filamentous staining. Blue color represents Hoechst staining to label the nuclei. Scale bar = 100 μ m. **B)** Quantification of percent GFAP expressing cells to total nuclei. In the right graph, “x” represents different data sets to account for variability. Data are represented as mean \pm s.e.m (n=3, * $p < 0.05$, one way ANOVA, Tukey’s post hoc test).

As astrocyte differentiation occurs at later stages of gestation and continues in the postnatal period (Semple *et al.*, 2013), it suggests that further maturation of NSCs is required to enable them to generate astrocytes. This also has been shown to be true *in vitro* (Krencik *et al.*, 2011, Shaltouki *et al.* 2013, Roybon *et al.*, 2013). Based on these studies, NSCs were cultured until

passage 40-45 (~ 7-8 months) and then differentiated for 14 days using the same three protocols as mentioned above. Expression of GFAP was studied by performing ICC (*Figure 18A*). With these higher passage NSCs, up to 50% (± 2.8 , $n=4$) of the cells expressed high levels of GFAP after differentiation (*Figure 18B*). Interestingly, this was achieved with the PD approach which only gave rise to 5% (± 1.8 , $n=3$) of high GFAP expressing cells from younger NSC passages (*Figure 17B*). Growth factor removal (NSC-/-) did not show the rise in the number of high GFAP astrocytes with increasing NSC passage and CNTF treatment only generated a mean of 30% with some variability between the data sets which is represented in *Figure 18B*. Also, it has to be noted that the number of high GFAP expressing cells increased up to 18% (± 1.8 , $n=4$) in the undifferentiated NSCs after prolonged culture time, again confirming the acquisition of a higher gliogenic potential of these cells with passaging.

The results from these experiments support a development dependent occurrence of different states of NSCs as shown by their ability to give rise to high GFAP expressing cells. Following this differentiation scheme, it is conceivable to establish a homogenous culture of 80-90% high GFAP expressing cells with NSCs of higher passage. In addition, it was observed that among different differentiation protocols tested, PD approach proved to be the most consistent one with minimum variability.

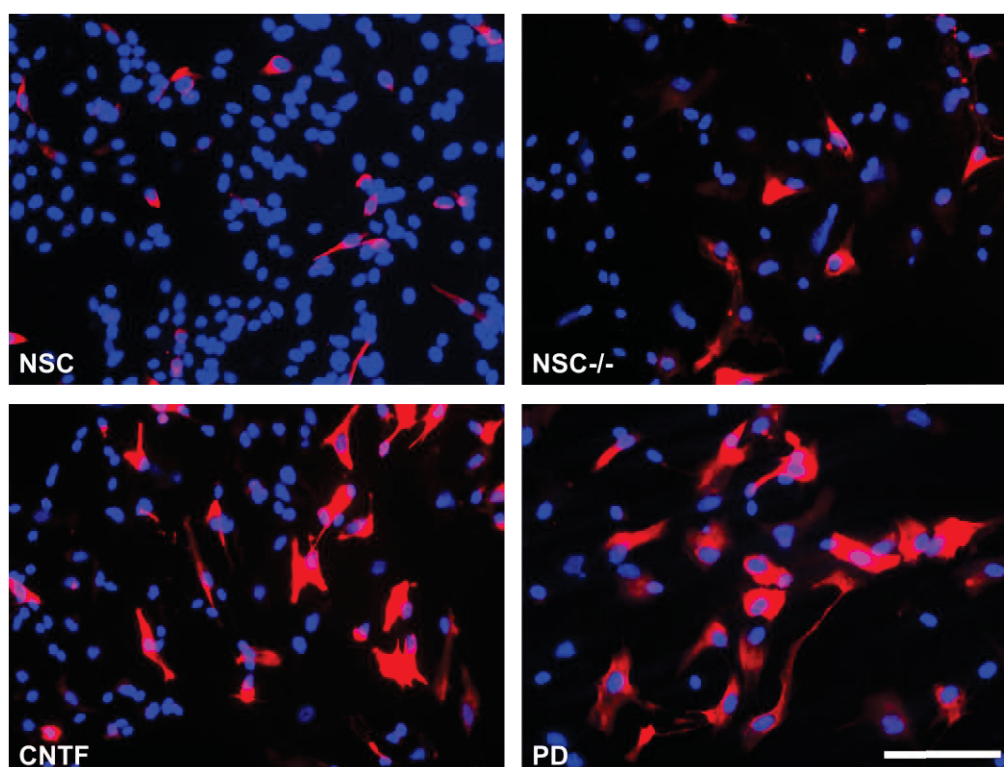
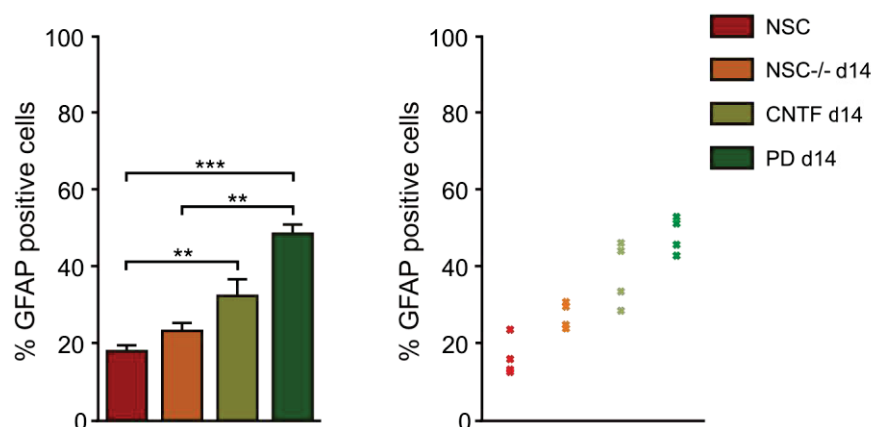
A**B**

Figure 18: Augmentation of GFAP positive cells with increasing passage of NSCs.

A) Immunostaining for GFAP (red) for NSCs at passage 40 or higher, high passage NSCs after 14 d of growth factor deprivation (NSC-/-), CNTF, or PD. Blue color represents Hoechst staining to label the nuclei. Scale bar = 100 μ m. **B)** Quantification of percent GFAP expressing cells to total nuclei. In the right graph, “x” represents different data sets to account for variability. Data are represented as mean \pm s.e.m (n=4, ** p < 0.01, *** p < 0.001, one way ANOVA, Tukey's post hoc test).

3.2.2 Triggering the gliogenic switch in early NSCs

Previous results have shown that a considerably long culture time of NSCs is required to differentiate them into high GFAP astrocytes. This brings in issues like prolonged waiting time and economic limitation to such an *in vitro* differentiation procedure. These limitations could be overcome by finding a mechanism to induce the gliogenic switch in NSCs. Several factors have

been reported to play an important role in triggering the glial lineage, especially at the epigenetic level (Hatada *et al.*, 2008). A previous study using mouse NSCs has shown that the exposure to high levels of FGF for a short time of 24 hours can bring about a change in histone 3 acetylation at the STAT binding site of the GFAP promoter, rendering it responsive to CNTF (Song and Ghosh, 2004). Taking lead from this study, passage 5-7 from newly generated NSCs (NSC1a, 1b and 2) were cultured in either E20F20 (EGF and FGF: 20 ng/ml each) or high FGF (EGF and FGF: 20 ng/ml and 100 ng/ml respectively) or high EGF (EGF and FGF: 100 ng/ml and 20 ng/ml respectively) medium for 7 days. High EGF was used based on the previous observation of increase in NF1A and CD44 when the medium was switched from FGF to EGF + FGF (Figure 16). Culture settings were referred to as uninduced, FGF induced and EGF induced respectively. At first, changes in the gliogenic potential of uninduced and induced cells were compared by performing ICC for CD44 (Figure 19A). The percentage of CD44 positive cells remained significantly unaltered in uninduced or FGF/EGF induced conditions, with a mean of 70-80% CD44 positive cells (Figure 19B). Unlike to high passage NSCs, growth factor dependent induction did not lead to an increased expression of GFAP in NSCs (Figure 19C). Undifferentiated NSCs from uninduced and induced conditions exhibited only 2-3% of high GFAP expressing cells (Figure 19D).

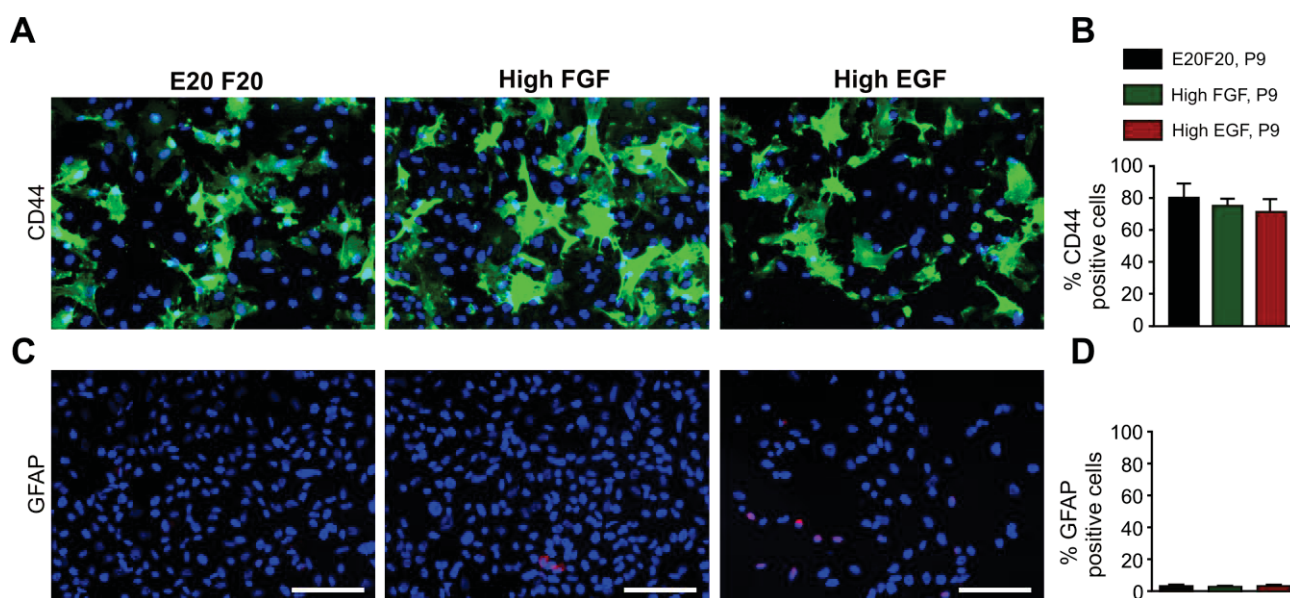


Figure 19: High level of CD44 expression in low passage NSCs.

A, C) Immunostaining for CD44 (green) and GFAP (red) in E20F20, high FGF and high EGF derived NSCs (passage 7-9). **B, D)** Quantification of percent CD44 (**B**) and GFAP (**D**) positive cells under E20F20 and induced conditions. E20F20= EGF and FGF (20 ng/ml each), high FGF= EGF (20 ng/ml), FGF (100 ng/ml) and high EGF= EGF (100 ng/ml) FGF (20 ng/ml). Data are represented as mean \pm s.e.m (n=4). No significant differences were observed in the expression of either CD44 or GFAP upon induction with high FGF or EGF.

To test the astrocytic differentiation potential of the different NSCs, uninduced and induced NSCs were subjected to astrocytic differentiation by different protocols (growth factor removal (NSC^{-/-}), CNTF or PD treatment for 24 days). The differentiation time was increased from the previously used 14 days to 24 days, as an effect was visible at the later time point. Differentiation was examined by performing ICC for GFAP in uninduced and induced NSC^{-/-}, CNTF and PD treated cells (*Figure 20A, C, E respectively*). For quantification, the induced cells were compared to their corresponding uninduced differentiation condition to calculate the fold change in GFAP expressing cells. The NSC^{-/-} and PD differentiation protocol did not show an effect of FGF or EGF induction on the yield of high GFAP expressing cells after 24 days (*Figure 20B, F*). However, by using CNTF for differentiation, we could successfully obtain a 50% (± 5.5 ; $n=4$, $p < 0.01$) increase in differentiation efficiency towards high GFAP expressing cells after FGF induction of these early NSCs. EGF induction also resulted in a 31% (± 4.7 , $n=4$) increase in the number of high GFAP expressing cells but the increase was not statistically significant (*Figure 20D*).

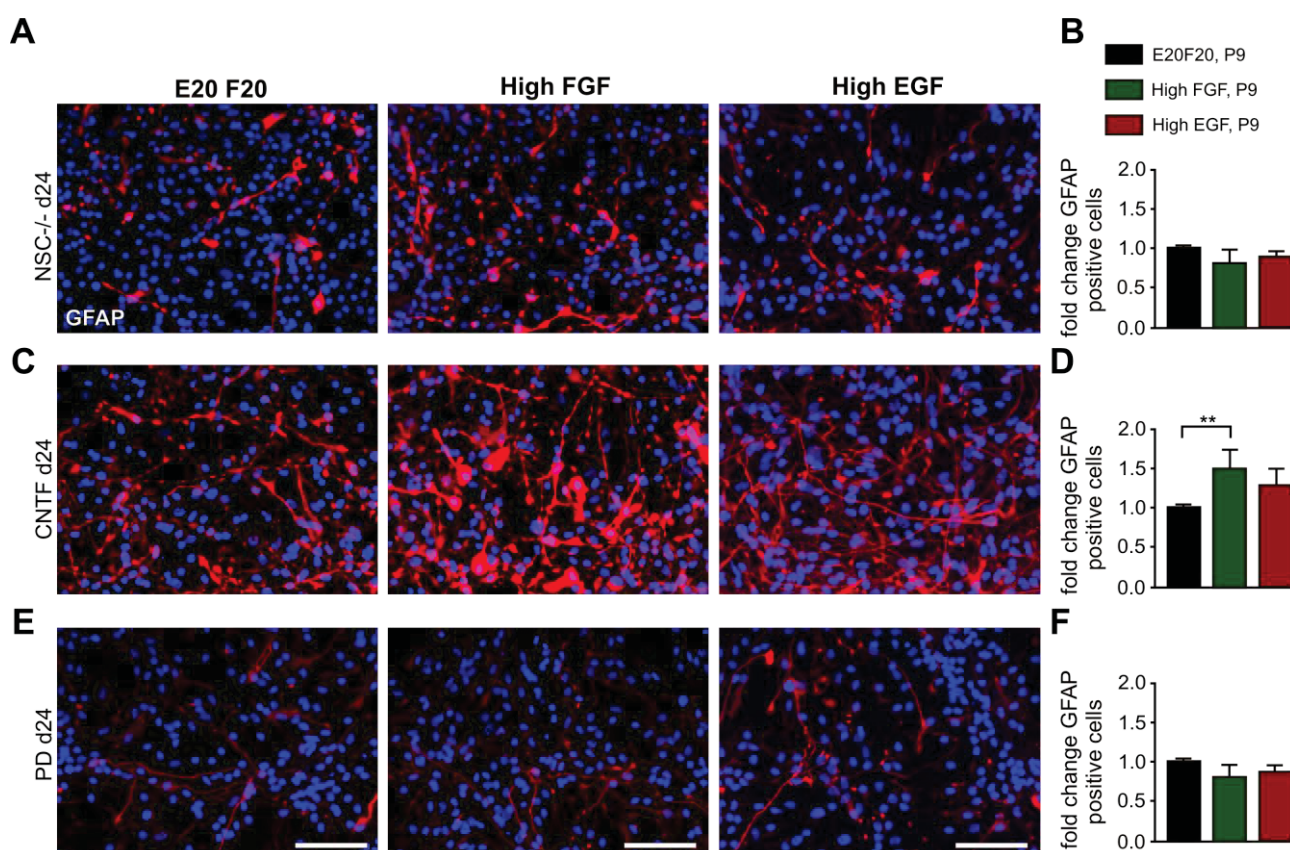


Figure 20: FGF dependent induction of gliogenic switch augments differentiation of early neural stem cells into high GFAP expressing astrocytes upon exposure to CNTF.

A, C, E) Expression of GFAP in E20F20, high FGF and high EGF derived NSCs (P 7-9) after 24 d of growth factor removal (NSC^{-/-}) (**A**), CNTF treatment (**C**) and PD treatment (**E**). Blue color represents Hoechst staining to label the nuclei. Scale bar = 100 μ m. **B, D, F**) Quantification of fold change GFAP positive cells to total nuclei from E20F20 to high FGF and high EGF derived cells after 24 d of NSC^{-/-}

condition **(B)**, CNTF treatment **(D)** and PD treatment **(E)**. E20F20= EGF and FGF (20 ng/ml each), high FGF= EGF (20 ng/ml) FGF (100 ng/ml) and high EGF= EGF (100 ng/ml) FGF (20 ng/ml). Data are represented as mean \pm s.e.m (n=4, ** p < 0.01, one way ANOVA, Tukey's post hoc test).

Overall, the induction of a gliogenic switch was established in early passage human neural stem cells, rendering them suitable for differentiation into about 50% of high GFAP expressing astrocytes in a time period of just 2 months. Without induction, it requires at least 7 months of NSC culture in order to attain a similar percentage of high GFAP expressing cells. With further characterization of these cells, it may offer a prospective time cutting and less expensive approach for differentiation of NSCs towards high GFAP expressing astrocytes.

3.3 Small molecule mediated differentiation of human iPSCs derived NSCs into low GFAP expressing astrocytes

3.3.1 Exit from the NSC stage in the presence of PD

Pertaining to glial heterogeneity and the presence of low GFAP expressing cells in the gray matter, it is incorrect to use GFAP as 'the' marker for astrocyte differentiation. Recently, transcriptome studies have highlighted another protein: ALDH1L1, as a pan astrocytic marker and it has been shown that a large number of cells labeled with ALDH1L1 does not co-localize with GFAP labeled cells, thereby emphasizing the underappreciated diversity of astrocytes (Cahoy *et al.*, 2008). This necessitates the generation of low GFAP expressing, physiologically functional astrocytes *in vitro* to enable their use for understanding astrocyte development as well as disease related aspects. Prior to this, there have been no studies attempting to generate solely this subtype of astrocytes in a defined way, as all the protocols rely on the expression of GFAP. Here, a small molecule based approach is described in order to differentiate NSCs towards low GFAP expressing astrocytes.

Subsequent to treatment of NSCs with the small molecule- PD0325901 (PD) for 14 days, morphological changes were observed under phase contrast (*Figure 21A*). The cells shape changed from small, spindle like NSCs to big and flat polygonal cells resembling cultured astrocytes. This drastic change in morphology was further confirmed by staining with Calcein AM dye which is taken by the cells and becomes fluorescent upon action of intracellular esterases (*Figure 21B*). As hydrolysis of Calcein AM is required to make it fluorescent and for its intracellular retention, labeling with this dye also accounts for lack of any considerable cell death in both NSCs and PD treated cultures.

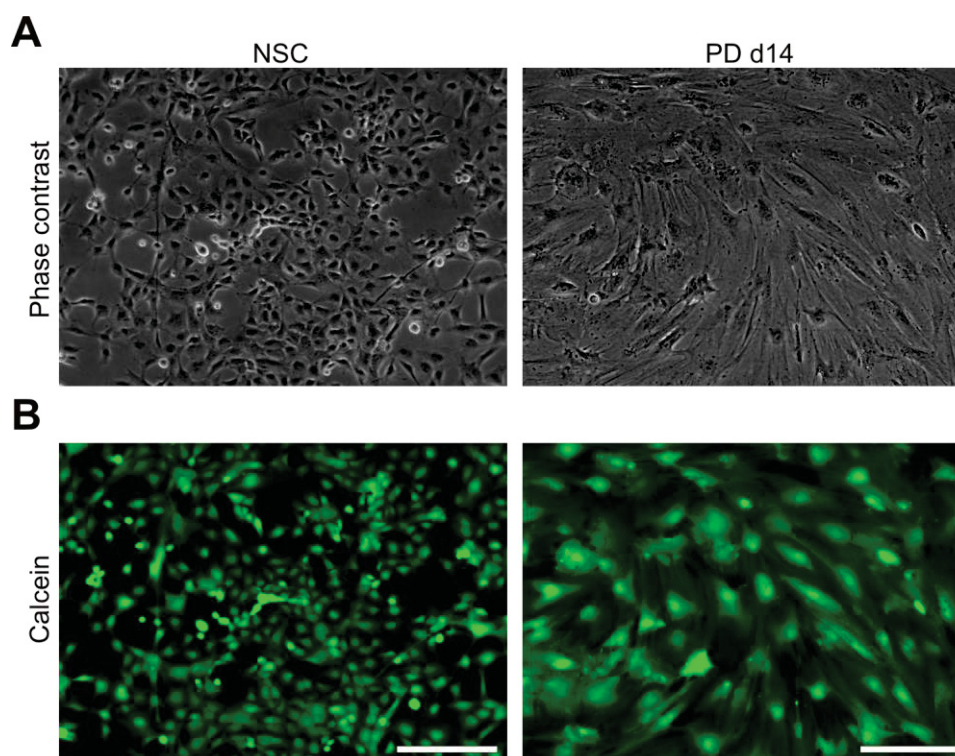


Figure 21: Morphological differences upon PD treatment in neural stem cells.

A) Phase contrast view of NSCs in E20F20 medium and after 14 d of PD treatment. **B)** Calcein based whole cell staining for NSCs and 14 d PD treated cells. Scale bar = 100 μ m. n=4.

PD is a well established inhibitor of MEK, which is a key pathway for cell proliferation. Therefore, next, 4 and 9 days PD treated cells were investigated for their proliferation property by staining for Ki67 protein, a widely used proliferation marker. Exit from neural stem cell stage was confirmed by staining with Sox2 (*Figure 22A*). Under the effect of PD treatment, the number of proliferating cells decreased significantly from 35% to 1% within 9 days. Along with proliferation, the expression of Sox2 also dropped down appreciably from 95% to less than 20% following 9 days of PD treatment (*Figure 22B*). This decline in proliferation marker- Ki67 and neural stem cell marker- Sox 2 was further supported by performing real time PCR for these two genes in NSCs, 4 and 9 days PD treated cells. As observed by ICC, the mRNA levels also decreased by 75% for Sox2 and 98% for Ki67 after exposure to PD for 9 days (*Figure 22C*).

To further evaluate the NSC profile of PD treated cells, qPCR was carried out for another conventional marker for NSCs- Nestin and several ARP markers- CD44 and NF1 family of transcription factors. There was a more than 50% reduction in Nestin at mRNA level. Also, we noted a similar decrease in CD44 and NF1A, however, the levels of NF1B, NF1C and NF1X were not significantly changed (*Figure 23*). This implies an early role of CD44 and NF1A in glial lineage restriction and a delayed role for NF1B, NF1C and NF1X.

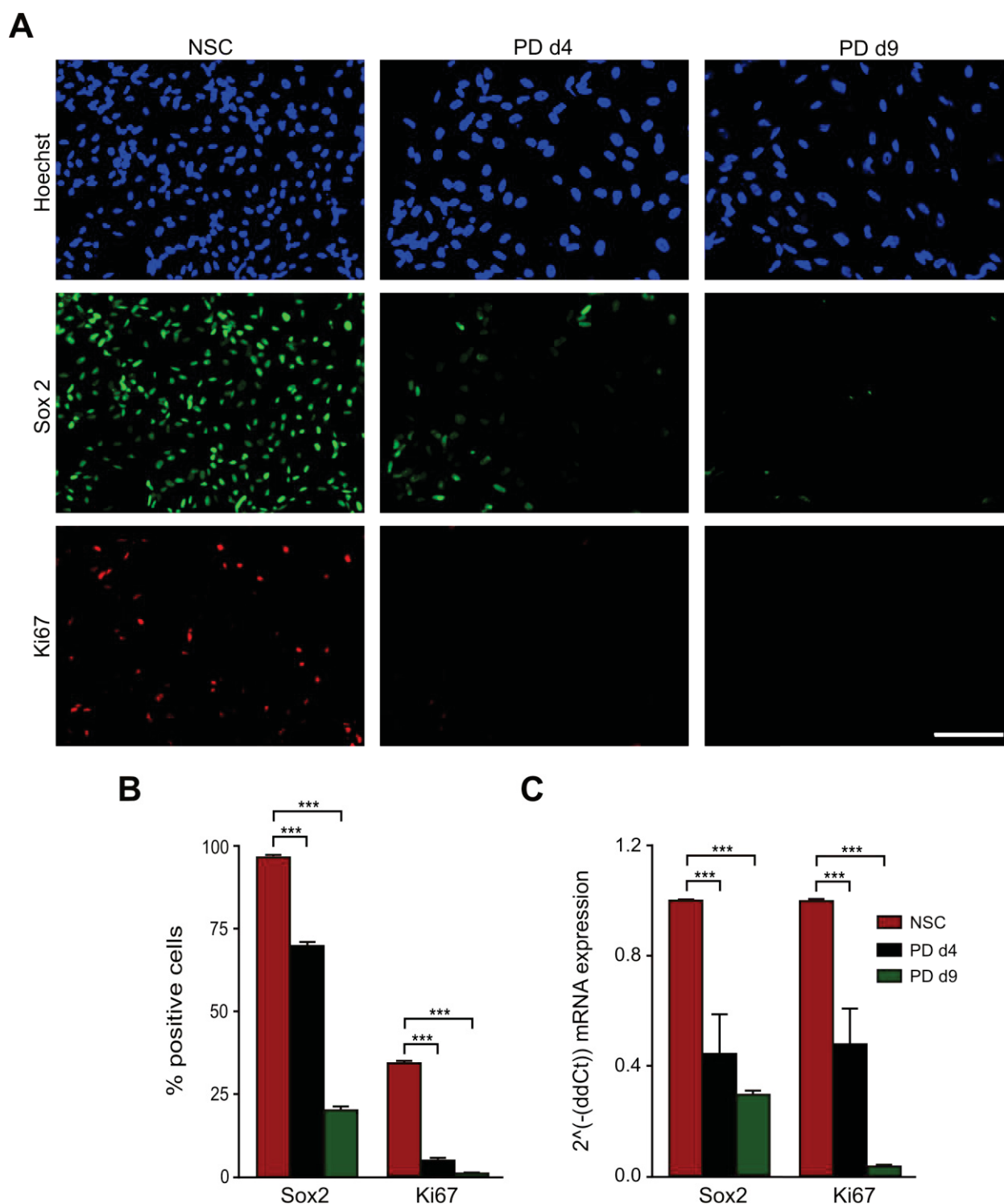


Figure 22: Decreased proliferation of neural stem cells after short term PD treatment.

A) Immunostaining for NSCs, 4 d and 9 d PD treated cells for Sox2 (green) and Ki67 (red). Blue color represents Hoechst staining to label the nuclei. Scale bar = 100 μ m. **B)** Quantification of immunostaining comparing percent of Sox2 and Ki67 positive cells to total nuclei in NSCs and PD treated cells at 4 d and 9 d. **C)** Further confirmation of reduction in Sox2 and Ki67 at mRNA level as illustrated by quantitative PCR for NSCs and 4 d, 9 d PD treated cells. Data are represented as mean \pm s.e.m (n=4, *** p < 0.001, one way ANOVA, Tukey's post hoc test).

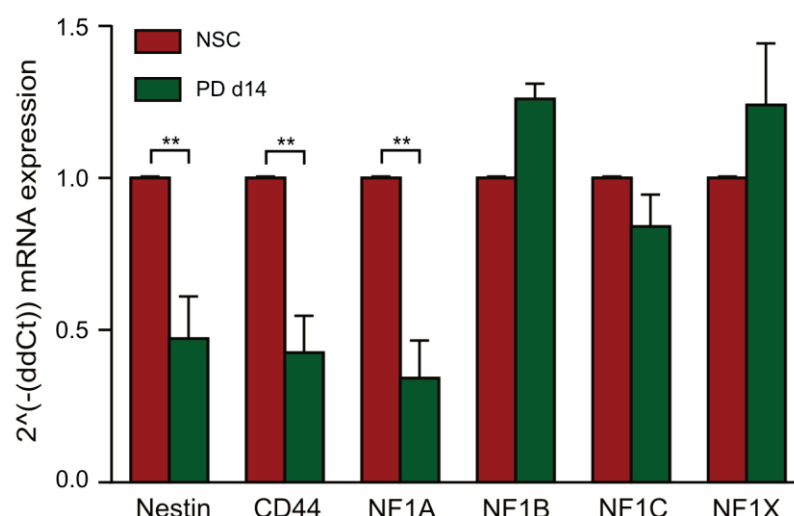
A

Figure 23: Reduction in NSCs and glial restricted progenitor markers in the presence of PD at mRNA level.

A) Quantitative PCR for neural stem cell marker: *Nestin* and glial progenitor markers: CD44, NF1A, NF1B, NF1C and NF1X after 14 d of PD treatment. Data are represented as mean \pm s.e.m (n=3, ** p < 0.01, one way ANOVA, Tukey's post hoc test).

In particular, these results show that treatment with PD shuts off the self renewal and proliferative state of NSCs, directing them towards an advanced gliogenic fate.

3.3.2 PD treated NSCs differentiate into low GFAP expressing astrocytes of cortical lineage

As the morphology of 14 days old PD treated cells resembles cultured astrocytes and also, owing to the exit from NSC state shown before, next we checked for the co-expression of an immature astrocyte marker- S100 β and the classical astrocyte marker- GFAP (*Figure 24A*). As observed by ICC, more than 90% of the cells were positive for S100 β after PD treatment compared to its expression in less than 20% of the NSCs. As shown before (*Figure 17*), the expression of high levels of GFAP was confined to only 5% of the PD treated cells and was not significantly different from the NSCs (*Figure 24B*). However, a low level of GFAP expression was present in most of the cells in the PD treated condition. To get a deeper understanding of the expression level of GFAP, several approaches were used. First, FACS based detection of GFAP expression was performed. It revealed a clear difference in the intensity of GFAP staining between NSCs and PD treated cells (*Figure 24C*). Geometric mean intensity of NSCs and PD treated cells was 2233.74 ± 26.53 CV and 30233.46 ± 32.10 CV respectively (CV = coefficient of variation). In addition, a scattered population in PD treated condition was detected, whereas NSCs were confined as a single population showing a low intensity of GFAP. These data align well with our ICC results. Further analysis of the protein levels of GFAP by western blot demonstrated a

remarkable 10 fold increase in the expression of GFAP after 14 days of PD treatment. Quantification is represented in terms of fold change considering PD as 1 because almost negligible expression of GFAP was visible for NSCs (*Figure 24D*). Similar result with a significant increase in GFAP after PD treatment was obtained at the mRNA level (*Figure 24E*). This could be explained by the small population (~5%) of high GFAP expressing cells and a low level of GFAP expression in the rest 95% of the cells which sums up and shows a significant difference between NSCs and PD treated cells in western blot and PCR.

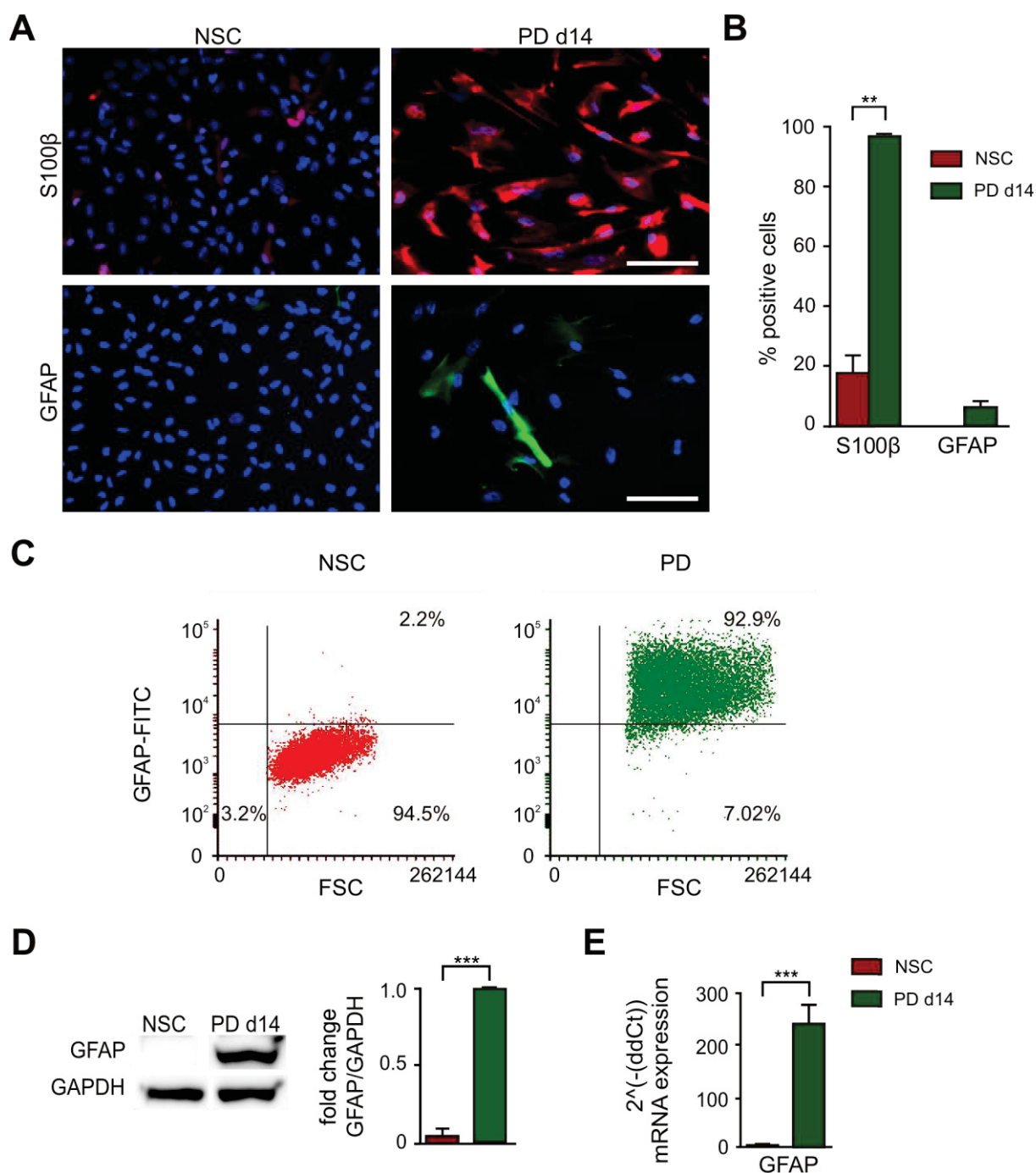


Figure 24: Low level of GFAP expression in PD treated cells. Legend on next page

A) Immunostaining for S100 β (red) and GFAP (green) in NSCs and 14 d PD treated cells. Blue color represents Hoechst staining to label the nuclei. Scale bar = 100 μ m. **B)** Quantification of immunostaining for S100 β and high GFAP expressing cells, represented as percent of positive cells to total number of nuclei. **C)** Flow cytometry based analysis of GFAP expression in NSCs and 14 d PD treated cells. **D)** Western blot and quantification for GFAP in terms of fold change in NSCs and cells exposed to PD for 14 d. **E)** qPCR to evaluate mRNA expression levels of GFAP in NSCs and 14 d PD treated cells. Data are represented as mean \pm s.e.m (n=3, ** p < 0.01, *** p < 0.001, unpaired t-test).

In order to determine whether the virtually pure population of low GFAP expressing cells generated by PD treatment display further astrocyte identity, the expression of several more mature astrocyte markers was investigated. Their astrocytic profile was confirmed by the expression of pan astrocyte marker- ALDH1L1 (*Figure 25A*), where more than 80% of the cells exhibited ALDH1L1 expression (*Figure 25B*). Maturity of the cells was further investigated by staining for glutamine synthetase (GS) enzyme and glutamate transporter- EAAT1 (*Figure 25C, E*). Approximately 90% of the PD treated cells expressed both GS and EAAT1, whereas the percentage of positive cells in NSCs for both of these markers remained less than 5% (*Figure 25D, F*).

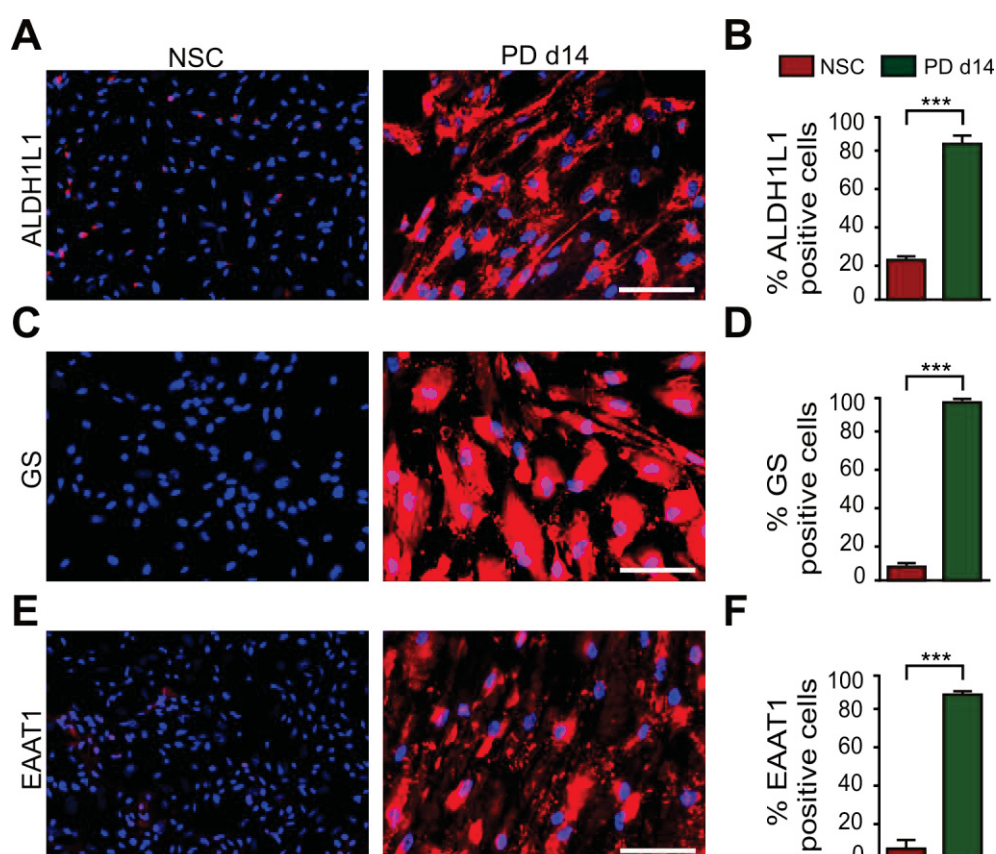


Figure 25: Expression of pan astrocytic and functional astrocyte markers in PD differentiated astrocytes by immunostaining.

A-F) Immunocytochemistry based analysis of expression level of pan astrocytic marker: ALDH1L1 (**A, B**) and functional astrocyte markers: GS (**C, D**) and EAAT1 (**E, F**) in NSCs and 14 d old, PD

treated low GFAP astrocytes. Blue color represents Hoechst staining to label the nuclei. Scale bar = 100 μ m. Data are represented as mean \pm s.e.m (n=3, *** p < 0.001, unpaired t-test).

In addition, an increase in ALDH1L1 and more than 5 fold upregulation of fatty acid metabolizing enzyme- Acsbg1 and gap junction coupling protein- Cx43 was also found at protein level by western blot (*Figure 26A-D*). Further, qPCR was used to confirm the increase in Cx43 and to investigate the expression of the synaptogenic protein- ApoE (*Göritz et al., 2002*) and another glutamate transporter- EAAT2 which is reported to be present in mature human astrocytes (*DeSilva et al., 2012*). The expression of all of these genes was augmented after 14 or 24 days of PD treatment. The mRNA levels of Cx43, ApoE and EAAT2 were found to be at least 5 fold higher after PD treatment as compared to NSCs (*Figure 26E*).

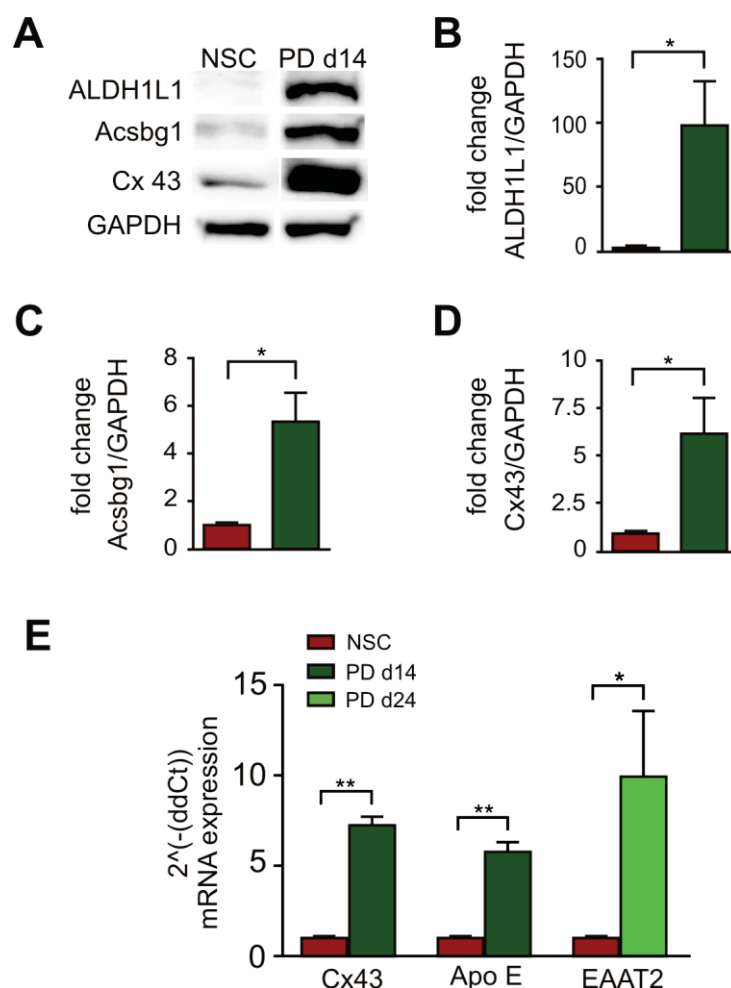


Figure 26: Expression of pan astrocytic and functional astrocyte markers in PD differentiated astrocytes.

A) Western blots to investigate expression levels of ALDH1L1, Acsbg1 and Cx43 in NSCs and 14 d PD treated cells. **B-D)** Quantification of western blots comparing fold change between NSC and low GFAP astrocytes for ALDH1L1 (**B**), Acsbg1 (**C**) and Cx43 (**D**). **E)** qPCR for mRNA expression levels of Cx43, ApoE in NSCs and 14 d PD treated cells and EAAT2 in 24 d PD treated cells. Data are represented as mean \pm s.e.m (n=3, * p < 0.05, ** p < 0.01, unpaired t-test).

Glial cells have been proved to be of immense importance in supporting neuronal functions. Astrocytes also play a vital role in the synapse formation, function and synaptic plasticity (Clarke *et al.*, 2013). Besides their function in brain physiology, astrocytes are powerful players of neurodegeneration in diseased conditions. Therefore, to get a better understanding of the role of astrocytes in health and disease, it would be very useful to have a neuron-astrocyte coculture system. As an active neuronal culture could be maintained in NBNS21S medium for 2-3 months (Nieweg *et al.*, 2015), therefore PD directed differentiation of astrocytes was tested in this medium which could be further employed for co-culture. Although the survival was good, but a slight morphological difference was observed in PD + NBNS21S differentiated astrocytes as compared to PD + NSC-/- medium, the former being bit smaller in size. In order to confirm the successful differentiation and maintenance of low levels of GFAP in PD + NBNS21S differentiated astrocytes, ICC was performed for previously defined astrocytic markers: S100 β , ALDH1L1 and GFAP (Figure 27A). Upon 14 days of differentiation, these cells displayed a significant upregulation of S100 β and ALDH1L1 in 99% of the cells, although hardly 1% of the cells were positive for GFAP (Figure 27B), thereby resembling the previously described low GFAP astrocytes. These data further illustrates the robustness of the PD mediated differentiation towards low GFAP astrocytes in different culture mediums.

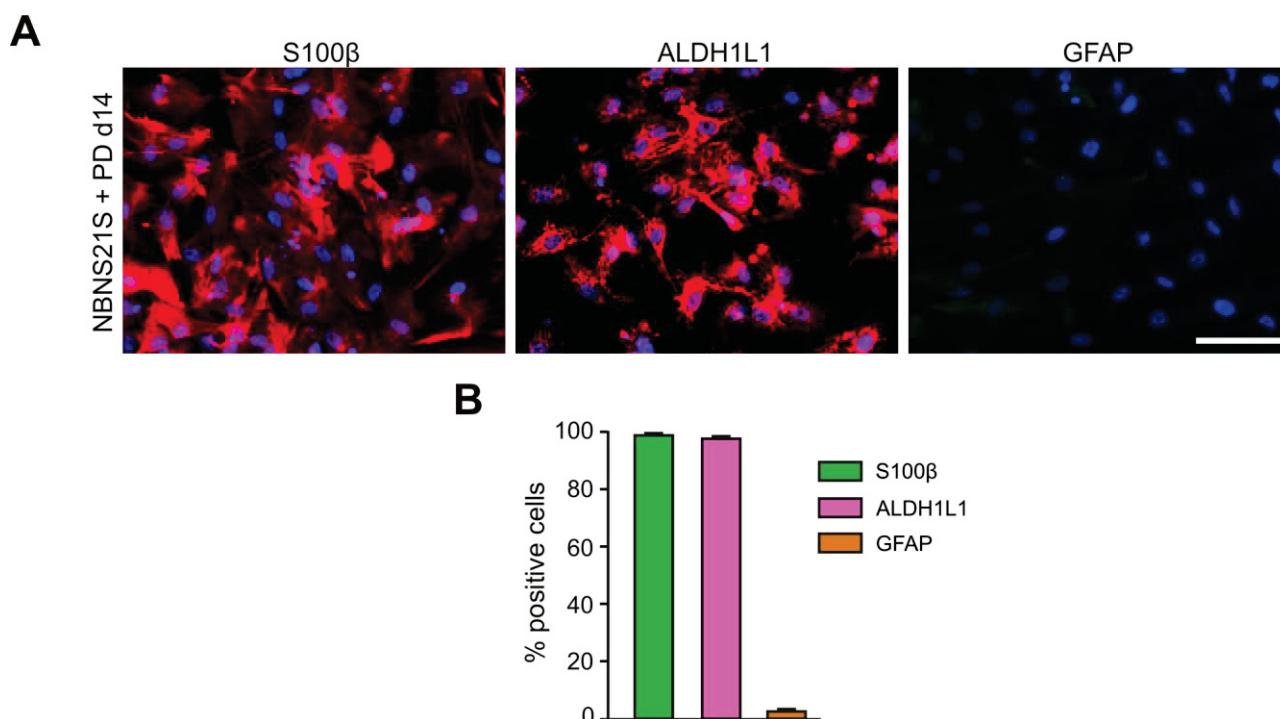


Figure 27: Maintenance of low GFAP levels in astrocytes differentiated in NBNS21S.

A) Immunostaining for S100 β , ALDH1L1 and GFAP in 14 d PD differentiated cells in NBNS21S medium. Blue color represents Hoechst staining to label the nuclei. Scale bar = 100 μ m. **B)** Quantification of percent of S100 β , ALDH1L1 and GFAP positive cells in astrocytes differentiated in NBNS21S. Data are represented as mean \pm s.e.m (n=4).

The generation of homogenous and mature human spinal cord astrocytes has been previously reported (Roybon *et al.*, 2013). Anterior and posterior lineage has been long known to be dependent on Shh and Wnt signaling. Here, the cortical lineage of iPSC derived NSCs as well as the maintenance of this lineage in the differentiated astrocytes was illustrated. This was done by performing ICC for forebrain markers- OTX2, LHX2 (Figure 28A, B) and the ventral identity markers- HOXB4 and NKX2.1 (Figure 28C, D). Almost 95% of the cells in NSCs and PD differentiated cultures were positive for both OTX2 and LHX2, while none of the cell expressed either HOXB4 or NKX2.1.

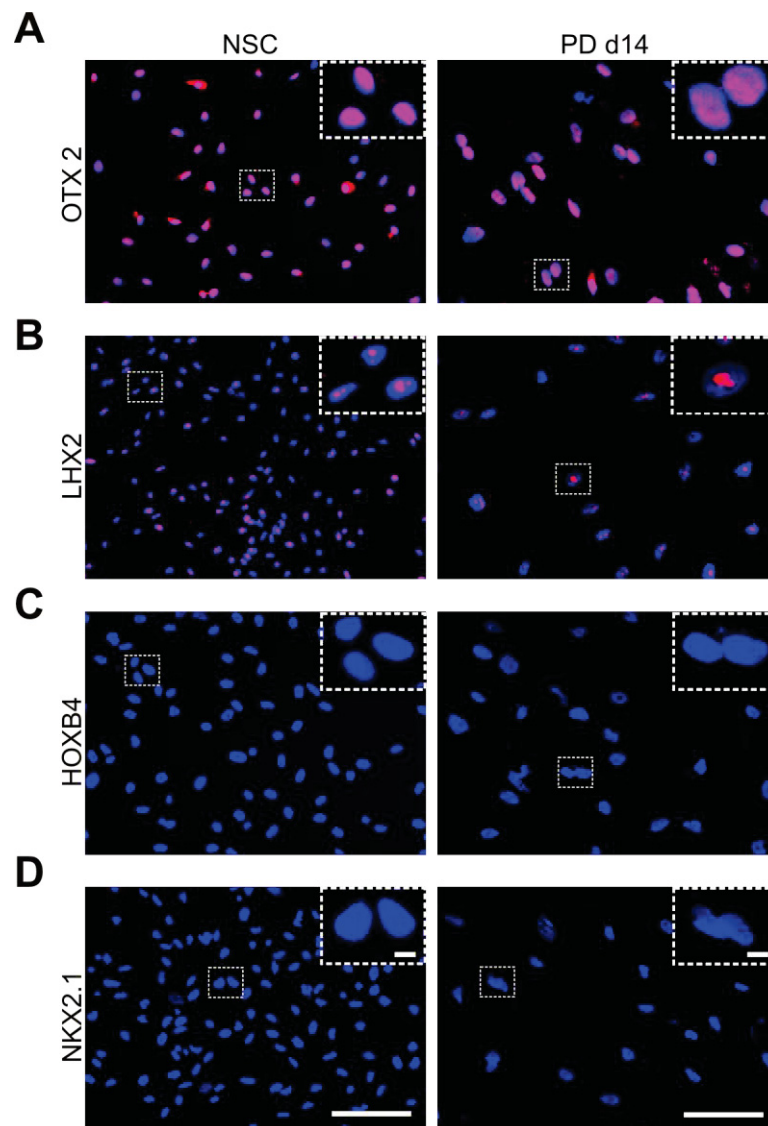


Figure 28: PD differentiated astrocytes exhibit cortical lineage.

A-D) Immunostaining for cortical markers: OTX2 (**A**), LHX2 (**B**) and ventral markers: HOXB4 (**C**), NKX2.1 (**D**) in NSCs and 14 d PD derived astrocytes. Blue color represents Hoechst staining to label the nuclei. White insets represent magnified view. Scale bar = 100 μ m.

The results from these different approaches show that, within 14 days, PD successfully differentiated 3-4 months old NSCs into low GFAP expressing cells of cortical lineage with astrocyte identity. These cells have properties of developmentally mature astrocytes as they are no longer proliferating and express several markers of mature astrocytes (ALDH1L1, Cx43, EAAT1, GS, EAAT2). Regarding the findings that PD is more efficient than CNTF in differentiating high GFAP expressing cells from high passage NSCs and is also able to generate virtually pure populations of low GFAP expressing cells with astrocyte identity from younger NSCs, it can be concluded that the invention of PD is an innovative approach for driving astrocyte differentiation.

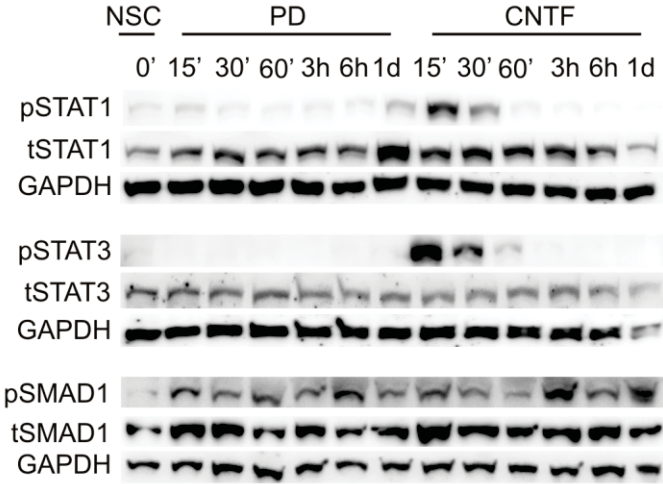
3.4 Signaling pathways involved in PD mediated astrocyte differentiation

3.4.1 PD mediates late onset of STAT1/3 phosphorylation during differentiation into low GFAP expressing astrocytes

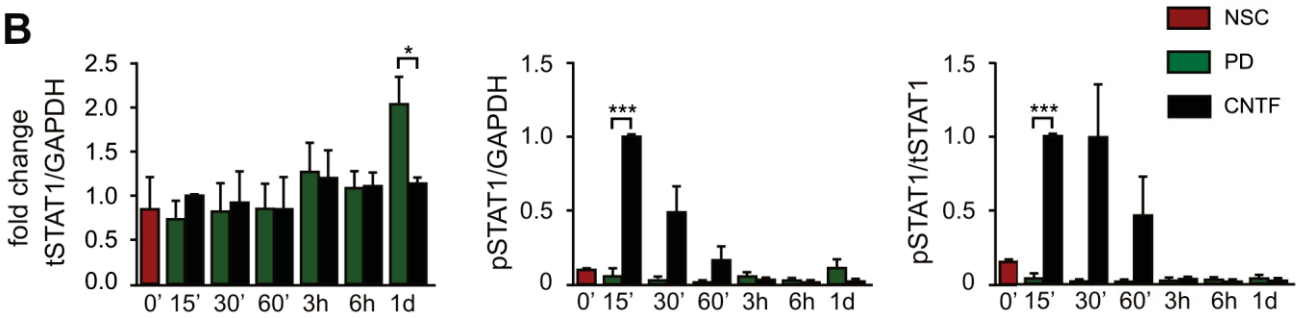
Since PD could be validated as a small molecule for efficient astrocyte differentiation without obvious pathway activation, the underlying mechanisms were thus investigated. Several pathways have been reported for the differentiation of astrocytes, out of which CNTF dependent STAT1/3 and BMP dependent SMAD1 phosphorylation are the most commonly validated ones (*Molofsky et al., 2012*). In order to understand the molecular mechanism by which PD mediates differentiation into astrocytes, changes in these two conventional astrocytic pathways were first investigated at early time points as usually reported for CNTF or BMP. NSCs were used as a negative control and CNTF as a positive control for comparison to PD. NSCs from passages 15-20 were treated with either PD or CNTF for 15, 30, 60 min, 3, 6 and 24 hours. Western blot was performed for: pSTAT1 (Tyr 701), pSTAT3 (Tyr 705), pSMAD1 (Ser 463), their corresponding total proteins and GAPDH (*Figure 29A*).

For analysis, fold change was calculated with respect to CNTF 15 min condition. As expected, the levels of pSTAT1/GAPDH and pSTAT1/tSTAT1 were up to 10 times higher in the first 30 min of CNTF treatment and pSTAT3/GAPDH and pSTAT3/tSTAT3 were increased by 20 fold until 1 hr of CNTF treatment. However, no increase in STAT1 and STAT3 phosphorylation was observed during 1 day of treatment with PD (*Figure 29B, C*). Interestingly, a significant augmentation of the expression of total STAT1 (tSTAT1) was detected after 1 day of PD treatment, whereas, its expression was almost consistent in the presence of CNTF (*Figure 29B*). No significant difference was found in the expression of tSTAT3 upon PD or CNTF treatment for 1 day. Next, the changes in total and phospho SMAD1 were examined.

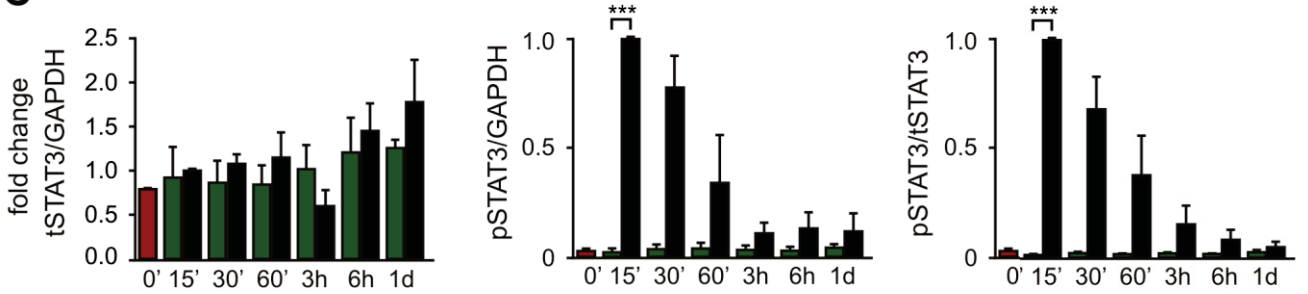
A



B



C



D

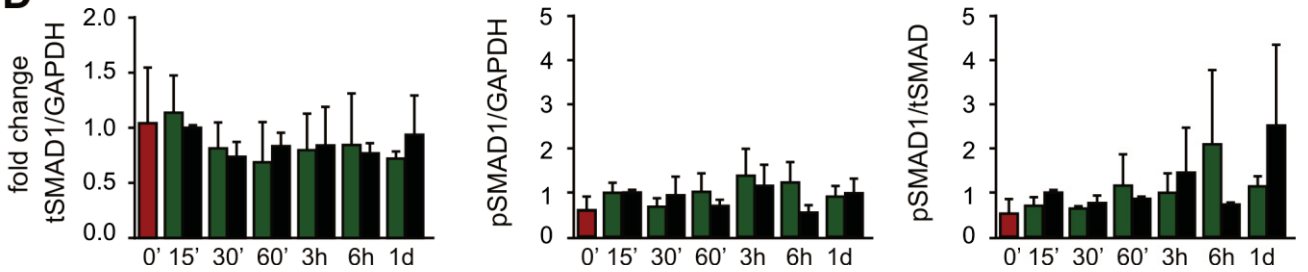


Figure 29: Absence of early phosphorylation of STAT1/3 and SMAD1 in the presence of PD.

A) Western blots for pSTAT1 (Tyr 701), pSTAT3 (Tyr 705), and pSMAD1 (Ser 463) to their corresponding total proteins and GAPDH after 15 min, 30 min, 60 min, 3 h, 6 h, and 1 d of PD and CNTF treatment. **B-D)** Quantification of western blots in terms of fold change with respect to CNTF 15 min for tSTAT1/GAPDH, pSTAT1/GAPDH and pSTAT1/tSTAT1 (**B**), tSTAT3/GAPDH, pSTAT3/GAPDH and pSTAT3/tSTAT3 (**C**), tSMAD1/GAPDH, pSMAD1/GAPDH and

pSMAD1/tSMAD1 (**D**). Data are represented as mean \pm s.e.m (n=3, * $p < 0.05$, *** $p < 0.001$, unpaired t-test).

The expression of tSMAD1 and its phosphorylation remained unchanged from NSCs to CNTF or PD differentiated cells. As CNTF is not known to activate the SMAD pathway, an increase in SMAD1 phosphorylation was not expected upon exposure of NSCs with CNTF (*Figure 29D*). From this early time point study, it was clear that PD does not follow the same differentiation timeline as usually reported for CNTF or BMP.

As STAT1/3 or SMAD1 are thought to be crucial for the expression of GFAP and the observed increase of tSTAT1 after PD treatment hints on the activation of an autoregulatory loop, described for the STAT1/3 pathway (*He et al., 2005*), their total and phospho protein levels were examined after 4 days of PD or CNTF treatment, using the similar experimental approach as employed for early time points (*Figure 30A*). Fold change was calculated with respect to 4 day CNTF treatment and NSCs were used as a negative control. As reported before for 1 day, the expression of tSTAT1 was higher in 4 day PD as compared to CNTF treated cells, with an 8 fold increase from NSCs and a 70% augmentation in comparison to CNTF. In addition, there was significantly 10 fold up regulation of pSTAT1/GAPDH and pSTAT1/tSTAT1 after 4 day of PD or CNTF treatment as compared to NSCs (*Figure 30B*). Similarly, a considerable 2 fold augmentation was detected in the expression of tSTAT3 upon exposure to PD in comparison to NSCs. Also, there was more than 2 fold and 10 fold increase in pSTAT3/GAPDH and pSTAT3/tSTAT3 in both 4 day PD and CNTF treated cells respectively (*Figure 30C*). Furthermore, the changes in total and phospho SMAD1 were investigated after 4 day treatment with PD or CNTF. However, no differences were observed in the expression of either total SMAD1 or its phosphorylated form between NSCs, PD and CNTF treated condition. Also, the expression of pSMAD1 in NSCs itself was quite variable (*Figure 30D*).

Taken together, the STAT1 and STAT3 signaling pathways have been shown to be involved in both PD and CNTF differentiation mechanisms, although their way of activation seems to differ in the two differentiation processes. The phosphorylation of STAT1 and STAT3 was delayed in the case of PD treated cells as compared to CNTF. Also, PD results in a noteworthy increase in tSTAT1 and tSTAT3. Moreover, STAT1 activation was found to be more prominent than STAT3 activation in PD treated cells.

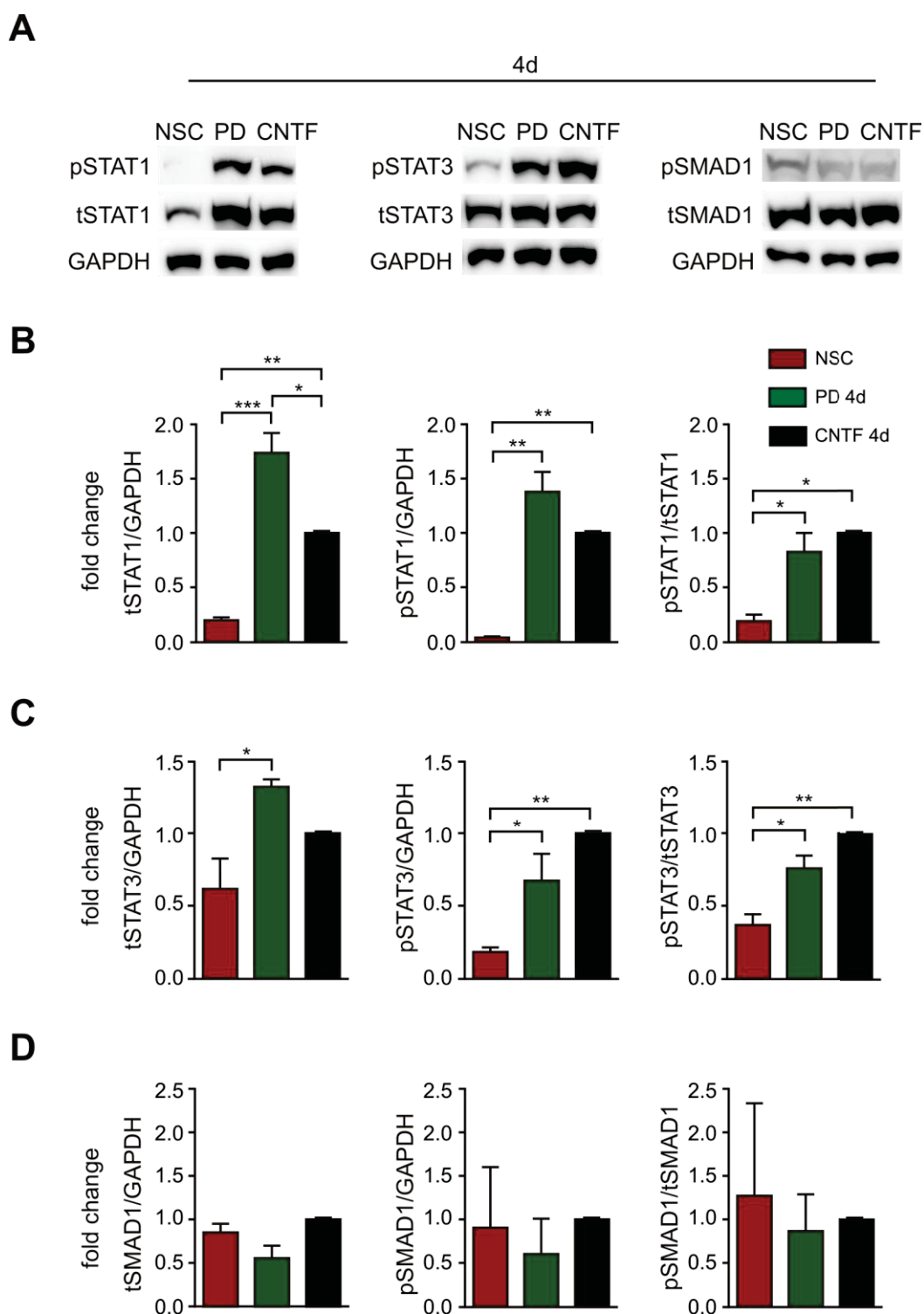


Figure 30: Late phosphorylation of STAT1/3 in the presence of PD.

A) Western blots for pSTAT1 (Tyr 701), pSTAT3 (Tyr 705), and pSMAD1 (Ser 463) to their corresponding total proteins and GAPDH after 4 d of PD and CNTF treatment. **B-D)** Quantification of western blots in terms of fold change with respect to CNTF 4 d for tSTAT1/GAPDH, pSTAT1/GAPDH and pSTAT1/tSTAT1 (**B**), tSTAT3/GAPDH, pSTAT3/GAPDH and pSTAT3/tSTAT3 (**C**), tSMAD1/GAPDH, pSMAD1/GAPDH and pSMAD1/tSMAD1 (**D**). Data are represented as mean \pm s.e.m (n=3, * p < 0.05, ** p < 0.01, *** p < 0.001, unpaired t-test).

3.4.2 PD mediates differentiation into low GFAP expressing astrocytes via Akt1 dependent pathway

Next, it was elucidated how inhibition of MEK dependent Erk1, 2 phosphorylation by PD leads to a delayed activation of STAT1/3. Akt1 phosphorylation by PI3kinase (PI3K) has been previously reported to result in formation of astrocytes by removing repressor from astrocytic genes (*Figure 3B*) (*Hermanson et al., 2002; Setoguchi et al., 2004*). Erk and Akt pathways share an upstream component Ras and inhibition of the Erk pathway has been shown to activate the Akt pathway in NGF stimulated PC12 cells (*Chen et al., 2012*). Following these reports, the phosphorylation status of Akt1 (Thr 308) was examined in the presence of PD and PD + 20 μ M LY294002 (LY- an inhibitor of PI3K) after 1 hr and 1 day of treatment. High doses of LY were avoided due to visible cell death at concentrations above 20 μ M. The phosphorylation of Erk1, 2 (Thr 202/Tyr 204) was also investigated to confirm the activity of PD (*Figure 31A*). For quantification, fold change was determined with respect to NSC control. Interestingly, a striking 3.8 fold upregulation of pAkt1 was observed after 1 day of PD treatment which was reduced in the presence of LY. Also, the activity of PD was confirmed by inhibition of Erk1, 2 phosphorylation after 1 hr and 1 day of PD application (*Figure 31B*). These results suggest a plausible role of Akt1 in directing astrocytic differentiation via PD.

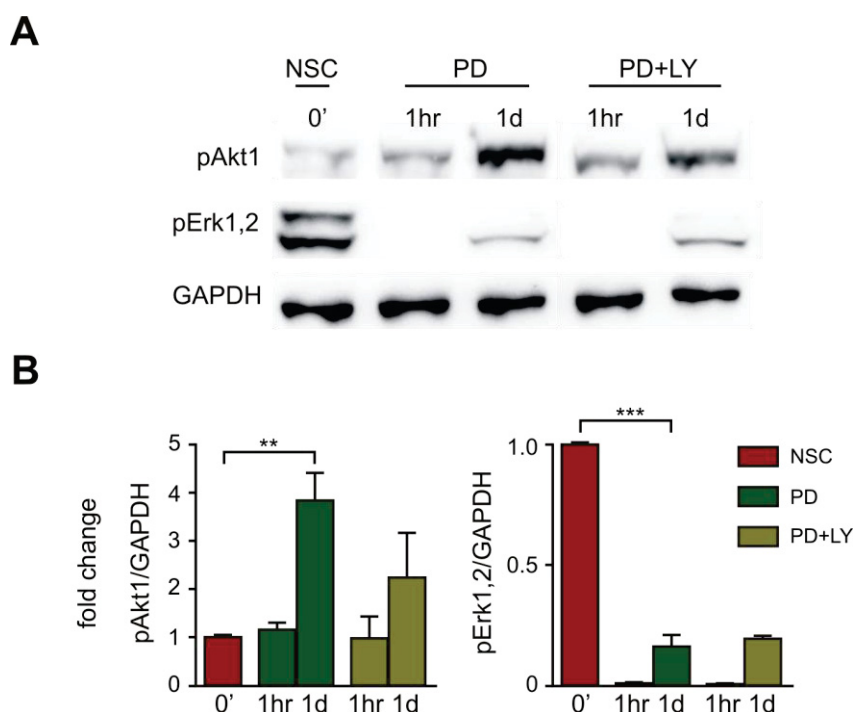


Figure 31: Increased phosphorylation of Akt1 upon exposure to PD.

A) Western blots for pAkt1 (Thr 308), pErk1, 2 (Thr 202, Tyr 204) and GAPDH after 1 h and 1 d of PD, PD+LY (20 μ M). **B)** Quantification of western blots in terms of fold change with respect to NSC control for pAkt1/GAPDH and pErk1, 2/GAPDH. Data are represented as mean \pm s.e.m (n=3, ** p < 0.01, *** p < 0.001, one way ANOVA, Tukey's post hoc test).

In order to further confirm the involvement of pAkt1 in PD mediated astrocyte differentiation, phosphorylation status of STAT1/3 was investigated in the presence or absence of PI3K inhibitor with or without PD treatment after 4 days (*Figure 32A, C*). NSCs without any treatment were used as control for calculating respective fold changes. As noted previously, the treatment of NSCs with PD resulted in a remarkable increase in both phospho and total STAT1, which was found to be significantly down regulated in the presence of LY (*Figure 32B*). In addition, augmented phosphorylation of STAT3 upon PD treatment was also abrogated in the presence of LY. However, the level of tSTAT3 remained significantly unaltered upon treatment with PD or LY or PD+LY (*Figure 32 D*). These data further strengthens our hypothesis of a PI3K-pAkt1 dependent activation of STAT1/3, resulting in the differentiation of low GFAP astrocytes in the presence of PD.

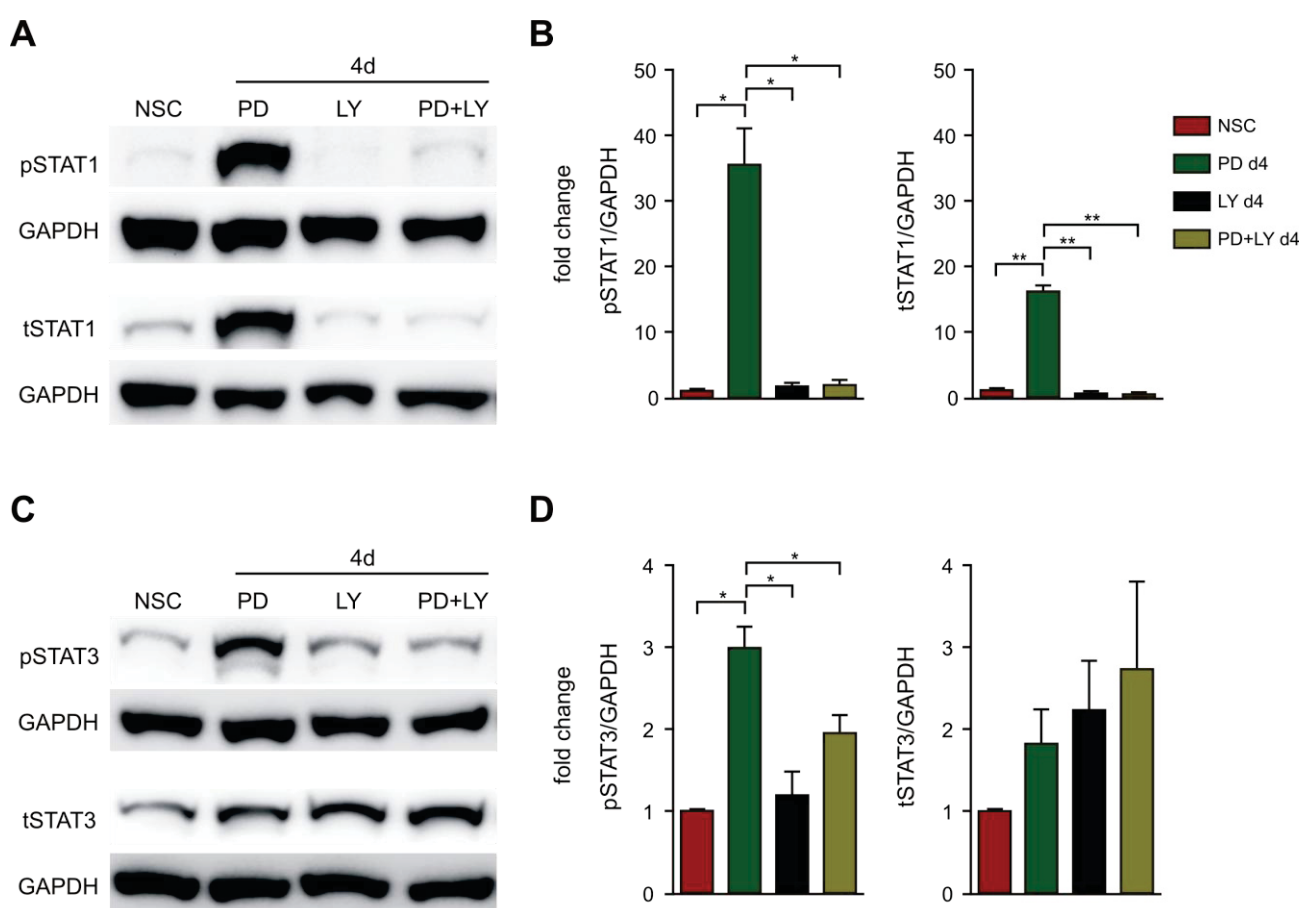


Figure 32: PI3K-pAKT1 dependent phosphorylation of STAT1/3 upon PD treatment.

A) Western blots for pSTAT1 (Tyr 701), tSTAT1 and GAPDH after 4 d of PD, LY, PD+LY (20 μ M). **B)** Quantification of western blots in terms of fold change with respect to NSC control for pSTAT1/GAPDH and tSTAT1/GAPDH. **C)** Western blots for pSTAT3 (Tyr 705), tSTAT3 and GAPDH after 4 d of PD, LY, PD+LY (20 μ M). **D)** Quantification of western blots in terms of fold change with respect to NSC control for pSTAT3/GAPDH and tSTAT3/GAPDH. Data are represented as mean \pm s.e.m (n=3, * p < 0.05, ** p < 0.01, one way ANOVA, Tukey's post hoc test).

Previously, a couple of studies have accounted for pAkt1 mediated phosphorylation of the gliogenic repressors Olig2 and NCoR. Once phosphorylated, these repressors are freed from the astrocytic genes and translocated from nucleus to cytoplasm, thereby allowing the formation of astrocytes (*Hermanson et al., 2002; Fukuda et al., 2004; Setoguchi et al., 2004*). To elucidate the importance of these gliogenic repressors in differentiation of PD derived low GFAP astrocytes, ICC was performed for total Olig2 and NCoR before and after 4 days of PD treatment (*Figure 33, 34*). Hoechst staining was performed to label the nucleus and use it as a region of interest (ROI) for analyzing the mean nuclear signal. The mean cytoplasmic signal was analyzed by generating ROIs in proximity of the nucleus. The ratio of mean nuclear to cytoplasmic signal was calculated from at least 250 cells per data set. In the case of NSCs, a differential expression of Olig2 was observed, with some cells displaying very high and other cells with comparatively low expression. However after PD treatment, the expression of Olig2 was more or less consistent between different cells and also between nucleus and cytoplasm. The ratio of nuclear to cytoplasmic mean intensity for Olig2 was $1.8 (\pm 0.089, n=3, p=0.002)$ in NSCs and $1 (\pm 0.046, n=3)$ after PD treatment (*Figure 33B*).

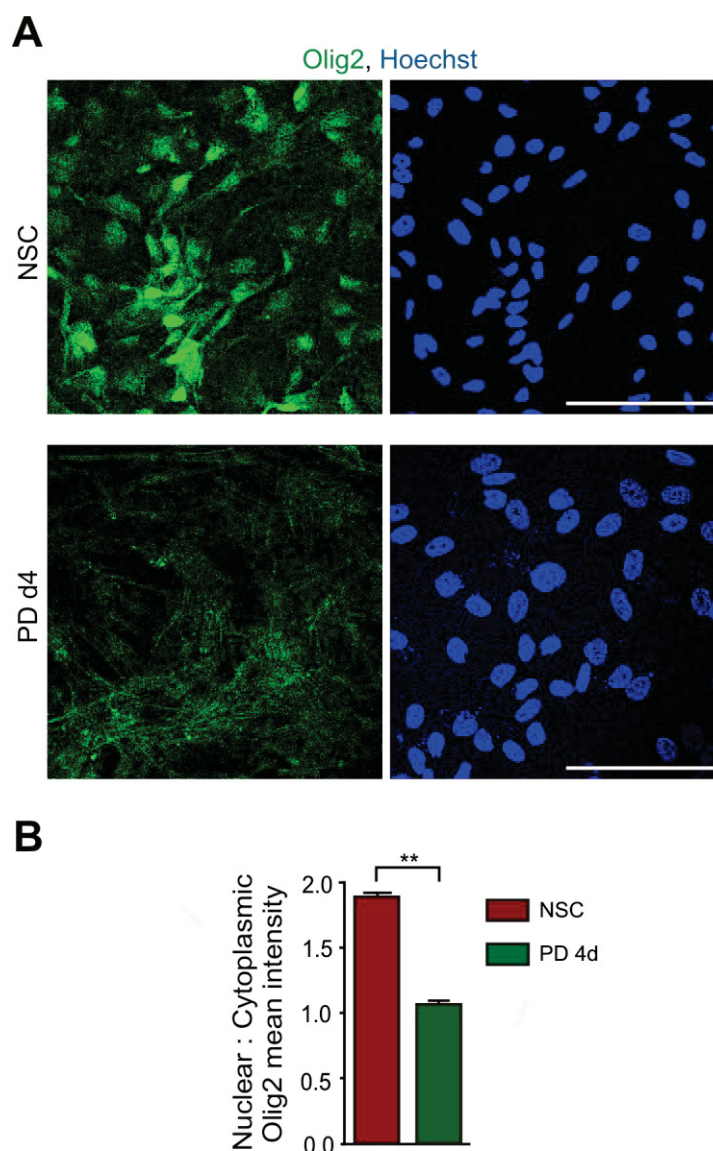


Figure 33: Nuclear export of Olig2 upon PD treatment.

A) Immunocytochemistry for Olig2 (green) in NSCs and after 4 d of PD treatment. Blue color represents Hoechst staining to label the nuclei. Scale bar = 100 μ m. **B)** Quantification of mean intensity for nuclear:cytoplasmic signal for Olig2 in NSCs and 4 d PD treated cells. Data are represented as mean \pm s.e.m (n=3, *** p < 0.001, unpaired t-test).

Regarding NCoR, both NSCs and PD treated cells expressed NCoR in the nucleus of almost all the cells, thereby ruling out a probable role of cytoplasmic translocation of this repressor as a prerequisite for PD mediated astrocyte differentiation (*Figure 34A*).

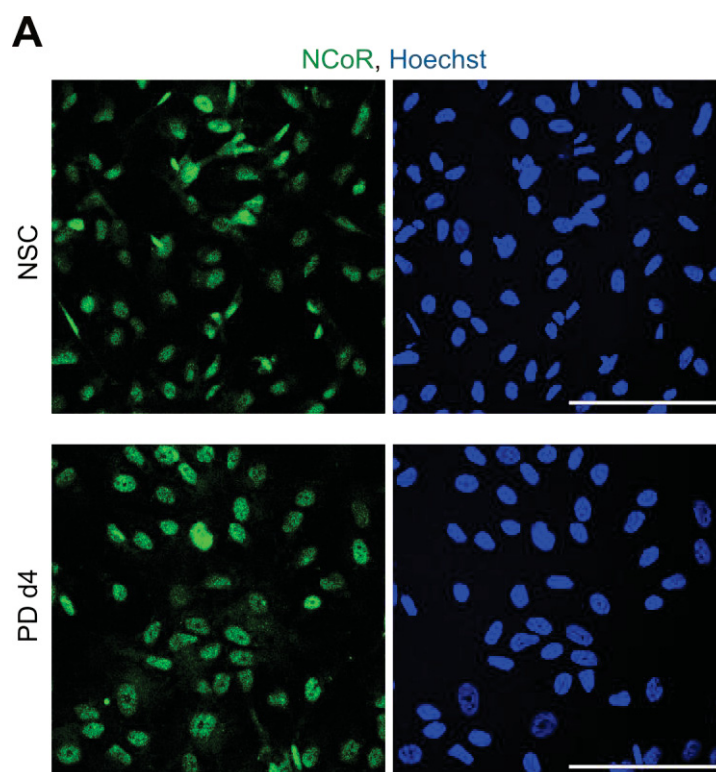


Figure 34: Maintenance of NCoR in the nucleus upon PD treatment.

A) Immunocytochemistry for NCoR (green) in NSCs and after 4 d of PD treatment. Blue color represents Hoechst staining to label the nuclei. Scale bar = 100 μ m, n=3.

Overall, these data suggest nuclear export of Olig2 as one of the downstream targets of PD mediated phosphorylation of Akt1. Whether PD mediates the differentiation of high GFAP expressing astrocytes from high passage NSCs by employing the same signaling pathways remains to be investigated.

3.5 Functional aspects of small molecule differentiated low GFAP astrocytes

3.5.1 Low GFAP astrocytes exhibit calcium transients typical of astrocytes

Calcium oscillations and waves in astrocytes are one of the most well studied mechanisms for the cells to respond to various stimuli and a mode of intra as well as intercellular signaling (*Scemes et al., 2006*). Here, the presence of calcium oscillations was examined in PD differentiated low GFAP astrocytes under different conditions which have been previously described for serum-free derived mouse astrocytes (*Foo et al., 2011*). Fluo-4 loaded NSCs and 14 days PD differentiated astrocytes were exposed to L-Glutamate (100 μ M) after acquiring 2 min of baseline calcium oscillations. The images were acquired for a total time of 10 min for both NSCs and PD. Images for both the cell types before and at different time points after substance application are

represented in *Figure 35A(i, ii)*. Almost 95% (± 0.001 , $n=3$) of PD differentiated astrocytes showed elevated intracellular calcium in response to L-Glutamate while only 45% (± 15.0 , $n=3$) of NSCs were responsive as analyzed within 100 sec of L-Glutamate application. Also, the calcium response of low GFAP astrocytes displayed a different kinetic, i.e. lasting longer than in NSCs (*Figure 35B, C*). These results show that also at a functional level, a differentiation towards astrocytes has taken place.

Next, the behavior of calcium oscillations was investigated upon exposure to ATP (100 μ M) in a similar way as done for L-Glutamate. Around 30% of NSCs and low GFAP cells responded to ATP but in a very diverse manner. NSCs responded with an increased but asynchronous calcium activity, whereas, low GFAP astrocytes exhibited a biphasic and highly synchronized response to ATP (*Figure 35D, E*). These findings suggest the presence of ionotropic and metabotropic purinergic receptors in low GFAP astrocytes, again proving a PD mediated differentiation at the functional level. Additionally, spontaneous calcium oscillations were also examined. 60% (± 18.61 , $n=3$) of NSCs had highly fluctuating calcium oscillations, while negligible number of low GFAP astrocytes exhibited any spontaneous calcium activity (*Figure 35H, I*). There is quite a lot of discrepancy for spontaneous calcium activity in astrocytes depending on the regional variations and also owing to the presence or absence of neurons (*Oberheim et al., 2012*). As these cells were cultured in the absence of neurons, no response was expected upon exposing them to high concentrations of KCl (50 mM) (*Figure 35F*). The small response seen in case of NSCs could be due to spontaneous activity as no major changes in fluorescence were observed immediately after application of KCl. Also, no activity was observed from low GFAP expressing astrocytes in response to KCl owing to the absence of neurons (*Figure 35G*).

Taken together, PD differentiated low GFAP astrocytes exhibited typical calcium responses described for cultured, serum free derived rodent astrocytes, whereas undifferentiated NSCs had different properties.

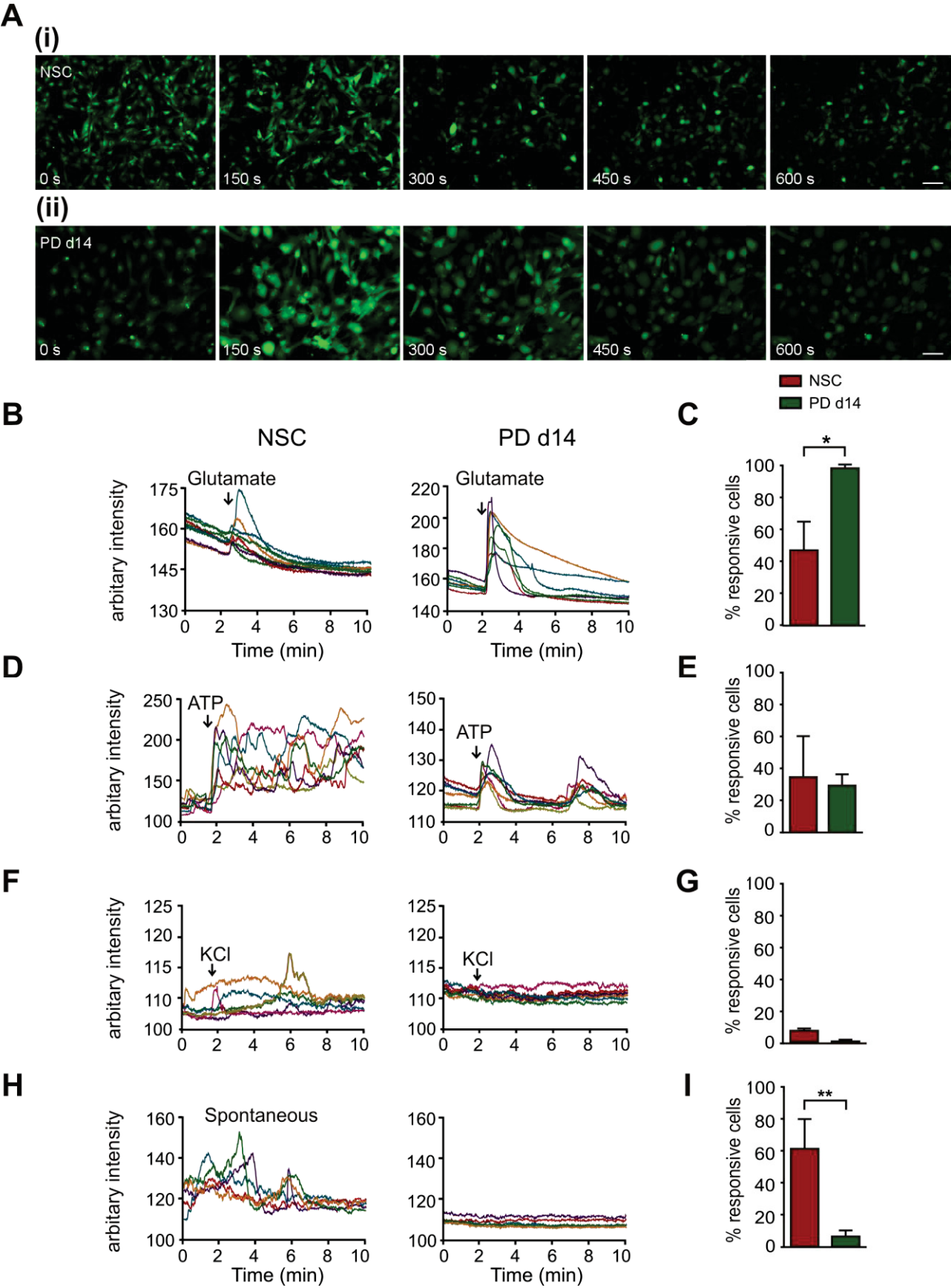


Figure 35: Calcium oscillations in PD differentiated low GFAP astrocytes upon exposure to stimulatory agents. Legend on next page

A) Fluo-4 loaded NSCs(**i**) and PD differentiated astrocytes(**ii**) at 0 s, 150 s, 300 s, 450 s and 600 s of calcium imaging. Cells were stimulated with addition of L-Glutamate (100 μ M) at 120 s. Scale bar = 100 μ m. **B,C)** Comparison of calcium oscillations in NSCs and PD differentiated astrocytes in response to L-Glutamate (100 μ M). **D,E)** Comparison of calcium oscillations in NSCs and PD differentiated astrocytes in response to ATP (100 μ M). **F,G)** Comparison of calcium oscillations in NSCs and PD differentiated astrocytes in response to KCl (50 mM). **H,I)** Comparison of spontaneous calcium oscillations in NSCs, and PD differentiated astrocytes and quantification in terms of percent responsive cells. Data are represented as mean \pm s.e.m (n=3, * p < 0.05, ** p < 0.01, unpaired t-test).

3.5.2 Low GFAP astrocytes exhibit sodium dependent glutamate uptake

Clearance of glutamate from the extracellular milieu by the glutamate transporters EAAT1 and EAAT2 is one of the major properties of astrocyte by which they prevents neurons from glutamate mediated excitotoxicity and shape synaptic responses. Also, glutamate taken up by the astrocytes is the main source of glutamine provided to neurons after amination by glutamine synthetase (Hertz, 2013). The ability to take up glutamate in PD differentiated low GFAP astrocytes was evaluated by incubating the cells for 2 hours, in a buffer containing L-Glutamate (50 μ M), in the presence or absence of the glutamate transporters inhibitor- *L-trans*-Pyrrolidine-2,4-dicarboxylic acid (PDC, 1 mM). Removal of Na⁺ from the buffer served as an additional control, as the glutamate transporters are Na⁺ dependent. By measuring the remaining glutamate in the extracellular solution under different conditions, it was found that PD differentiated astrocytes displayed a transporter dependent uptake of glutamate which was significantly decreased by more than 25% (\pm 8.2, n=6, p=0.0035) in the presence of PDC and 60% (\pm 14.1, n=6, p=0.00079) after removal of Na⁺ (Figure 36A).

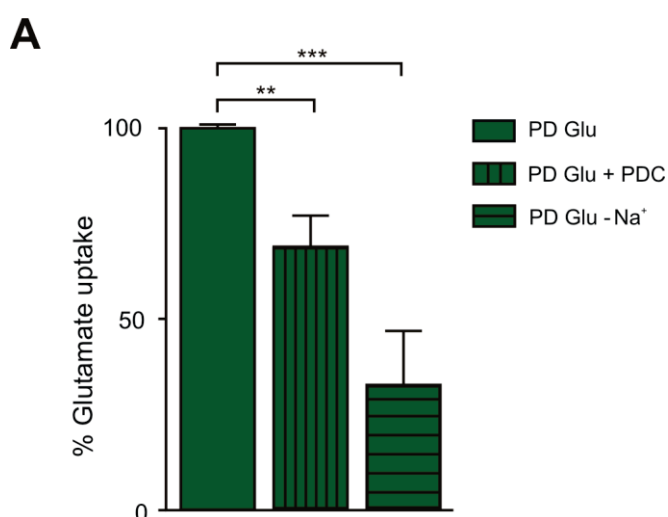


Figure 36: L-Glutamate uptake by PD differentiated low GFAP astrocytes.

A) Glutamate uptake capacity of PD differentiated astrocytes after 2 h incubation of the cells with L-Glutamate (50 μ M), either in the presence or absence of PDC (1 mM) or Na⁺ as negative controls. Data are represented as mean \pm s.e.m (n=6, ** p < 0.01, *** p < 0.001, unpaired t-test).

Collectively, these data demonstrate the functional potential of low GFAP astrocytes. In the previous data, the presence of Cx43 and glutamate transporters (EAAT1 and EAAT2) was shown at mRNA or protein level. Here, the evidence for them to be functionally active is provided.

3.5.3 Low GFAP astrocytes respond to reactive stimuli

Astrocytes turn reactive in response to injury and disease. This is marked by a profound increase in the release of inflammatory cytokines and chemokines as well as change in the cell morphology. The response of the cell may vary depending on the type of injury which also decides whether it is protective or detrimental to neurons (*Zamanian et al., 2012*). A pro-inflammatory cytokine- TNF α and bacterial endotoxin- LPS, which are known to trigger gliosis *in vitro* were employed to explore the potential of PD differentiated low GFAP astrocytes to turn reactive. NSCs and 14 day old astrocytes were exposed to either TNF α (50 ng/ml) or LPS (100 ng/ml) for 24 hours, followed by performing qPCR for reactive astrocyte markers. PD differentiated cells demonstrated a remarkable increase in *Serpina3n* and *Lcn2* upon exposure to TNF α (*Figure 37A*). NSCs also exhibited a tremendous increase in *Serpina3n* and a slight but significant increase in *Lcn2* upon exposure to TNF α (*Figure 37B*). This could be the result of upregulated NF-KB dependent STAT signaling pathway in NSCs. GFAP was significantly down-regulated in both NSCs and PD differentiated astrocytes upon treatment with TNF α (*Figure 37A, B*). These results confirm the earlier reports describing no effect of TNF α on intracellular GFAP expression (*Edwards et al., 2006; Roybon et al., 2013*) even after 7 days of exposure.

In contrast to TNF α , LPS did not lead to a significant enhancement in any of the reactivity marker in NSCs (*Figure 37D*). Whereas, in PD differentiated astrocytes, a small but significant increase was found for *Serpina3n* and GFAP. However, no significant difference was seen in *Lcn2* expression (*Figure 37C*). These data show that low GFAP astrocytes are able to react to inflammatory stimuli with different responses, depending on the type of insult.

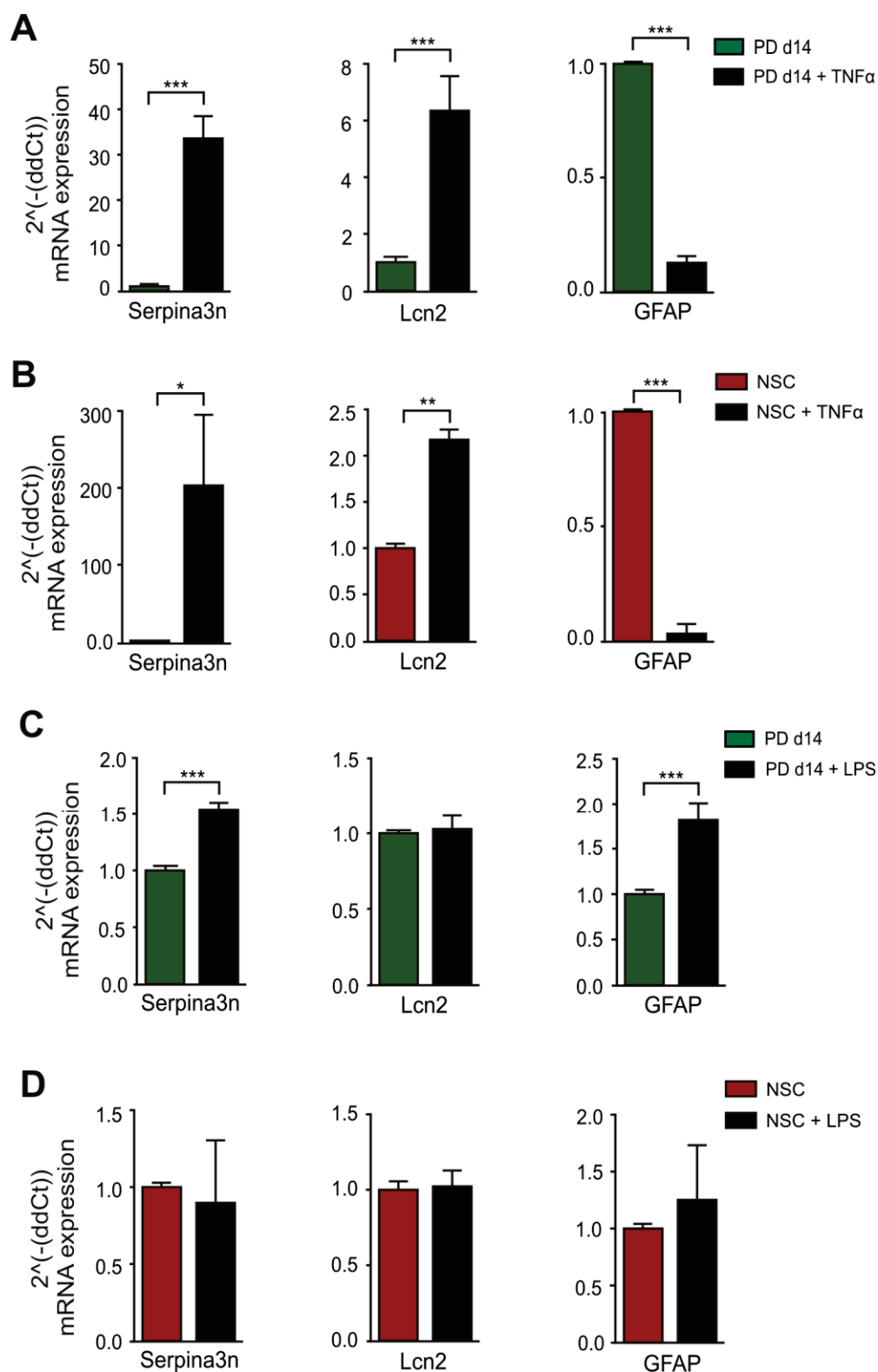


Figure 37: PD differentiated low GFAP astrocytes respond to inflammatory stimuli by augmenting markers for reactivity.

A,B) qPCR for Serpina3n, Lcn2 and GFAP after 1 d of TNFα treatment (50 ng/ml) for 14 d PD differentiated astrocytes (**A**) and NSCs (**B**). **C,D)** qPCR for Serpina3n, Lcn2 and GFAP after 1 d of LPS treatment (100 ng/ml) for 14 d PD differentiated astrocytes(**C**) and NSCs(**D**). Data are represented as mean ± s.e.m (n=3, * p < 0.05, ** p < 0.01, *** p < 0.001, unpaired t-test).

Astrocytes have been earlier reported to be highly sensitive to changes in pH of the extracellular medium, mimicking environmental changes occurring in injured tissue and acquire an irreversible reactive state, with an increased intracellular level of GFAP (*Giffard et al., 1990; 2000*). For this assay, 14 day PD treated cells were exposed to a low pH buffer (6.8) for 10 hours. Longer time point could not be followed due to visible cell death starting at the later stages. 14 day PD differentiated low GFAP astrocytes cultured in pH 7.4 buffer were considered as a control (*Figure 38A*). After this 10 hour period, a significant increase was found in GFAP expression in $\sim 32\%$ (± 3.19 , $n=3$, $p=0.02$) of cells exposed to acidic condition (*Figure 38B*).

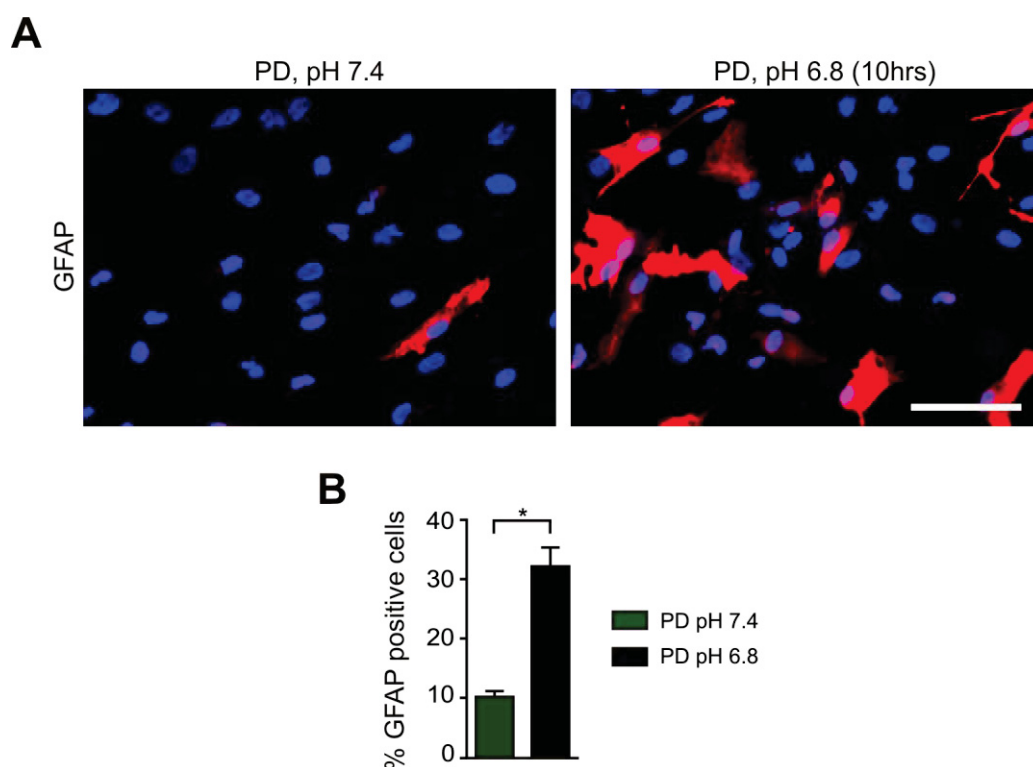


Figure 38: PD differentiated cells exhibit increased GFAP expression under acidic conditions .

A) Immunostaining for GFAP (red) for 14 d PD differentiated cells maintained under pH 7.4 and the cells exposed to pH 6.8 for 10 h. Blue color represents Hoechst staining to label the nuclei. Scale bar = 100 μ m. **B)** Quantification of percent of GFAP positive cells to total number of nuclei under normal and acidic condition. Data are represented as mean \pm s.e.m ($n=3$, * $p < 0.05$, unpaired t-test).

Overall, these data along with the previous results confirm the ability of low GFAP astrocytes to be functionally active and responsive to various kinds of reactivity assays.

4. Discussion

In this study, a novel small molecule based approach for differentiation of iPSC derived NSCs towards astrocytes has been developed. The differentiation protocol proved to be not only more consistent and faster than CNTF induced differentiation; it also enabled generation of high and low GFAP expressing astrocytes from different states of NSCs upon treatment with the same small molecule. The differentiated astrocytes were characterized by investigating the expression of different astrocyte specific markers like ALDH1L1, Cx43, GS, EAAT2 and others. Additionally, the functional properties of differentiated astrocytes were elucidated by ATP and L-Glutamate stimulated calcium transients, glutamate uptake capacity and their ability to turn reactive upon exposure to acidic or inflammatory conditions. Furthermore, the small molecule mediated differentiation towards low GFAP astrocytes was found to be dependent on PI3K-pAkt1 directed STAT1/3 signaling and nuclear export of Olig2 transcription factor. Also, a growth factor based approach to trigger astrocyte differentiation potential of early NSCs has been described.

4.1 Derivation of neural stem cells from iPSCs and characterization of their gliogenic potential

Studies have shown that coordinated inhibition of BMP and Activin/Nodal signaling, i.e. dual inhibition of SMAD, directs a highly efficient neuroectoderm specification (*Chambers et al., 2009*). A previously described combination of small molecules- SB431542 and Dorsomorphin was employed to promote neural induction of iPSCs mediated via dual SMAD inhibition. Dorsomorphin was earlier reported to block BMP type 1 receptor ALK2, 4 and 6; thereby BMP mediated SMAD1/5/8 phosphorylation (*Morizane et al., 2011*). SB431542- a known antagonist of TGF- β signaling inhibits Smad2/3 and Smad1/5 phosphorylation by ALK 4, 5 and 7 receptors (*Inman et al., 2002*). To generate indefinitely self-renewing NSCs from neuroepithelial cells, NSCs were maintained in EGF and FGF. These two growth factors are crucial for maintaining self renewing and proliferative potential of the stem cells (*Reynold et al., 1992; Pollard et al., 2008*). NSC identity was first characterized by evaluating the mRNA expression level of previously established markers: a) class VI intermediate filament protein- Nestin and b) NSC specific transcription factor Sox2, both of which were found to be almost consistent among different NSC lines tested in this study (*Lendahl et al., 1990; D'Amour et al., 2003*) (*Figure 13A*).

As the main goal of this study was to differentiate NSCs towards astrocytes, a characteristic marker profile had to be determined and validated in order to estimate the astrocytic potential of these cells. According to our current understanding of astrocyte development (mostly from the spinal cord studies), a temporal expression of gliogenic markers has been reported, starting with A2B5 and going to more specifically astrocyte restricted progenitor markers- Sox9, NF1A, NF1B, EGFR, STAT3, CD44, NF1C and NF1X. It is still not clear whether or not these markers follow the same temporal pattern in cortical development and whether or not the expression level of early markers is retained throughout development.

To determine the astrogenic potential of different NSC lines which had been initially generated under varying conditions, the expression of aforementioned markers was investigated. The expression of NF1A was high in lines E and F, whereas these lines exhibited minimal CD44 at both mRNA and protein level (*Figure 13A, B*). In contrary, expression of NF1A decreased in NSC line K as it displayed high levels of CD44 which suggests an early role of NF1A (*Deneen et al., 2006; Kang et al., 2012*) and delayed role of CD44 (*Liu et al., 2004*) in astrocyte development. A2B5, a ganglioside detecting antibody, was used as a general gliogenic marker, however, only a few cells in NSC line E and F were positive for it compared to line K (*Figure 13B*), pointing to a more neurogenic stage of these two lines. It also reflects the degree of heterogeneity within each line. For a deeper investigation of the gliogenic potential, two more lines- NSC B and O were analyzed by quantitative PCR, along with NSC line K. NSC line B displayed minimal expression of CD44, EGFR, STAT3 and NF1B as compared to line K and O, thus suggesting that line B could be still in the neurogenic phase. The consistent level of NF1C and NF1X among different lines indicates a delayed role of these two transcription factors (*Figure 14A*). These observations follow the previous knockdown studies where, NF1B has been shown to initially regulate FGFR and EAAT1 expression and later control GFAP; and NF1C, NF1X have been found to be important in inducing GFAP and SPARCL1 expression later in astrocyte development (*Mason et al., 2009; Wilczynska et al., 2009*). The gliogenic potential of these lines was additionally confirmed by differentiating them with the small molecule based approach for 9 days. It was observed that the lines which were still in the neurogenic stage exhibits tremendous cell death within 1-3 days of differentiation, while no significant cell death was seen in the gliogenic lines (data not shown). Based on these results, it was concluded that NSC line K and O exhibited the maximum gliogenic potential among the tested lines and therefore would be suitable to conduct astrocyte differentiation.

Another important question was to figure out an appropriate passage number under defined NSC culture conditions, for using these lines for astrocyte differentiation as both *in vivo* and *in vitro* studies have reported efficient astrocyte differentiation only late in development (*Krencik et al., 2011; Roybon et al., 2013; Semple et al., 2013*). Therefore, new NSC lines were generated from iPSCs and analyzed for NSC and gliogenic markers with increased passaging by performing immunostaining and qPCR. As shown in *Figure 15A, B* and *16A*; A2B5, CD44 and NF1A were augmented with increased passaging, with almost 100% positive cells at passage 10-12. Although the mRNA levels of Nestin were found to be slightly reduced, but the expression at protein level was conserved in all the cells with increased passage thereby confirming the maintenance of NSC stage. Depending on literature and my previous results on the delayed role of NF1B, NF1C and NF1X, their expression was examined at higher passages; all of which were doubled with increase in passage from P16 to P23 (*Figure 15C*).

To elucidate the underlying mechanism of glial induction in the culture system, the expression of astrocyte restricted markers were compared at P5 and P10 in different culture medium, containing FGF alone or EGF + FGF (10 ng/ml each). The presence of FGF in the culture medium can indirectly affect gliogenic potential as it renders early NSCs to be responsive to EGF via induction of EGF receptor (EGFR) (*Viti et al., 2003*). The responsiveness to EGF coincides with the acquisition of gliogenic potential in these cells as shown by the *in vitro* differentiation potential of NSCs isolated at E10 and E17 from the mouse brain (*Ciccolini et al., 1998 Kilpatrick et al., 1995*). Also, it has been shown that, with increased EGFR expression, there is an upregulation of STAT3 and thus enhanced phospho-STAT3 in the presence of LIF, thereby directing NSCs towards astrocytes (*Viti et al., 2003*). Thus, as expected, FGF increases the gliogenic potential over time, which explains the up regulation of both NF1A and CD44 with increased culture duration. However, the NSCs at P5, when exposed to EGF + FGF medium were able to exhibit a similar augmentation in gliogenic markers which was observed at P10 in FGF alone medium (*Figure 16A, B*). This indicates that, NSCs kept in FGF alone are able to maintain their neurogenic fate for some passages, whereas, the presence of EGF induces gliogenic potential already at early passages. Similar observations have been reported before in NSCs derived from mouse embryonic stem (ES) cells (*Sanalkumar et al., 2010*) and were used by *Serio et al., 2013*; to enrich for ARPs in iPSC derived NSC cultures by a prolonged culture period in EGF + LIF.

4.2 Differentiation of NSCs towards high GFAP expressing astrocytes

Earlier, differentiation into astrocytes and maintenance of primary astrocytes was usually carried out in serum containing media as it serves as a rich source of growth factors, vitamins, proteins and trace elements. However, gradually it was realized that serum may not be an ideal choice for cell culture due to several reasons. Besides the ethical concerns associated with obtaining serum from unborn calves, batch to batch variations in the serum constituents have been found due to seasonal and continental differences, thereby resulting in inconsistent data. In addition, serum may pose a mode of contamination as approximately 20-50% of the commercially available serum has been found to contain viruses (*Wessman et al., 1999*). Furthermore, the astrocytes derived from serum containing medium have been found to be highly non physiological, displaying a different gene expression profile and functional properties than their serum free counterparts and *in vivo* cortical astrocytes. Indeed, the gene expression profile of serum cultured astrocytes has been shown to be a mixture of developing and reactive astrocytes (*Foo et al., 2011; Zamanian et al., 2012*). To overcome these issues, it became necessary to establish a serum free, defined and replicable culture medium for the differentiation of astrocytes. Mostly, this is achieved by using a chemically defined medium supplemented with expensive growth factors and cytokines like CNTF or cardiotrophin or BMP and LIF. Growth factor deprived medium and CNTF has been previously used to generate astrocytes from rodent or human ES cells (*Lillien et al., 1998; Zhang et al., 2001*). In addition to these two approaches, in this study, a small molecule- PD0325901 (an inhibitor of MEK pathway) was employed to direct differentiation of NSCs into astrocytes. Earlier, PD has been used as a replacement for BMP and LIF in serum free mouse ES cell cultures to inhibit differentiation via MAPK pathway and to activate STAT3 pathway required to maintain their self renewing capacity (*Ying et al., 2008*). Since, BMP and LIF are well established mediators of astrocytic differentiation in humans; acting through phosphorylation of SMAD and STAT pathways (*Nakashima et al., 1999*), PD was used as a replacement protocol for BMP and LIF. Additionally, a couple of studies have previously demonstrated differences in the astrocytes differentiated with BMP or CNTF in terms of the expression of markers like Cx43, EAAT2, AKAP12, GDNF and their role in promoting functional recovery after spinal cord injury (*Davies et al., 2011; Okano-Uchida et al., 2013*). Following these reports, it would be interesting to see whether differentiation with PD or CNTF would lead to different types of astrocytes. Very low dose of PD (0.25 μ M) was used as this was found to be sufficient to promote astrocyte differentiation as investigated through qPCR for astrocyte genes- CD44, AldoC, and GFAP (*Figure 8*). Moreover, as PD is an inhibitor for

MAPK, which is one of the central pathways for cell survival, therefore higher doses could have been lethal to the cells.

Based on the expression of CD44 at P12 in almost all the cells, these cells were considered to possess ARP properties and should be able to give rise to astrocytes. Therefore, initially the astrocyte differentiation was performed using NSCs between passage 15-20 using above mentioned three approaches for 14 days. Growth factor removal was expected to decrease cell proliferation and hinder sustenance of the stem cell stage. A number of published protocols for astrocyte differentiation have employed this strategy before for both rodent and human cells (*Schwindt et al., 2009*). In alignment with the previous reports, growth factor deprivation was able to induce astrocyte differentiation in human iPSCs with around 30% rise in high GFAP expressing cells; however, this approach appeared to be quite variable in our system (*Figure 17B, C*). This could be attributed to the secretion of growth factors by NSCs themselves which in turn can compete with the differentiation step. Therefore, use of an agent for e.g. CNTF or BMP and LIF to push these cells towards astrocytes would be another option. However, an increase in high GFAP expressing cells was not achieved by CNTF or PD treatment. Thus, although most of the cells at these experimental passages were CD44 positive, they were still not mature enough to get converted into high GFAP expressing astrocytes.

A previous report has emphasized the need for culture duration of almost 6 months for iPSC derived NSCs to let them attain the potential for astrocyte differentiation (*Krencik et al., 2011*). Following this approach, the differentiation was performed using higher passage cells (higher than P40), which lead to an increase in the number of high GFAP expressing cells (*Figure 18B*). Notably, the highest yield (50%) could be achieved with the small molecule approach, invented in this study. Self differentiation upon growth factor removal was not so efficient, and also the addition of CNTF could increase the percent of differentiated cells to only 30% (*Figure 18 A, B*). The total yield could probably be improved by further differentiation of the cells for much longer duration, which poses a limitation for continuous supply of these cells required for disease modeling. These data also support the previous finding of *Krencik et al., 2011*; where long culture time of almost 6 months for NSCs was found to be necessary for obtaining a homogenous population of 70-80% GFAP expressing cells after CNTF differentiation. Interestingly, the MAPK pathway, which is inhibited by PD, has recently been proved to be essential for regulating the gliogenic switch and thus the generation of ARPs, giving rise to high GFAP expressing cells (*Li et al., 2012*). The present data however show that, final astrocyte differentiation can occur

independent of MAPK, suggesting the need for further investigation in elucidating the temporal role of MAPK during astrocyte development by performing *in vivo* studies.

4.3 Induction of the gliogenic switch

To further improve the protocol and reduce the differentiation time to some extent, it would be important to trigger the gliogenic switch in early NSCs. Epigenetics of the GFAP gene have been previously shown to play an imperative role in this by modulating the binding ability of STAT to the promoter region. In the neurogenic phase, the promoter region of GFAP is hypermethylated at lys 9 of histone 3. A previous study demonstrated that by using a combination of small molecule-5 Azacytidine (AzaC) and Trichostatin A (TSA), the inhibitors for DNA methyltransferase (DNMT) and class I and II histone deacetyltransferase (HDAC) respectively, it is possible to direct epigenetic changes on the astrocytic gene promoter sites (CD44, GFAP, S100B and AQP4), thus inducing the gliogenic fate of NSCs (*Majumder et al., 2013*). First, a similar approach was tried using AzaC and TSA alone or in combination at a concentration ranging from 10 nM to 2.5 μ M for AzaC and 1 nM to 200 nM for TSA. However, a tremendous cell death was observed within 1 day of treatment even at the lowest concentrations (data not shown). This could be the result of *a*) AzaC mediated inhibition of DNMT1, which is required for survival of NSCs at embryonic stages as shown by using conditional knockout of DNMT1 and *b*) TSA mediated blockade of HDAC5 which has been shown to be vital for NSCs proliferation. Later in the development, at around E15.5 in rodents, the endogenous levels of DNMT1 are greatly reduced, thereby promoting gliogenesis (*Fan et al., 2001; Sun et al., 2007*).

Furthermore, exposure to high dose of FGF for 24 h in mouse stem cells has been previously shown to specifically demethylate the GFAP promoter site, rendering it free for the binding of STAT, thereby allowing CNTF to function (*Song et al., 2004*). In addition, as mentioned before, FGF has also been known to promote the gliogenic lineage by increasing the expression of EGFR (*Figure 2A, C*). These findings have been confirmed *in vivo* in a recent study, showing that the MAPK pathway is essential for the occurrence of ARPs during brain development (*Li et al., 2012*). However, another study postulated that FGF maintains multipotent lineage of NSCs, promoting expression of proneural genes at early stage and astrocytes later in development and EGF was shown to enhance gliogenesis when ES cells were maintained solely in one of these growth factors. Also, they observed that FGF and EGF exposure may be a deciding factor for the morphological variations in the GFAP positive cells being formed, FGF giving rise to fibroblast like and EGF to radial glia like astrocytes (*Sanalkumar et al., 2010*). For a better perception of

the role of growth factors in triggering the gliogenic switch, we used either of these growth factor at a higher dose (100 ng/ml) along with optimal concentration of the other (20 ng/ml) for one week (referred to as high FGF and high EGF) and then examined its effect on the gliogenic potential of NSCs. As the main objective of the experiment was to cut down the time required for differentiation towards high GFAP expressing astrocytes, therefore very low passage (P7-P9) NSCs were used. The percentage of CD44 positive cells was almost 80% in all the three conditions (uninduced, high FGF and high EGF) (*Figure 19A, B*). Also, NSCs retained a low GFAP expression in the presence of growth factors, which suggested a need of differentiation factors to push them towards astrocytes (*Figure 19C, D*). This was done by growth factor removal, the CNTF or PD approach as used before. Differentiation time was increased to 24 d as the NSCs used were at very low passage. The removal of growth factors alone didn't bring any further improvement in the number of GFAP expressing cells as it might need a longer differentiation time without addition of any external differentiation factor. However, in the presence of CNTF, the percentage of GFAP positive cells increased significantly by up to 50% after high FGF treatment and a non significant 31% increase was attained with high EGF. On the other hand, PD cells retained a very minimal expression of high GFAP expressing cells even after induction (*Figure 19 E, F*). The results obtained, seem to follow the FGF pathway shown by *Song et al., 2004* in mouse cells, whereas EGF proved to be ineffective in inducing the differentiation into high GFAP expressing cells with low passage NSCs. One of the reasons for this could be that not all the NSCs were EGF responsive at this passage. This suggests that after maintenance of NSCs for more passages (15-20), there might be a sufficient expression of EGFR on all the cells, rendering them responsive to EGF which would increase the chances for astrocytic differentiation upon EGF induction. Also, no prominent morphological differences were observed after FGF or EGF induction and differentiation. With these results it was concluded that it is possible to induce differentiation of almost 50% of human NSCs towards high GFAP expressing astrocytes within a period of two months by exposure to high doses of growth factors. Further, a complete characterization of these cells with other astrocytic markers and functional assays would support the use of this protocol on a regular basis. Besides this, it is to be noted that although 80% of NSCs expressed CD44, but only 30% of uninduced and 50% high FGF induced cells could be successfully differentiated into astrocytes after 24 d CNTF exposure. This highlights the necessity to explore better markers for identifying astrocyte precursors which may differ between rodents and humans.

4.4 Differentiation of NSCs towards low GFAP expressing astrocytes in the presence of PD

Until now, most of the published protocols for differentiation of astrocytes from pluripotent stem cells (independent of the use of serum or culture duration) judge differentiation efficiency exclusively by the expression of GFAP (*Krencik et al. 2011; Gupta et al., 2012; Shaltouki et al., 2013; Serio et al., 2013; Wang et al., 2013; Williams et al., 2014*). One less defined protocol has considered reduced expression of GFAP upon maturation of astrocytes, however it is focusing on the generation of spinal cord astrocytes and employs long term differentiation in FBS containing medium (*Roybon et al., 2013*). Another study on the generation of low GFAP expressing astrocytes fails to prove any of their astrocyte like characteristics except showing increased reactivity upon exposure to serum (*Paşca et al., 2015*). However, in the last decade, the heterogeneity of astrocytes in different regions of the brain have been widely explored, both at anatomical and molecular level. GFAP has been proved not to be “the marker” for all types of astrocytes, as it shows weak expression in gray matter protoplasmic astrocytes, which are the major type of astrocytes in the brain. Another problem with using only GFAP as the marker to define astrocytic population is that it is also expressed in the adult type B stem cells as well as it is upregulated in reactive astrocytes. For a better characterization of astrocytes, a spectrum of other pan astrocytic markers has been postulated, for e.g. ALDH1L1, ApoE, Glutamine synthetase, Clusterin, AQP4, Aldolase3, Cystatin 3 (*Bachoo et al., 2004; Oberheim et al., 2006; Cahoy et al., 2008*). Considering astrocyte heterogeneity, it is important to study their development and distinct role in pathology. Establishing culture systems for individual subtypes of astrocytes offers a possible way for such investigations.

Based on the previous results with the exposure of 15-20 passage NSCs to PD, a sudden change in NSCs morphology was observed within 3 days and; after 14 days of treatment the treated cells appeared quite similar to astrocytes cultured with serum, being converted into big, flat cells in the phase contrast (*Figure 21A*). The change in morphology was more clearly visible after staining the cells with membrane permeant, lipophilic dye- calcein (*Figure 21B*). Also, as PD is an established blocker for MAPK pathway, one could expect a negative effect on cell survival. But, as all of the 14 days PD treated cells stained with calcein, it accounted for lack of cell death upon PD treatment as the dye fluoresces only when acted upon by cellular esterases, thereby making it one the commonly used dyes for live dead assays. Furthermore, another expected effect of PD treatment would be decreased proliferation due to blockade of MAPK. Investigation of cell proliferation marker- Ki67 (*Brown et al., 2002*) revealed a significant reduction within 4 days of

PD treatment both at mRNA and protein level. A similar reduction was observed in the expression of Sox2, one of the widely used NSC markers (*Figure 22A, B, C*). In addition, impeding of Sox 2 is also related to maturation of astrocytes, as its expression is known to be maintained in the early, dividing stage of astrocyte formation (*Komitava et al., 2004*). Also, in rodents, it is known to be induced in case of injury resulting in reactive gliosis (*Bani-Yaghoub M et al., 2006*). Further, reduction in the NSC marker- Nestin supported the hypothesis of a departed NSC stage in PD treated cells (*Figure 23A*). Next, the mRNA expression pattern of previously described ARP markers- CD44, NF1A, NF1B, NF1C and NF1X was examined. Among the NF1 genes, only NF1A showed a significant downregulation after PD treatment. It is known to be expressed early on in astrogenesis, forming a complex with Sox9 to induce the astrocytic lineage. The other NF1 factors remained unchanged, as their role is confined to regulating astrocyte maturation and GFAP expression (*Mason et al., 2009; Wilczynska et al., 2009; Kang et al., 2012*). Earlier results also suggest a similar temporal pattern for NF1 genes during progressive glial restriction of NSCs (*Figure 14A, 15C and 16B*). They are only upregulated in higher NSC passages (*Figure 15C*), which were later shown to give rise to higher number of GFAP expressing cells. CD44 has been described as “the” ARP marker in rodents, shown to be expressed at late stages of astrogenesis, giving rise to a high GFAP expressing population upon exposure to serum (*Liu et al., 2004*). In human NSCs, at least 80% CD44 expressing cells were observed within 2-3 months of NSCs culture, however, only 30% of these cells expressed high levels of GFAP upon differentiation (*Figure 19B, 20C*). However, around 80% of the cells expressed other astrocytic markers like ALDH1L1, GS or EAAT1 (*Figure 25B, D and F*). Therefore, CD44 was confirmed as an ARP marker, labeling cells that can upregulate astrocytic markers other than GFAP after differentiation. Furthermore, it is postulated that NF1A acts as early (cells die after PD treatment), CD44 as intermediate and NF1B, NF1C and NF1X as late astrocyte lineage markers. 14 day PD treated cells displayed a decrease in early and intermediate but maintain late ARP markers at mRNA level (*Figure 23A*). These data, besides implying that PD treated cells are no longer in a proliferative neural stem cell stage, also hints towards their progression into a late astrocytic lineage.

As the previous data suggested astrocytic lineage of PD treated cells, subsequent examination of S100 β (an early astrocyte marker) stained above 90% of cells differentiated for 14 days, thereby strengthening our idea of PD mediated astrocytic differentiation. However, staining with the classical astrocyte marker GFAP exhibited no significant increase from NSCs to PD differentiated astrocytes, with a maximum of 5% high GFAP expressing cells after PD treatment (*Figure 24A, B*). This could lead to two different conclusions: a) 14 days PD differentiated cells

were still at an immature astrocyte stage and needs to be cultured for much longer duration to express a homogenous high GFAP expressing population, b) PD differentiated cells were low GFAP expressing astrocytes corresponding to previous reports on the existence of low GFAP expressing cells in rodents (*Bachoo et al., 2004; Kimelberg et al., 2004; Cahoy et al., 2008*). To resolve this issue, it was decided to first characterize the expression of GFAP by other possible techniques like FACS and western blot for protein level expression and realtime PCR for mRNA analysis. Employing these three different approaches, a clear increase in the intensity of GFAP staining was observed from NSCs stage to PD differentiated cells by FACS (*Figure 24C*); as well by western blot (*Figure 24D*). Also the mRNA level of GFAP in PD differentiated astrocytes was tremendously higher than NSCs (*Figure 24E*). These data pointed towards a low GFAP expression in all the PD differentiated cells (as seen by FACS), while 5% of them expressed high GFAP (as shown by immunostaining), thereby leading to the view of a homogenous population of low GFAP expressing cells upon treatment with PD. As stated in *Krencik et al., 2013*; great care was taken for GFAP antibody dilution, exposure time during imaging, thresholding, and counting of high GFAP expressing cells with immunostaining as these factors can critically change result and conclusion.

Concerning the problem related to astrocyte identity, several studies have been done to discover pan-astrocyte markers and also to understand the molecular differences in a region specific manner (*Bachoo et al., 2004; Lovatt et al., 2007; Cahoy et al., 2008; Doyle et al., 2008; Yang et al., 2011*). A couple of studies have described ALDH1L1, a folate metabolizing enzyme, to be expressed specifically in astrocytes in rat and mouse brain, making it one of the most widely accepted pan-astrocyte marker (*Neymeyer et al., 1997; Cahoy et al., 2008; Doyle et al., 2008*). Another such marker is GS, which also labels all the astrocytes irrespective of region and their GFAP expression (*Anlauf et al., 2013*). At the functional level, the presence of glutamate transporters- EAAT1 and EAAT2 in astrocytes have been reported in a number of studies (*Shibata et al., 1997; Regan et al., 2007*). Also their expression peaks at postnatal stages, especially for EAAT2 (*DeSilva et al., 2012*). Therefore, to further establish astrocytic characteristics of PD differentiated low GFAP astrocytes, staining was performed for ALDH1L1, GS and EAAT1, all of which stained more than 90% of 14 days differentiated cells (*Figure 25A-F*). Further confirmation of ALDH1L1 was done by performing western blots (*Figure 26B*). Transcriptome studies of astrocytes have also revealed their enrichment with a lipid metabolizing enzyme- *Acsbg1* and a synaptogenic protein- *ApoE* (*Cahoy et al., 2008*). Another characteristic hallmark of astrocytes is the presence of gap junction protein- *Cx43*, whereas oligodendrocytes predominantly express *Cx32*. Heterogeneity of astrocytes on the basis of gap junction coupling

has also been previously reported, for e.g. layer 1 and 2/3 cortical networks are transversely coupled while layer 5/6 exhibits circular coupling. In addition, extent of coupling has also been found to vary among protoplasmic and fibrous astrocytes, the former exhibiting high coupling (Haas *et al.*, 2006; Theis *et al.*, 2012). The presence of all of these markers- Acsbg1, Cx43, ApoE was found either by western blot or quantitative PCR or both in PD differentiated astrocytes after 14 days (Figure 26C, D and E). The upregulation of EAAT2 was however only observed at a later time point of 24 days, which also coincides with the previous reports showing delayed expression of EAAT2 or requirement of the presence of neurons for its increasing expression (DeSilva *et al.*, 2012). The robustness of the protocol for differentiation into low GFAP astrocytes upon PD treatment was also tested by using neuronal culture medium- NBNS21S, which would further support the development of a co-culture system. All the PD differentiated cells in NBNS21S medium expressed S100 β and ALDH1L1, however the levels of GFAP were maintained low (Figure 27A, B). With the expression of these different astrocyte restricted markers, it was concluded that these low GFAP expressing cells are astrocytes. Also, the presence of EAAT1 and EAAT2 strongly supports the notion of them to be functionally active. In addition, several studies postulate the presence of S100 β positive but GFAP negative protoplasmic astrocytes to be NG2 cells (oligodendrocyte precursor cells). However, such cells do not express EAAT1 and EAAT2 which are restricted to astrocytic function (Walz *et al.*, 2000). This suggests that PD differentiated S100 β and low GFAP expressing cells are not NG2 cells.

When using PD derived low GFAP cells for disease modeling, it would be crucial to know their regional identity. Previously it has been shown that hiPSC derived neural cells express anterior markers ubiquitously due to endogenous Wnt signaling, but they can be pushed towards hindbrain identity with the use of morphogens like Shh or RA (Martinez-Barbera *et al.*, 2001; Li *et al.*, 2005). Lately, use of small molecule inhibitors such as puromorphamine, LDN193189, XAV939 etc. have also been described to mediate a similar effect, thereby efficiently replacing morphogens like Shh and Wnt (Hu *et al.*, 2010; Maroof *et al.*, 2013). The anterior progenitors are usually characterized by the expression of widely accepted transcription factors like OTX2, LHX2, FOXG1, SIX3 while the ones in hindbrain exhibits the presence of HOX family of proteins and NKX2.1 (Bajpai *et al.*, 2009; Li *et al.*, 2009). Using these rostrocaudal fate specifying molecules, a few studies have published the differentiation of iPSCs or hES cells into either a heterogeneous or a homogenous population of region specific astrocytes (Krencik *et al.*, 2011; Shaltouki *et al.*, 2013; Roybon *et al.*, 2013). Owing to the lack of patterning factors in the current PD protocol, anterior brain identity as expressed by the markers OTX2 and LHX2 was found in NSCs and its maintenance was also observed in the low GFAP astrocytes (Figure 28A,

B). However, posterior patterning wasn't tried by the use of any stimulating agent like SHH or RA or small molecule, because of which no expression of ventral markers like HOXB4 or NKX2.1 was seen in either NSCs or astrocytes, but it remains an open possibility and can be further pursued (*Figure 28C, D*). Based on their regional identity, these cells could be employed for studying the diseases effecting forebrain regions like Rett syndrome, AD, PD, AIDS etc.

4.5 Signaling cascade for PD mediated astrocyte differentiation

For decades, it has been known that once the gliogenic switch is triggered by underlying epigenetic modifications, astrogliogenesis is mediated by a pool of IL-6 family of cytokines (CNTF, LIF, CT-1) which binds to gp130 or LIFRb and converges at the JAK-STAT signaling pathway, leading to the transcription of GFAP and S100 β . This is mediated by interaction of phosphorylated STAT1/3 with the p300/CBP activator complex. Once activated, STAT1/3 directs various components of the JAK-STAT pathway to trigger an auto regulatory loop, thereby further promoting astrogliogenesis. Moreover, knockdown studies of gp130 or LIFRb have clearly demonstrated a defective astrogliogenesis (*Nakashima et al., 1999; He et al., 2005*). On the other hand, BMP2 activates SMAD1 and acts synergistically with LIF to form a pSMAD1-p300/CBP-pSTAT1/3 complex (*Nakashima et al., 1999*).

Therefore, to elucidate the primary mechanism for PD mediated astrocytic differentiation, investigation of the phosphorylation status of STAT1/3 as well as SMAD1 was the first choice. As the effect of growth factor response is known to occur within 15 min and is sustained for up to 2 hrs of their application (*Song et al., 2004, Hong et al., 2014*), a similar time range was selected from 15 min to 1 d (15min, 30 min, 60 min, 3 h, 6h, 1d). As usually reported for CNTF, a remarkable increase in pSTAT1/3 was observed within 15 min of CNTF application which was sustained for up to 60 min, followed by a slight decrease. Notably, no phosphorylation of STAT1/3 was observed after PD treatment for up to 1 d (*Figure 29A, B and C*). However, an increase in the expression of total STAT1 was observed after 1d of PD treatment. In addition, neither CNTF nor PD mediated phosphorylation of SMAD1 until 1 d of treatment (*Figure 29D*). Previously, a knock out study of STAT3 has shown ablation of GFAP expression, suggesting its prime role in astrocyte differentiation (*Hong et al., 2014*). As low and high levels of GFAP expression were observed in all the PD treated cells (*Figure 18B, 24C*), a later time point of 4 d was further investigated for phosphorylation of STAT1/3 as well as SMAD. Levels of phospho or total SMAD1 remained unchanged even with the increased treatment duration and were observed to be highly variable (*Figure 30D*). Phosphorylation of both STAT1 and STAT3 and a significant augmentation of total STAT1/3 in both 4d PD and CNTF treated condition was found at this

timepoint (*Figure 30A, B and C*). The increase in total STAT1/3 could be attributed to an auto-regulatory feedback loop (*He et al., 2005*). Notably, the expression of total STAT1 was increased by around 8.5 as compared to a lower 2 fold increase in total STAT3 after PD treatment. Moreover, the level of total STAT1 was significantly higher in PD as compared to CNTF treated cells, indicating a prominent role of STAT1 in PD differentiated astrocytes. *Hong et al., 2014* has shown the expression of more STAT3 in white matter and enhanced STAT1 in the gray matter of spinal cord after E16.5 in rodents. As low GFAP protoplasmic astrocytes are the major subtype present in the gray matter, these observations further hint on a protoplasmic identity of the low GFAP astrocytes differentiated by PD. My data signify the necessity for further exploration of STAT1/3 signaling using pan astrocytic markers in conjunction with GFAP, which might provide clues for diverse differentiation pathways for astroglial subtypes.

Previously, using double mutant mice for MEK1/2 in progenitors at mid embryogenesis, MEK1/2 signaling has been proved to be crucial for attaining glial competence and allowing cytokine mediated LIFR-STAT3 differentiation towards astrocytes (*Li et al., 2012*). The MAPK pathway was also reported to play a crucial role earlier in neurodevelopment, at the time of neurogenesis. Using E12-13 mouse models, a couple of other studies have reported the enhancement of neurogenesis upon activation of MEK-C/EBP signaling in the presence of FGF2 or PDGF and inhibition of gliogenesis (*Ménard et al., 2002; Paquin et al., 2005*). These studies already show that MAPK signaling plays diverse roles during neural development, depending on the developmental stage. In the current study, the MEK inhibitor PD0325901 was employed to direct final astrocyte differentiation. This suggests that, the stage at which the NSCs were treated with PD for astrocyte differentiation, they had already acquired gliogenic potential. This is supported by my observation of tremendous cell death upon treatment of NSCs at early neurogenic passages (up to P6-7) with PD.

However, the link on how MEK inhibition can lead to STAT activation is still missing as LIF/CNTF/IL-6 receptor does not occur. To explore the possibility of involvement of a surrogate pathway, the PI3K/Akt1 was investigated. Several hints from the literature lead to the assumption that this pathway may be implicated in astrocyte development. Phosphorylation of Akt1 was shown to release two known glial repressors, namely NCoR and Olig2 from the GFAP promoter (*Hermanson et al. 2002; Setoguchi et al., 2004*). Its upstream modulator PI3K is known to be activated in the presence of CNTF (*Hermanson et al. 2002; Setoguchi et al., 2004*) and FGF (*Goetz et al., 2013*). In addition, action of heregulin via ErbB receptor activates PI3K/Akt pathway which is known to result in glial maturation (*Shaltouki et al., 2013*). All these studies

show the importance of Akt signaling in astrocyte differentiation. Moreover, Erk and Akt pathways balance proliferation versus differentiation in stem cells. pAkt has been earlier reported to be a determining factor for cells to undergo differentiation in the presence of growth factors and abrogation of PI3K by overexpression of its endogenous inhibitor- PTEN decreases the number of differentiating cells (*Otaegi et al., 2006; Chen et al., 2012*). Importantly, Erk and Akt pathways share the upstream component Ras and inhibition of the Erk pathway activates the Akt pathway in NGF stimulated PC12 cells (*Chen et al., 2012*). Here, pAkt1 was found to be augmented within 1 day of PD treatment, while pErk1, 2 were down regulated (*Figure 31 A, B*). Therefore, in my differentiation protocol, PD mediated inhibition of pErk1, 2 and activation of pAkt1 might be the underlying mechanism for differentiation into astrocytes within a short time of 14 days. Also, previous reports have demonstrated pAkt1 mediated phosphorylation of STAT1/3 in oncogenesis (*Han et al., 2010*) which could explain the CNTF receptor independent activation of STAT1/3. LY294002, an inhibitor of PI3K is used widely to block phosphorylation of Akt1. (*Setoguchi et al., 2004; Chen et al., 2011*). Following this approach, using LY with and without PD, phosphorylation of STAT1/3 and total STAT1 expression was found to be dependent on activation of the PI3kinase pathway (*Figure 32A-D*). Phosphorylation of STAT1/3 is considered to be one of the requirements to initiate astrocyte differentiation. Therefore, the involvement of PI3K-pAkt1 in STAT1/3 phosphorylation is the postulated pathway for PD mediated astrocyte differentiation. However, a direct link between phosphorylation of Akt1 and STAT1/3 has not been reported in astrocyte differentiation and needs further investigation *in vivo*. Additionally, phosphorylation of Akt1 might also aid in maturation of PD differentiated astrocytes as it has been previously implicated to increase transcription of EAAT2 in primary astrocytes cultured from neonatal rat brain (*Li et al., 2006*).

Once phosphorylated, pAkt1 is translocated from the plasma membrane to act upon its intracellular targets and nuclear transcription factors. Prior studies have reported two important players in the regulation of pAkt1 mediated differentiation into astrocytes- NCoR and Olig2. Olig2 has been mostly associated with the development of oligodendrocytes. At the same time, it acts as a repressor of astrocyte formation by inhibiting access of the CBP/p300 complex to STAT3 at the GFAP promoter region. Cytokines such as CNTF and LIF mediate PI3K dependent phosphorylation of Akt1, which in turn results in Ser30 phosphorylation of Olig2. Phosphorylated Olig2 is then directed out of the nucleus in a CRM1 dependent manner, thereby releasing CBP/p300 from the repressor and allowing transcription of astrocytic genes (*Fukuda et al., 2004; Setoguchi et al., 2004*). Like Olig2, NCoR null mutants have been shown to undergo premature astrocyte differentiation, implying its role as a repressor of astrocytic genes. Also,

NCoR has been shown to hinder astrocytic differentiation by forming a nuclear complex with the presenilin cleaved intracellular domain of ErbB4. Nuclear export of NCoR is another mechanism by which pAkt promotes astrogliogenesis (*Hermanson et al. 2002; Sardi et al., 2006*). Upon examination of nuclear and cytoplasmic localization of both NCoR and Olig2, a significant reduction was observed in the nuclear expression of Olig2 in 4 day PD treated cells, whereas NCoR expression in the nucleus was not affected, thereby suggesting independent roles of both repressors (*Figure 33, 34*). However, whether NCoR and Olig2 works together or independently still remains to be addressed *in vivo*. Also, it is not clear if astrocyte genes other than GFAP are also under the regulation of Olig2 and NCoR, again highlighting the poorly understood mechanism of astrocyte development and heterogeneity.

Together, these data suggests that PI3K-pAkt1 acts as a surrogate pathway mediating astrocyte differentiation through removal of Olig2 repressor and also phosphorylating STAT1/3 in the absence of Erk signaling.

4.6 Functional activity of PD derived low GFAP expressing astrocytes

Pioneering work over the last two decades has enlightened the importance of astrocytes in maintaining metabolic and functional integrity of the brain and spinal cord. Their properties of K^+ spatial buffering from areas of high neuronal activity; scavenging heavy metals like lead and toxic substance like glutamate; regulation of pH, ion concentration and osmolarity, regulating cerebral blood flow, serving neurons with nutritional fuel makes them indispensable for normal functioning of the brain. Also, besides guiding and strengthening the neuronal synapses during development, astrocytes have been postulated to control neuronal activity by releasing gliotransmitters with the emerging concept of tripartite synapses (*Araque et al., 1999*). As we differentiated astrocytes in a short time of 14 days, it was necessary to investigate whether or not they exhibit functional properties.

Although astrocytes are electrically passive cells, but they are known to express a large number of metabotropic receptors which modulate their intracellular calcium in response to neuronal activity, thereby making astrocytes chemically excitable. These intracellular calcium transients can travel long distances from one cell to the other either in an IP3 mediated gap junction dependent way or through activation of purinergic receptors on the adjacent cells via released ATP, resulting in a mode for intercellular communication (*Leybaert et al., 1998; Cotrina et al., 2000; Fam et al., 2000; Höfer et al., 2002*). These mechanisms, first observed in cultured astrocytes was later found to be true *in vivo*, exhibiting a very high level of complexity in terms

of variable responses in the cell soma and astrocytic processes (*Cornell-Bell et al., 1990; Aguado et al., 2002; Shigetomi et al., 2010; Kuga et al., 2011*). The stimulus involved in evoking these calcium transients in astrocytes might vary from region to region, for e.g. cerebral astrocytes have been shown to respond to ATP, NO, glutamate and norepinephrine whereas hippocampal astrocytes respond to ATP, glutamate, GABA, acetylcholine, prostaglandins and endocannabinoids (*Oberheim et al., 2012*). PD derived low GFAP astrocytes were tested for their response to L-glutamate as well as ATP in comparison to NSCs (*Figure 35B-E*). Highly synchronous calcium oscillations were observed upon stimulation of low GFAP astrocytes with glutamate. With ATP, not all of the PD derived astrocytes exhibited calcium oscillations, however, the response was synchronous and biphasic. Along with this, PD derived low GFAP astrocytes displayed no spontaneous calcium oscillations owing to the absence of neurons in these cultures. By blocking neuronal activity by tetrodotoxin, several studies have reported the presence of neuron activity independent calcium waves in astrocytic cultures (*Nett et al., 2002; Parri et al., 2003*). However, the presence of such intrinsic calcium oscillations is subject to regional heterogeneity and needs further investigation. In comparison to low GFAP astrocytes, around 50% of NSCs exhibited spontaneous calcium transients (*Figure 35H, I*). This property of NSCs has been demonstrated in the proliferating ventricular zone cells and is considered to occur during waves of proliferation and depend on the activity of hemichannels, purinergic ATP receptors and IP3 signaling. Blockade of ATP receptor result in decreased proliferation of NSCs due to inhibition of the spatially and temporally coordinated spread of calcium waves (*Weismann et al., 2004*). The increased frequency of calcium oscillations in NSCs in response to ATP, observed in the present study, could be attributed to the presence of P2Y1 receptors and connexin hemichannels. A lack of response of NSCs and PD derived astrocytes to KCl (*Figure 35F*) is attributed to the absence of neurons in these cultures as *in situ* studies have shown that the application of KCl evokes neuronal activity which in turn promotes calcium oscillations in astrocytes due to the released glutamate (*Pasti et al., 1997*). In terms of calcium transients, PD differentiated low GFAP astrocytes proved to be more close to previously described *in vivo* like astrocytes derived from the mouse cortex by immunopanning. Also, they lacked the culture induced artifacts known to occur due to the action of serum (*Foo et al., 2011*).

One of the most significant properties of astrocytes is to clear the extracellular glutamate released during neuronal activity. This prevents accumulation of extracellular glutamate, which is neurotoxic at higher concentrations and helps to shape the postsynaptic response of excitatory synapses. It is mediated by the activation of astrocytic glutamate transporters EAAT1 and

EAAT2 which take up glutamate in a sodium and potassium coupled manner. The immediate conversion of glutamate into glutamine by the astrocyte specific enzyme glutamine synthetase maintains an internal glutamate concentration up to 50 μM , thereby allowing a continuous uptake of glutamate (*Beal et al., 2006*). Major illustration of the importance of astrocytic glutamate uptake was provided by the pioneering work of Rothstein and coworkers, where the use of EAAT1/2 antisense oligonucleotides resulted in neuronal degeneration (*Rothstein et al., 1993*). Also, null mutants of sodium dependent GLT1 have been shown to exhibit spontaneous seizures and reduced postnatal survival (*Tanaka et al., 1997*). Moreover, several of the neurodegenerative disorders like ALS, AD, HD and infectious diseases like AIDS are marked by reduced glutamate uptake owing to abrogated expression of EAAT2 or GS (*Maragakis et al., 2006*). Upon testing the glutamate clearance ability of 14 d PD differentiated low GFAP astrocytes, they were found to exhibit sodium dependent uptake of glutamate from the extracellular solution (*Figure 36*). This signifies the presence of functional glutamate transporters and receptors in these differentiated astrocytes. A further increase in their glutamate uptake capacity might be achieved upon coculture with neurons as it has been previously shown to increase the expression of glutamate transporters on astrocytes (*Yang et al., 2010*).

Besides down regulation of GS and EAAT2 in various pathologies, astrocytes also turn reactive in response to several cytokines, toxic agents and neurological diseases and this property of astrocytes is considered to be an innate immune mechanism of the brain. The expression of a number of receptors, especially, pattern recognition receptors on astrocytes alarms them for the presence of infectious particles and organisms, increased concentrations of cytokines etc.; thereby activating a multitude of signaling cascades involved in rendering these cells reactive. Additionally, miRNAs 145 and 181 have been found to regulate GFAP and cytokine expression respectively; and therefore might modulate astrocyte reactivity. Although microglia are the major immune cells of the brain, astrocytes also play an important role by releasing several cytokines responsible for the invasion of peripheral immune cells and an increased BBB permeability. From the studies on several brain regions in neurodegenerative disorders like AD, PD, ALS, ischemia and HD by using animal models and patient samples, reactive astrocytes have been found to exist even before neuronal cell death and onset of symptoms (*Ben Haim et al., 2015*). *In vitro* studies to investigate the properties of reactive astrocytes are usually performed by the exposure to an array of growth factors and proinflammatory cytokines like TGF β , LIF, TNF α , IL1 β , IL6 etc, where the response has been shown to vary depending on the type of molecule used (*Roybon et al., 2013*). Besides increasing cell size and GFAP expression, reactive astrocytes exhibit altered expression of a wide range of molecules like Vimentin, Nestin, Cx43, AQP4, glutamate

transporters, thrombospondins, NO, NOS, ATP etc. which may vary depending on the type of insult (*Sofroniew et al., 2010*). Recently, a study using mouse models of ischemia and LPS induced toxicity performed genome wide analysis of reactive astrocytes and postulated enhanced expression of Serpina3n (a serine protease inhibitor) and Lcn2 as the hallmarks of reactivity (*Zamanian et al., 2012*). Lcn2 has also been previously associated with reactive astrocytes by acting as an autocrine modulator of their morphology, migration and survival and is also considered to induce neuronal cell death (*Roybon et al., 2013*). Based on these reports, the ability of PD differentiated low GFAP astrocytes to turn reactive was investigated by exposing them to TNF α or LPS. TNF α mediated increase in Serpina3n and Lcn2 and LPS mediated upregulation in Serpina3n and GFAP was observed in PD differentiated cells after 1 day of treatment (*Figure 37A, C*). However, NSCs also exhibited augmentation of Serpina3n and Lcn2 post TNF α treatment (*Figure 37B*) which could be the result of activation of NF- κ B mediated signaling (*Widera et al., 2006; Pugazhenti et al., 2013*). However, no effect was observed upon exposure of NSCs to LPS (*Figure 37D*). As reported in a few publications for human and rat astrocytes, no increase in GFAP was observed upon TNF α treatment of PD differentiated cells (*Figure 37A*) (*Edwards et al., 2006; Roybon et al., 2013*). Additionally, no visible cell death or proliferation was observed within this treatment time.

Upregulation of GFAP is a major hallmark of astrocyte reactivity. Further examination of the ability of low GFAP astrocytes to enhance GFAP expression would thus strengthen their functional properties. A decrease in extracellular and intracellular pH due to lactic acidosis is usually associated with cerebral ischemia. In a previous study, astrocytes have been shown to be more sensitive to reduced pH than neurons, where pH < 4.2 killed the cultured rat glia in less than 10 min while neurons still survived 10 min exposure to pH < 3.8 (*Goldmann et al., 1989*). Interestingly, extracellular acidosis has been shown to prevent neurons from glutamate mediated excitotoxicity. On the other hand, astrocytes react to increased acidosis by undergoing increased reactivity, characterized by high expression of GFAP and cell death within 24 hrs even at pH < 6.4 (*Giffard et al., 1990*). In primary cultures from neonatal mouse brain and astrocytes differentiated from rat forebrain progenitor cells, the sensitivity of astrocytes to acidic environment was shown to be regulated by sodium bicarbonate cotransporter and Ca²⁺ channels (*Oh et al., 1995; Giffard et al., 2000*). Similar experiments in 14 day PD differentiated astrocytes displayed increased expression of GFAP, rendering up to 32% of the cells GFAP positive within 10 hr exposure to pH 6.8 (*Figure 38A, B*). pH 6.8 was chosen as this is the pH value usually reported in ischemic rat brain (*Kraig et al., 1986*) and experimental conditions were limited to 10

hr due to visible cell death upon longer exposure to acidic pH. With these results, once again, the biological relevance of PD differentiated low GFAP astrocytes was confirmed.

Taken together, in this study, it was shown that MEK signaling plays an important role in different stages of *in vitro* mimicked neural development, allowing differentiation of distinct neural subtypes at each specific stage. In early NSCs, MEK signaling is indispensable for the survival of neurogenic NSCs and its inhibition leads to massive cell death in low passage NSCs. Further on in neural development, MEK signaling is essential for the induction of the gliogenic switch, thereby converting multipotent NSCs into ARPs. In intermediate NSC or early ARP stages, inhibition of MEK generates low GFAP expressing astrocytes. Late ARPs generate high GFAP expressing astrocytes, probably due to epigenetic changes opening the GFAP promoter. Combining this innovative protocol for the generation of homogenous populations of astrocyte subtypes with high end technologies like RNA sequencing, opens future prospects to elucidate novel markers for high and low GFAP expressing astrocytes. These markers could be further validated in animal and human tissue. It will also allow deciphering differences in the gliogenic molecular signature of low and high passage NSCs. A need to develop better cortical ARP markers reflecting the differentiation potential is emphasized by this study. Implantation of differentiated low and high GFAP astrocytes in mouse models would aid in mapping their *in vivo* fate restriction and also show, whether the *in vitro* generated astrocytes can acquire the typical *in vivo* morphology of mature astrocytes. The results of the unconventional activation of STAT1/3 signaling ask for probing signaling cascades directing differentiation towards low and high GFAP astrocytes using pan astrocyte markers.

Importantly, this model system provides physiologically functional cortical astrocytes which could be employed for disease modeling using patient derived iPSCs. Based on the expression pattern of different astrocyte markers and functional properties of PD differentiated low GFAP astrocytes, it can also be concluded that they can serve as a potential model system to study the functional differences between low and high GFAP cells, for example, in context to their effect on neuronal network activity and plasticity.

5. References

- Aguado F, Espinosa-Parrilla JF, Carmona MA *et al.* Neuronal activity regulates correlated network properties of spontaneous calcium transients in astrocytes in situ. *J Neurosci.* 22(21):9430-44. 2002.
- Alexander DB, Goldberg GS. Transfer of biologically important molecules between cells through gap junction channels. *Curr Med Chem.* 10(19):2045-58. 2003.
- Allen NJ, Bennett ML, Foo LC *et al.* Astrocyte glypicans 4 and 6 promote formation of excitatory synapses via GluA1 AMPA receptors. *Nature.* 486(7403):410-4. 2012.
- Angulo-Rojo C, Manning-Cela R1, Aguirre A *et al.* Involvement of the Notch pathway in terminal astrocytic differentiation: role of PKA. *ASN Neuro.* 5(5):e00130. 2013.
- Anlauf E, Derouiche A. Glutamine Synthetase as an Astrocytic Marker: Its Cell Type and Vesicle Localization. *Front Endocrinol (Lausanne).* 4:144. 2013.
- Araque A, Carmignoto G, Haydon PG *et al.* Gliotransmitters travel in time and space. *Neuron.* 81(4):728-39. 2014.
- Araque A, Parpura V, Sanzgiri RP *et al.* Tripartite synapses: glia, the unacknowledged partner. *Trends Neurosci.* 22(5):208-15. 1999.
- Aschner M. Neuron-astrocyte interactions: implications for cellular energetics and antioxidant levels. *Neurotoxicology.* 21(6):1101-7. 2000.
- Azevedo FA, Carvalho LR, Grinberg LT *et al.* Equal numbers of neuronal and nonneuronal cells make the human brain an isometrically scaled-up primate brain. *J Comp Neurol.* 513(5):532-41. 2009.
- Bachoo RM, Kim RS, Ligon KL *et al.* Molecular diversity of astrocytes with implications for neurological disorders. *Proc Natl Acad Sci U S A.* 101(22):8384-9. 2004.
- Bajetto A, Bonavia R, Barbero S *et al.* Characterization of chemokines and their receptors in the central nervous system: physiopathological implications. *J Neurochem.* 82(6):1311-29. 2002.
- Bajpai R, Coppola G, Kaul M *et al.* Molecular stages of rapid and uniform neuralization of human embryonic stem cells. *Cell Death Differ.* 16(6):807-25. 2009.
- Bani-Yaghoub M, Tremblay RG, Lei JX *et al.* Role of Sox2 in the development of the mouse neocortex. *Dev Biol.* 295(1):52-66. 2006.
- Barnabé-Heider F, Wasylnka JA, Fernandes KJ *et al.* Evidence that embryonic neurons regulate the onset of cortical gliogenesis via cardiotrophin-1. *Neuron.* 48(2):253-65. 2005.
- Ben Haim L, Carrillo-de Sauvage MA, Ceyzeriat K *et al.* Elusive roles for reactive astrocytes in neurodegenerative diseases. *Front Cell Neurosci.* 9:278. 2015.
- Berl S, Lajtha A, Waelsch H. Amino Acid and Protein Metabolism - VI Cerebral Compartments of Glutamic Acid Metabolism. *J Neurochem.* 7:186-197. 1961.
- Bolton S, Greenwood K, Hamilton N *et al.* Regulation of the astrocyte resting membrane potential by cyclic AMP and protein kinase A. *Glia.* 54(4):316-28. 2006.
- Bonni A, Sun Y, Nadal-Vicens M *et al.* Regulation of gliogenesis in the central nervous system by the JAK-STAT signaling pathway. *Science.* 278(5337):477-83. 1997.
- Brown DC & Gatter KC. Ki67 protein: the immaculate deception? *Histopathology.* 40(1):2-11. 2002.

- Buffo A, Rite I, Tripathi P *et al.* Origin and progeny of reactive gliosis: A source of multipotent cells in the injured brain. *Proc Natl Acad Sci U S A.* 105(9):3581-6. 2008.
- Cahoy JD, Emery B, Kaushal A *et al.* A transcriptome database for astrocytes, neurons, and oligodendrocytes: a new resource for understanding brain development and function. *J Neurosci.* 28(1):264-78. 2008.
- Cai N, Kurachi M, Shibasaki K *et al.* CD44-positive cells are candidates for astrocyte precursor cells in developing mouse cerebellum. *Cerebellum.* 11(1):181-93. 2012.
- Cebolla B, Fernández-Pérez A, Perea G *et al.* DREAM mediates cAMP-dependent, Ca²⁺-induced stimulation of GFAP gene expression and regulates cortical astroglialogenesis. *J Neurosci.* 28(26):6703-13. 2008.
- Chambers SM, Fasano CA, Papapetrou EP *et al.* Highly efficient neural conversion of human ES and iPS cells by dual inhibition of SMAD signaling. *Nat Biotechnol.* 27(3):275-80. 2009.
- Chen G, Gulbranson DR, Hou Z *et al.* Chemically defined conditions for human iPSC derivation and culture. *Nat Methods.* 8(5):424-9. 2011.
- Chen JY, Lin JR, Cimprich KA *et al.* A two-dimensional ERK-AKT signaling code for an NGF-triggered cell-fate decision. *Mol Cell.* 45(2):196-209. 2012.
- Chen T, Dent SY. Chromatin modifiers and remodelers: regulators of cellular differentiation. *Nat Rev Genet.* 15(2):93-106. 2014.
- Chen Y, Stevens B, Chang J *et al.* NS21: re-defined and modified supplement B27 for neuronal cultures. *J Neurosci Methods.* 171(2):239-47. 2008.
- Ciccolini F, Svendsen CN. Fibroblast growth factor 2 (FGF-2) promotes acquisition of epidermal growth factor (EGF) responsiveness in mouse striatal precursor cells: identification of neural precursors responding to both EGF and FGF-2. *J Neurosci.* 18(19):7869-80. 1998.
- Clancy B, Darlington RB, Finlay BL. Translating developmental time across mammalian species. *Neuroscience.* 105(1):7-17. 2001.
- Clarke LE, Barres BA. Emerging roles of astrocytes in neural circuit development. *Nat Rev Neurosci.* 14(5):311-21. 2013.
- Cornell-Bell AH, Finkbeiner SM, Cooper MS *et al.* Glutamate induces calcium waves in cultured astrocytes: long-range glial signaling. *Science.* 247(4941):470-3. 1990.
- Cotrina ML, Lin JH, López-García JC *et al.* ATP-mediated glia signaling. *J Neurosci.* 20(8):2835-44. 2000.
- D'Amour KA, Gage FH. Genetic and functional differences between multipotent neural and pluripotent embryonic stem cells. *Proc Natl Acad Sci U S A.* 100 Suppl 1:11866-72. 2003.
- Dang CV. MYC on the path to cancer. *Cell.* 149(1):22-35. 2012.
- Davies SJ, Shih CH, Noble M *et al.* Transplantation of specific human astrocytes promotes functional recovery after spinal cord injury. *PLoS One.* 6(3):e17328. 2011.
- Deneen B, Ho R, Lukaszewicz A *et al.* The transcription factor NFIA controls the onset of gliogenesis in the developing spinal cord. *Neuron.* 52(6):953-68. 2006.
- DeSilva TM, Borenstein NS, Volpe JJ *et al.* Expression of EAAT2 in neurons and protoplasmic astrocytes during human cortical development. *J Comp Neurol.* 520(17):3912-32. 2012.
- Dimos JT, Rodolfa KT, Niakan KK *et al.* Induced pluripotent stem cells generated from patients with ALS can be differentiated into motor neurons. *Science.* 321(5893):1218-21. 2008.

- Donato R, Sorci G, Riuzzi F *et al.* S100B's double life: intracellular regulator and extracellular signal. *Biochim Biophys Acta.* 1793(6):1008-22. 2009.
- Doyle JP, Dougherty JD, Heiman M *et al.* Application of a translational profiling approach for the comparative analysis of CNS cell types. *Cell.* 135(4):749-62. 2008.
- Edwards MM, Robinson SR. TNF alpha affects the expression of GFAP and S100B: implications for Alzheimer's disease. *J Neural Transm.* 113(11):1709-15. 2006.
- Eid T, Tu N, Lee TS *et al.* Regulation of astrocyte glutamine synthetase in epilepsy. *Neurochem Int.* 63(7):670-81. 2013.
- Fam SR, Gallagher CJ, Salter MW *et al.* P2Y(1) purinoceptor-mediated Ca(2+) signaling and Ca(2+) wave propagation in dorsal spinal cord astrocytes. *J Neurosci.* 20(8):2800-8. 2000.
- Fan G, Beard C, Chen RZ *et al.* DNA hypomethylation perturbs the function and survival of CNS neurons in postnatal animals. *J Neurosci.* 21(3):788-97. 2001.
- Fangfang Bi, Cao Huang, Jianbin Tong *et al.* Reactive astrocytes secrete lcn2 to promote neuron death. *Proc Natl Acad Sci U S A.* 110(10):4069–4074. 2013.
- Fernanda M.P. Tonelli, Anderson K. Santos, Dawidson A *et al.* Stem Cells and Calcium Signaling. *Adv Exp Med Biol.* 740: 891–916. 2012.
- Florio M, Huttner WB. Neural progenitors, neurogenesis and the evolution of the neocortex. *Development.* 141(11):2182-94. 2014.
- Foo LC, Allen NJ, Bushong EA *et al.* Development of a method for the purification and culture of rodent astrocytes. *Neuron.* 71(5):799-811. 2011.
- Frankland PW, Miller FD. Regenerating your senses: multiple roles for neurogenesis in the adult brain. *Nat Neurosci.* 11(10):1124-6. 2008.
- Freitas-Andrade M, Naus CC. Astrocytes in neuroprotection and neurodegeneration: The role of connexin43 and pannexin1. *Neuroscience.* S0306-4522(15)00376-0. 2015.
- Fukuda S, Kondo T, Takebayashi H *et al.* Negative regulatory effect of an oligodendrocytic bHLH factor OLIG2 on the astrocytic differentiation pathway. *Cell Death Differ.* 11(2):196-202. 2004.
- Gadea A, Schinelli S, Gallo V. Endothelin-1 regulates astrocyte proliferation and reactive gliosis via a JNK/c-Jun signaling pathway. *J Neurosci.* 28(10):2394-408. 2008.
- Gaiano N, Nye JS, Fishell G. Radial glial identity is promoted by Notch1 signaling in the murine forebrain. *Neuron.* 26(2):395-404. 2000.
- Ge W, Martinowich K, Wu X *et al.* Notch signaling promotes astroglialogenesis via direct CSL-mediated glial gene activation. *J Neurosci Res.* 69(6):848-60. 2002.
- Giffard RG, Monyer H, Choi DW. Selective vulnerability of cultured cortical glia to injury by extracellular acidosis. *Brain Res.* 530(1):138-41. 1990.
- Giffard RG, Papadopoulos MC, van Hooft JA *et al.* The electrogenic sodium bicarbonate cotransporter: developmental expression in rat brain and possible role in acid vulnerability. *J Neurosci.* 20(3):1001-8. 2000.
- Glaser T, Pollard SM, Smith A. Tripotential differentiation of adherently expandable neural stem (NS) cells. *PLoS One.* 2(3):e298. 2007.
- Goetz R, Mohammadi M. Exploring mechanisms of FGF signalling through the lens of structural biology. *Nat Rev Mol Cell Biol.* 14(3):166-80. 2013.

- Goldman SA, Pulsinelli WA, Clarke WY *et al.* The effects of extracellular acidosis on neurons and glia in vitro. *J Cereb Blood Flow Metab.* 9(4):471-7. 1989.
- Gómez-Gonzalo M, Losi G, Chiavegato A *et al.* An excitatory loop with astrocytes contributes to drive neurons to seizure threshold. *PLoS Biol.* 8(4):e1000352. 2010.
- Göritz C, Mauch DH, Nägler K. Role of glia-derived cholesterol in synaptogenesis: new revelations in the synapse-glia affair. *J Physiol Paris.* 96(3-4):257-63. 2002.
- Gruetter R. Glycogen: the forgotten cerebral energy store. *J Neurosci Res.* 74(2):179-83. 2003.
- Gupta K, Patani R, Baxter P *et al.* Human embryonic stem cell derived astrocytes mediate non-cell-autonomous neuroprotection through endogenous and drug-induced mechanisms. *Cell Death Differ.* 19(5):779-87. 2012.
- Haas B, Schipke CG, Peters O *et al.* Activity-dependent ATP-waves in the mouse neocortex are independent from astrocytic calcium waves. *Cereb Cortex.* 16(2):237-46. 2006.
- Han SS, Williams LA, Eggan KC. Constructing and deconstructing stem cell models of neurological disease. *Neuron.* 70(4):626-44. 2011.
- Han SS, Yun H, Son DJ *et al.* NF-kappaB/STAT3/PI3K signaling crosstalk in iMyc E mu B lymphoma. *Mol Cancer.* 9:97. doi: 10.1186/1476-4598-9-97. 2010.
- Han X, Chen M, Wang F *et al.* Forebrain engraftment by human glial progenitor cells enhances synaptic plasticity and learning in adult mice. *Cell Stem Cell.* 12(3):342-53. 2013.
- Hatada I, Namihira M, Morita S *et al.* Astrocyte-specific genes are generally demethylated in neural precursor cells prior to astrocytic differentiation. *PLoS One.* 3(9):e3189. 2008.
- He F, Ge W, Martinowich K *et al.* A positive autoregulatory loop of Jak-STAT signaling controls the onset of astroglialogenesis. *Nat Neurosci.* 8(5):616-25. 2005.
- Hermanson O, Jepsen K, Rosenfeld MG *et al.* N-CoR controls differentiation of neural stem cells into astrocytes. *Nature.* 419(6910):934-9. 2002.
- Höfer T, Venance L, Giaume C. Control and plasticity of intercellular calcium waves in astrocytes: a modeling approach. *J Neurosci.* 22(12):4850-9. 2002.
- Hong S, Song MR. STAT3 but not STAT1 is required for astrocyte differentiation. *PLoS One.* 9(1):e86851. 2014.
- Hou P, Li Y, Zhang X *et al.* Pluripotent stem cells induced from mouse somatic cells by small-molecule compounds. *Science.* 341(6146):651-4. 2013.
- <http://www.embl.de/eamnet/html/calcium/dyes/fluorescentdyes3.htm>
- Hu BY, Zhang SC. Differentiation of spinal motor neurons from pluripotent human stem cells. *Nat Protoc.* 4(9):1295-304. 2009.
- Hu BY, Zhang SC. Directed differentiation of neural-stem cells and subtype-specific neurons from hESCs. *Methods Mol Biol.* 636:123-37. 2010.
- Huttner A, Rakic P. Diagnosis in a dish: your skin can help your brain. *Nat Med.* 17(12):1558-9. 2011.
- Ichikawa M, Shiga T, Hirata Y. Spatial and temporal pattern of postnatal proliferation of glial cells in the parietal cortex of the rat. *Brain Res.* 285(2):181-7. 1983.
- Iino M, Goto K, Kakegawa W *et al.* Glia-synapse interaction through Ca²⁺-permeable AMPA receptors in Bergmann glia. *Science.* 292(5518):926-9. 2001.

- Iliff JJ, Wang M, Liao Y *et al.* A paravascular pathway facilitates CSF flow through the brain parenchyma and the clearance of interstitial solutes, including amyloid β . *Sci Transl Med.* 4(147):147ra111. 2012.
- Inman GJ, Nicolás FJ, Callahan JF *et al.* SB-431542 is a potent and specific inhibitor of transforming growth factor-beta superfamily type I activin receptor-like kinase (ALK) receptors ALK4, ALK5, and ALK7. *Mol Pharmacol.* 62(1):65-74. 2002.
- Inoue H, Nagata N, Kurokawa H *et al.* iPS cells: a game changer for future medicine. *EMBO J.* 33(5):409-17. 2014.
- Ishibashi T, Dakin KA, Stevens B *et al.* Astrocytes promote myelination in response to electrical impulses. *Neuron.* 49(6):823-32. 2006.
- Kang P, Lee HK, Glasgow SM *et al.* Sox9 and NFIA coordinate a transcriptional regulatory cascade during the initiation of gliogenesis. *Neuron.* 74(1):79-94. 2012.
- Kessaris N, Pringle N, Richardson WD. Specification of CNS glia from neural stem cells in the embryonic neuroepithelium. *Philos Trans R Soc Lond B Biol Sci.* 363(1489):71-85. 2008.
- Khakh BS, Sofroniew MV. Diversity of astrocyte functions and phenotypes in neural circuits. *Nat Neurosci.* 18(7):942-52. 2015.
- Kilpatrick TJ, Bartlett PF. Cloned multipotential precursors from the mouse cerebrum require FGF-2, whereas glial restricted precursors are stimulated with either FGF-2 or EGF. *J Neurosci.* 15(5 Pt 1):3653-61. 1995.
- Kimelberg HK. The problem of astrocyte identity. *Neurochem Int.* 45(2-3):191-202. 2004.
- Koblar SA, Turnley AM, Classon BJ *et al.* Neural precursor differentiation into astrocytes requires signaling through the leukemia inhibitory factor receptor. *Proc Natl Acad Sci U S A.* 95(6):3178-81. 1998.
- Kraig RP, Pulsinelli WA, Plum F. Carbonic acid buffer changes during complete brain ischemia. *Am J Physiol.* 250(3 Pt 2):R348-57. 1986.
- Krencik R, Hokanson KC, Narayan AR *et al.* Dysregulation of astrocyte extracellular signaling in Costello syndrome. *Sci Transl Med.* 7(286):286ra66. 2015.
- Krencik R, Weick JP, Liu Y *et al.* Specification of transplantable astroglial subtypes from human pluripotent stem cells. *Nat Biotechnol.* 29(6):528-34. 2011.
- Kriegstein A, Alvarez-Buylla A. The glial nature of embryonic and adult neural stem cells. *Annu Rev Neurosci.* 32:149-84. 2009.
- Kucukdereli H, Allen NJ, Lee AT *et al.* Control of excitatory CNS synaptogenesis by astrocyte-secreted proteins Hevin and SPARC. *Proc Natl Acad Sci U S A.* 108(32):E440-9. 2011.
- Kuga N, Sasaki T, Takahara Y *et al.* Large-scale calcium waves traveling through astrocytic networks in vivo. *J Neurosci.* 31(7):2607-14. 2011.
- LaMonica BE, Lui JH, Wang X *et al.* OSVZ progenitors in the human cortex: an updated perspective on neurodevelopmental disease. *Curr Opin Neurobiol.* 22(5):747-53. 2012.
- Langer J, Stephan J, Theis M *et al.* Gap junctions mediate intercellular spread of sodium between hippocampal astrocytes in situ. *Glia.* 60(2):239-52. 2012.
- Leif Hertz. The Glutamate–Glutamine (GABA) Cycle: Importance of Late Postnatal Development and Potential Reciprocal Interactions between Biosynthesis and Degradation. *Front Endocrinol.* 4: 59. 2013.

- Lendahl U, Zimmerman LB, McKay RD. CNS stem cells express a new class of intermediate filament protein. *Cell*. 60(4):585-95. 1990.
- Levison SW, Jiang FJ, Stoltzfus OK *et al*. IL-6-type cytokines enhance epidermal growth factor-stimulated astrocyte proliferation. *Glia*. 32(3):328-37. 2000.
- Leybaert L, Paemeleire K, Strahonja A *et al*. Inositol-trisphosphate-dependent intercellular calcium signaling in and between astrocytes and endothelial cells. *Glia*. 24(4):398-407. 1998.
- Li LB, Toan SV, Zeleniaia O *et al*. Regulation of astrocytic glutamate transporter expression by Akt: evidence for a selective transcriptional effect on the GLT-1/EAAT2 subtype. *J Neurochem*. 97(3):759-71. 2006.
- Li X, Newbern JM, Wu Y. MEK is a Key Regulator of Gliogenesis in the Developing Brain. *Neuron*. 75(6):1035-50. 2012.
- Li XJ, Du ZW, Zarnowska ED *et al*. Specification of motoneurons from human embryonic stem cells. *Nat Biotechnol*. 23(2):215-21. 2005.
- Liddel S, Barres B. SnapShot: Astrocytes in Health and Disease. *Cell*. 162(5):1170-1170.e1. 2015.
- Lillien L, Raphael H. BMP and FGF regulate the development of EGF-responsive neural progenitor cells. *Development*. 127(22):4993-5005. 2000.
- Lillien LE, Sendtner M, Rohrer H *et al*. Type-2 astrocyte development in rat brain cultures is initiated by a CNTF-like protein produced by type-1 astrocytes. *Neuron*. 1(6):485-94. 1988.
- Li X, Newbern JM, Wu Y *et al*. MEK is a Key Regulator of Gliogenesis in the Developing Brain. *Neuron*. 75(6):1035-50. 2012.
- Lin T, Wu S. Reprogramming with Small Molecules instead of Exogenous Transcription Factors. *Stem Cells Int*. 2015:794632. 2015.
- Liu Y, Han SS, Wu Y *et al*. CD44 expression identifies astrocyte-restricted precursor cells. *Dev Biol*. 276(1):31-46. 2004.
- Livak KJ, Schmittgen TD. Analysis of relative gene expression data using real-time quantitative PCR and the 2(-Delta Delta C(T)) Method. *Methods*. 25(4):402-8. 2001.
- Lovatt D, Sonnewald U, Waagepetersen HS *et al*. The transcriptome and metabolic gene signature of protoplasmic astrocytes in the adult murine cortex. *J Neurosci*. 2007 Nov 7;27(45):12255-66. 2007.
- Lui JH, Hansen DV, Kriegstein AR. Development and evolution of the human neocortex. *Cell*. 146(1):18-36. 2011.
- Lund P. L-Glutamine and L-Glutamate: UV-Method with Glutaminase and Glutamate Dehydrogenase. *Methods of Enzymatic Analysis*. 8. 357-363 1986.
- Magistretti PJ, Sorg O, Naichen Y *et al*. Regulation of astrocyte energy metabolism by neurotransmitters. *Ren Physiol Biochem*. 17(3-4):168-71. 1994.
- Majumder A, Dhara SK, Swetenburg R *et al*. Inhibition of DNA methyltransferases and histone deacetylases induces astrocytic differentiation of neural progenitors. *Stem Cell Res*. 11(1):574-86. 2013.
- Malmersjö S, Rebellato P, Smedler E *et al*. Neural progenitors organize in small-world networks to promote cell proliferation. *Proc Natl Acad Sci U S A*. 110(16):E1524-32. 2013.
- Maragakis NJ, Rothstein JD. Mechanisms of Disease: astrocytes in neurodegenerative disease. *Nat Clin Pract Neurol*. 2(12):679-89. 2006.

- Maroof AM, Keros S, Tyson JA *et al.* Directed differentiation and functional maturation of cortical interneurons from human embryonic stem cells. *Cell Stem Cell*. 12(5):559-72. 2013.
- Marshall CA, Novitsch BG, Goldman JE. Olig2 directs astrocyte and oligodendrocyte formation in postnatal subventricular zone cells. *J Neurosci*. 25(32):7289-98. 2005.
- Martinez-Barbera JP, Signore M, Boyl PP *et al.* Regionalisation of anterior neuroectoderm and its competence in responding to forebrain and midbrain inducing activities depend on mutual antagonism between OTX2 and GBX2. *Development*. 128(23):4789-800. 2001.
- Mason S, Piper M, Gronostajski RM *et al.* Nuclear factor one transcription factors in CNS development. *Mol Neurobiol*. 39(1):10-23. 2009.
- Mauch DH, Nagler K, Schumacher S *et al.* CNS synaptogenesis promoted by glia-derived cholesterol. *Science*. 294(5545):1354-7. 2001.
- Mearow KM, Mill JF, Vitkovic L. The ontogeny and localization of glutamine synthetase gene expression in rat brain. *Brain Res Mol Brain Res*. 6(4):223-32. 1989.
- Menard C, Hein P, Paquin A *et al.* An essential role for a MEK-C/EBP pathway during growth factor-regulated cortical neurogenesis. *Neuron*. 36(4):597-610. 2002.
- Meyer-Franke A, Shen S, Barres BA. Astrocytes induce oligodendrocyte processes to align with and adhere to axons. *Mol Cell Neurosci*. 14(4-5):385-97. 1999.
- Mi H, Haeberle H, Barres BA. Induction of astrocyte differentiation by endothelial cells. *J Neurosci*. 21(5):1538-47. 2001.
- Mila Komitova, Peter S. Eriksson. Sox-2 is expressed by neural progenitors and astroglia in the adult rat brain. *Neurosci Lett*. 369(1):24-7. 2004.
- Molofsky AV, Krencik R, Ullian EM *et al.* Astrocytes and disease: a neurodevelopmental perspective. *Genes Dev*. 26(9):891-907. 2012.
- Morizane A, Doi D, Kikuchi T *et al.* Small-molecule inhibitors of bone morphogenic protein and activin/nodal signals promote highly efficient neural induction from human pluripotent stem cells. *J Neurosci Res*. 89(2):117-26. 2011.
- Morrison SJ. Pten-uating neural growth. *Nat Med*. 8(1):16-8. 2002.
- MuhChyi C, Juliandi B, Matsuda T *et al.* Epigenetic regulation of neural stem cell fate during corticogenesis. *Int J Dev Neurosci*. 31(6):424-33. 2013.
- Nadarajah B, Parnavelas JG. Modes of neuronal migration in the developing cerebral cortex. *Nat Rev Neurosci*. 3(6):423-32. 2002.
- Nagao M, Campbell K, Burns K. Coordinated control of self-renewal and differentiation of neural stem cells by Myc and the p19ARF-p53 pathway. *J Cell Biol*. 183(7):1243-57. 2008.
- Naka-Kaneda H, Nakamura S, Igarashi M. The miR-17/106-p38 axis is a key regulator of the neurogenic-to-gliogenic transition in developing neural stem/progenitor cells. *Proc Natl Acad Sci U S A*. 111(4):1604-9. 2014.
- Nakashima K, Wiese S, Yanagisawa M *et al.* Developmental requirement of gp130 signaling in neuronal survival and astrocyte differentiation. *J Neurosci*. 19(13):5429-34. 1999.
- Nakashima K, Yanagisawa M, Arakawa H *et al.* Astrocyte differentiation mediated by LIF in cooperation with BMP2. *FEBS Lett*. 457(1):43-6. 1999.
- Nakashima K, Yanagisawa M, Arakawa H *et al.* Synergistic signaling in fetal brain by STAT3-Smad1 complex bridged by p300. *Science*. 284(5413):479-82. 1999.

- Namihira M, Kohyama J, Semi K *et al.* Committed neuronal precursors confer astrocytic potential on residual neural precursor cells. *Dev Cell*. 16(2):245-55. 2009.
- Namihira M, Nakashima K. Mechanisms of astrocytogenesis in the mammalian brain. *Curr Opin Neurobiol*. 23(6):921-7. 2013.
- Navarrete M, Araque A. Endocannabinoids mediate neuron-astrocyte communication. *Neuron*. 57(6):883-93. 2008.
- Neary JT, Zimmermann H. Trophic functions of nucleotides in the central nervous system. *Trends Neurosci*. 32(4):189-98. 2009.
- Nett WJ, Oloff SH, McCarthy KD. Hippocampal astrocytes in situ exhibit calcium oscillations that occur independent of neuronal activity. *J Neurophysiol*. 87(1):528-37. 2002.
- Neymeyer V, Tephly TR, Miller MW. Folate and 10-formyltetrahydrofolate dehydrogenase (FDH) expression in the central nervous system of the mature rat. *Brain Res*. 766(1-2):195-204. 1997.
- Niederreither K, Dollé P. Retinoic acid in development: towards an integrated view. *Nat Rev Genet*. 9(7):541-53. 2008.
- Nieto M, Schuurmans C, Britz O *et al.* Neural bHLH genes control the neuronal versus glial fate decision in cortical progenitors. *Neuron*. 29(2):401-13. 2001.
- Nieweg K, Andreyeva A, van Stegen B *et al.* Alzheimer's disease-related amyloid- β induces synaptotoxicity in human iPS cell-derived neurons. *Cell Death and Dis*. 6:e1709. 2015.
- Noctor SC, Martínez-Cerdeño V, Ivic L *et al.* Cortical neurons arise in symmetric and asymmetric division zones and migrate through specific phases. *Nat Neurosci*. 7(2):136-44. 2004.
- Oberheim NA, Goldman SA, Nedergaard M. Heterogeneity of astrocytic form and function. *Methods Mol Biol*. 814:23-45. 2012.
- Oberheim NA, Wang X, Goldman S *et al.* Astrocytic complexity distinguishes the human brain. *Trends Neurosci*. 29(10):547-53. 2006.
- Oh TH, Markelonis GJ, Von Visger JR *et al.* Acidic pH rapidly increases immunoreactivity of glial fibrillary acidic protein in cultured astrocytes. *Glia*. 13(4):319-22. 1995.
- Okano-Uchida T, Naruse M, Ikezawa T *et al.* Cerebellar neural stem cells differentiate into two distinct types of astrocytes in response to CNTF and BMP2. *Neurosci Lett*. 552:15-20. 2013.
- O'Leary DD, Chou SJ, Sahara S. Area patterning of the mammalian cortex. *Neuron*. 56(2):252-69. 2007.
- Ota M, Ito K. BMP and FGF-2 regulate neurogenin-2 expression and the differentiation of sensory neurons and glia. *Dev Dyn*. 235(3):646-55. 2006.
- Owada Y, Yoshimoto T, Kondo H. Spatio-temporally differential expression of genes for three members of fatty acid binding proteins in developing and mature rat brains. *J Chem Neuroanat*. 12(2):113-22. 1996.
- Pang ZP, Yang N, Vierbuchen T. Induction of human neuronal cells by defined transcription factors. *Nature*. 476(7359):220-3. 2011.
- Paquin A, Barnabé-Heider F, Kageyama R *et al.* CCAAT/enhancer-binding protein phosphorylation biases cortical precursors to generate neurons rather than astrocytes in vivo. *J Neurosci*. 25(46):10747-58. 2005.
- Parri HR, Crunelli V. The role of Ca²⁺ in the generation of spontaneous astrocytic Ca²⁺ oscillations. *Neuroscience*. 120(4):979-92. 2003.

- Paşca AM, Sloan SA, Clarke LE *et al.* Functional cortical neurons and astrocytes from human pluripotent stem cells in 3D culture. *Nat Methods*. 12(7):671-8. 2015.
- Pasti L, Volterra A, Pozzan T *et al.* Intracellular calcium oscillations in astrocytes: a highly plastic, bidirectional form of communication between neurons and astrocytes in situ. *J Neurosci*. 17(20):7817-30. 1997.
- Pekny M, Pekna M. Astrocyte reactivity and reactive astrogliosis: costs and benefits. *Physiol Rev*. 94(4):1077-98. 2014.
- Pfriege FW. Role of glial cells in the formation and maintenance of synapses. *Brain Res Rev*. 63(1-2):39-46. 2010.
- Pollard SM, Wallbank R, Tomlinson S *et al.* Fibroblast growth factor induces a neural stem cell phenotype in foetal forebrain progenitors and during embryonic stem cell differentiation. *Mol Cell Neurosci*. 38(3):393-403. 2008.
- Pringle NP, Yu WP, Howell M *et al.* Fgfr3 expression by astrocytes and their precursors: evidence that astrocytes and oligodendrocytes originate in distinct neuroepithelial domains. *Development*. 130(1):93-102. 2003.
- Pugazhenth S, Zhang Y, Bouchard R *et al.* Induction of an inflammatory loop by interleukin-1 β and tumor necrosis factor- α involves NF- κ B and STAT-1 in differentiated human neuroprogenitor cells. *PLoS One*. ;8(7):e69585. 2013.
- Rajan P, McKay RD. Multiple routes to astrocytic differentiation in the CNS. *J Neurosci*. 18(10):3620-9. 1998.
- Rao MS, Malik N. Assessing iPSC reprogramming methods for their suitability in translational medicine. *J Cell Biochem*. 113(10):3061-8. 2012.
- Raponi E, Agnes F, Delphin C *et al.* S100B expression defines a state in which GFAP-expressing cells lose their neural stem cell potential and acquire a more mature developmental stage. *Glia*. 55(2):165-77. 2007.
- Regan MR, Huang YH, Kim YS *et al.* Variations in promoter activity reveal a differential expression and physiology of glutamate transporters by glia in the developing and mature CNS. *J Neurosci*. 27(25):6607-19. 2007.
- Reynolds BA, Tetzlaff W, Weiss S. A multipotent EGF-responsive striatal embryonic progenitor cell produces neurons and astrocytes. *J Neurosci*. 12(11):4565-74. 1992.
- Rodríguez-Rivera NS, Molina-Hernández A, Sánchez-Cruz E *et al.* Activated Notch1 is a stronger astrocytic stimulus than leukemia inhibitory factor for rat neural stem cells. *Int J Dev Biol*. 53(7):947-53. 2009.
- Rothstein JD, Jin L, Dykes-Hoberg M *et al.* Chronic inhibition of glutamate uptake produces a model of slow neurotoxicity. *Proc Natl Acad Sci U S A*. 90(14):6591-5. 1993.
- Rowitch DH, Kriegstein AR. Developmental genetics of vertebrate glial-cell specification. *Nature*. 468(7321):214-22. 2010.
- Roybon L, Lamas NJ, Garcia-Diaz A *et al.* Human stem cell-derived spinal cord astrocytes with defined mature or reactive phenotypes. *Cell Rep*. 4(5):1035-48. 2013.
- Sahlender DA, Savtchouk I2, Volterra A. What do we know about gliotransmitter release from astrocytes? *Philos Trans R Soc Lond B Biol Sci*. 369(1654):20130592. 2014.
- Sanalkumar R, Vidyanand S, Lalitha Indulekha C *et al.* Neuronal vs. glial fate of embryonic stem cell-derived neural progenitors (ES-NPs) is determined by FGF2/EGF during proliferation. *J Mol Neurosci*. 42(1):17-27. 2010.

- Sardi SP, Murtie J, Koirala S *et al.* Presenilin-dependent ErbB4 nuclear signaling regulates the timing of astrogenesis in the developing brain. *Cell*. 127(1):185-97. 2006.
- Scemes E, Giaume C. Astrocyte calcium waves: what they are and what they do. *Glia*. 54(7):716-25. 2006.
- Schwindt TT, Motta FL, Gabriela F B *et al.* Effects of FGF-2 and EGF removal on the differentiation of mouse neural precursor cells. *An Acad Bras Cienc*. 81(3):443-52. 2009.
- Semple BD, Blomgren K, Gimlin K *et al.* Brain development in rodents and humans: Identifying benchmarks of maturation and vulnerability to injury across species. *Prog Neurobiol*. 106-107:1-16. 2013.
- Serio A, Bilican B, Barmada SJ *et al.* Astrocyte pathology and the absence of non-cell autonomy in an induced pluripotent stem cell model of TDP-43 proteinopathy. *Proc Natl Acad Sci U S A*. 2013 Mar 19;110(12):4697-702. 2013.
- Setoguchi T, Kondo T. Nuclear export of OLIG2 in neural stem cells is essential for ciliary neurotrophic factor-induced astrocyte differentiation. *J Cell Biol*. 166(7):963-8. 2004.
- Shaltouki A, Peng J, Liu Q *et al.* Efficient generation of astrocytes from human pluripotent stem cells in defined conditions. *Stem Cells*. 31(5):941-52. 2013.
- Shenoy A, Danial M, Blleloch RH. Let-7 and miR-125 cooperate to prime progenitors for astroglialogenesis. *EMBO J*. 34(9):1180-94. 2015.
- Shibata T, Yamada K, Watanabe M *et al.* Glutamate transporter GLAST is expressed in the radial glia-astrocyte lineage of developing mouse spinal cord. *J Neurosci*. 17(23):9212-9. 1997.
- Shigetomi E, Kracun S, Sofroniew MV *et al.* A genetically targeted optical sensor to monitor calcium signals in astrocyte processes. *Nat Neurosci*. 13(6):759-66. 2010.
- Smith PK, Krohn RI, Hermanson GT *et al.* Measurement of protein using bicinchoninic acid. *Anal Biochem*. 150(1):76-85. 1985.
- Sofroniew MV, Vinters HV. Astrocytes: biology and pathology. *Acta Neuropathol*. 119(1):7-35. 2010.
- Sofroniew MV. Molecular dissection of reactive astrogliosis and glial scar formation. *Trends Neurosci*. 32(12):638-47. 2009.
- Song MR, Ghosh A. FGF2-induced chromatin remodeling regulates CNTF-mediated gene expression and astrocyte differentiation. *Nat Neurosci*. 7(3):229-35. 2004.
- Song SY, Kato C, Adachi E *et al.* Expression of an acyl-CoA synthetase, lipidosin, in astrocytes of the murine brain and its up-regulation during remyelination following cuprizone-induced demyelination. *J Neurosci Res*. 85(16):3586-97. 2007
- Steele-Perkins G, Plachez C, Butz KG, Yang G *et al.* The transcription factor gene Nfib is essential for both lung maturation and brain development. *Mol Cell Biol*. 25(2):685-98. 2005.
- Stevens B, Allen NJ, Vazquez LE *et al.* The classical complement cascade mediates CNS synapse elimination. *Cell*. 131(6):1164-78. 2007.
- Stolt CC, Lommes P, Sock E *et al.* The Sox9 transcription factor determines glial fate choice in the developing spinal cord. *Genes Dev*. 17(13):1677-89. 2003.
- Sun G, Yu RT, Evans RM *et al.* Orphan nuclear receptor TLX recruits histone deacetylases to repress transcription and regulate neural stem cell proliferation. *Proc Natl Acad Sci U S A*. 104(39):15282-7. 2007.

- Sun Y, Nadal-Vicens M, Misono S *et al.* Neurogenin promotes neurogenesis and inhibits glial differentiation by independent mechanisms. *Cell*. 104(3):365-76. 2001.
- Takahashi K, Tanabe K, Ohnuki M. Induction of pluripotent stem cells from adult human fibroblasts by defined factors. *Cell*. 131(5):861-72. 2007.
- Takahashi K, Yamanaka S. Induction of pluripotent stem cells from mouse embryonic and adult fibroblast cultures by defined factors. *Cell*. 126(4):663-76. 2006.
- Takano T, Tian GF, Peng W *et al.* Astrocyte-mediated control of cerebral blood flow. *Nat Neurosci*. 9(2):260-7. 2006.
- Tanaka K, Watase K, Manabe T *et al.* Epilepsy and exacerbation of brain injury in mice lacking the glutamate transporter GLT-1. *Science*. 276(5319):1699-702. 1997.
- Theis M, Giaume C. Connexin-based intercellular communication and astrocyte heterogeneity. *Brain Res*. 1487:88-98. 2012.
- Tsuyama J, Bunt J, Richards LJ *et al.* MicroRNA-153 Regulates the Acquisition of Gliogenic Competence by Neural Stem Cells. *Stem Cell Reports*. S2213-6711(15)00187-3. 2015.
- Ullensvang K, Lehre KP, Storm-Mathisen J *et al.* Differential developmental expression of the two rat brain glutamate transporter proteins GLAST and GLT. *Eur J Neurosci*. 9(8):1646-55. 1997.
- Urayama S, Semi K, Sanosaka T *et al.* Chromatin accessibility at a STAT3 target site is altered prior to astrocyte differentiation. *Cell Struct Funct*. 38(1):55-66. 2013.
- Verkman AS. Knock-out models reveal new aquaporin functions. *Handb Exp Pharmacol*. (190):359-81. 2009.
- Vidal SE, Amlani B, Chen T. Combinatorial modulation of signaling pathways reveals cell-type-specific requirements for highly efficient and synchronous iPSC reprogramming. *Stem Cell Reports*. 3(4):574-84. 2014.
- Vierbuchen T, Ostermeier A, Pang ZP *et al.* Direct conversion of fibroblasts to functional neurons by defined factors. *Nature*. 463(7284):1035-41. 2010.
- Viti J, Feathers A, Phillips J *et al.* Epidermal growth factor receptors control competence to interpret leukemia inhibitory factor as an astrocyte inducer in developing cortex. *J Neurosci*. 23(8):3385-93. 2003.
- Vives V, Alonso G, Solal AC *et al.* Visualization of S100B-positive neurons and glia in the central nervous system of EGFP transgenic mice. *J Comp Neurol*. 457(4):404-19. 2003.
- Volterra A, Liaudet N, Savtchouk I. Astrocyte Ca²⁺ signaling: an unexpected complexity. *Nat Rev Neurosci*. 15(5):327-35. 2014.
- Vong KI, Leung CK, Behringer RR *et al.* Sox9 is critical for suppression of neurogenesis but not initiation of gliogenesis in the cerebellum. *Mol Brain*. 12;8:25. 2015.
- Walther EU, Dichgans M, Maricich SM *et al.* Genomic sequences of aldolase C (Zebirin II) direct lacZ expression exclusively in non-neuronal cells of transgenic mice. *Proc Natl Acad Sci U S A*. 95(5):2615-20. 1998.
- Walz W, Hertz L. Intense furosemide-sensitive potassium accumulation in astrocytes in the presence of pathologically high extracellular potassium levels. *J Cereb Blood Flow Metab*. 4(2):301-4. 1984.
- Walz W. Controversy surrounding the existence of discrete functional classes of astrocytes in adult gray matter. *Glia*. 31(2):95-103. 2000.

- Wang S, Bates J, Li X *et al.* Human iPSC-derived oligodendrocyte progenitor cells can myelinate and rescue a mouse model of congenital hypomyelination. *Cell Stem Cell*. 12(2):252-64. 2013.
- Weissman TA, Riquelme PA, Ivic L *et al.* Calcium waves propagate through radial glial cells and modulate proliferation in the developing neocortex. *Neuron*. 43(5):647-61. 2004.
- Wessman SJ, Levings RL. Benefits and risks due to animal serum used in cell culture production. *Dev Biol Stand*. 99:3-8. 1999.
- Widera D, Mikenberg I, Elvers M *et al.* Tumor necrosis factor alpha triggers proliferation of adult neural stem cells via IKK/NF-kappaB signaling. *BMC Neurosci*. 7:64. 2006.
- Wilczynska KM, Singh SK, Adams B *et al.* Nuclear factor I isoforms regulate gene expression during the differentiation of human neural progenitors to astrocytes. *Stem Cells*. 27(5):1173-81. 2009.
- Wilhelmsson U, Bushong EA, Price DL *et al.* Redefining the concept of reactive astrocytes as cells that remain within their unique domains upon reaction to injury. *Proc Natl Acad Sci U S A*. 103(46):17513-8. 2006.
- Williams EC, Zhong X, Mohamed A *et al.* Mutant astrocytes differentiated from Rett syndrome patients-specific iPSCs have adverse effects on wild-type neurons. *Hum Mol Genet*. 23(11):2968-80. 2014.
- Xu Q, Bernardo A, Walker D *et al.* Profile and regulation of apolipoprotein E (ApoE) expression in the CNS in mice with targeting of green fluorescent protein gene to the ApoE locus. *J Neurosci*. 26(19):4985-94. 2006.
- Xu XH, Zhong Z. Disease modeling and drug screening for neurological diseases using human induced pluripotent stem cells. *Acta Pharmacol Sin*. 34(6):755-64. 2013.
- Yanagisawa M, Nakashima K, Takizawa T *et al.* Signaling crosstalk underlying synergistic induction of astrocyte differentiation by BMPs and IL-6 family of cytokines. *FEBS Lett*. 489(2-3):139-43. 2001.
- Yang Y, Gozen O, Vidensky S *et al.* Epigenetic regulation of neuron-dependent induction of astroglial synaptic protein GLT1. *Glia*. 58(3):277-86. doi: 10.1002/glia.20922. 2010.
- Yang Y, Higashimori H, Morel L. Developmental maturation of astrocytes and pathogenesis of neurodevelopmental disorders. *J Neurodev Disord*. 5(1):22. 2013.
- Yang Y, Vidensky S, Jin L *et al.* Molecular comparison of GLT1+ and ALDH1L1+ astrocytes in vivo in astroglial reporter mice. *Glia*. 59(2):200-7. 2011.
- Ying QL, Wray J, Nichols J *et al.* The ground state of embryonic stem cell self-renewal. *Nature*. 453(7194):519-23. 2008.
- Yu F, Li J, Chen H *et al.* Kruppel-like factor 4 (KLF4) is required for maintenance of breast cancer stem cells and for cell migration and invasion. *Oncogene*. 30(18):2161-72. 2011.
- Yu J, Vodyanik MA, Smuga-Otto K *et al.* Induced pluripotent stem cell lines derived from human somatic cells. *Science*. 318(5858):1917-20. 2007.
- Zaehres H, Kögler G, Arauzo-Bravo MJ *et al.* Induction of pluripotency in human cord blood unrestricted somatic stem cells. *Exp Hematol*. 38(9):809-18, 818.e1-2. 2010.
- Zamanian JL, Xu L, Foo LC *et al.* Genomic analysis of reactive astrogliosis. *J Neurosci*. 32(18):6391-410. 2012.
- Zhang L, Zhao W, Li B *et al.* TNF-alpha induced over-expression of GFAP is associated with MAPKs. *Neuroreport*. 11(2):409-12. 2000.

- Zhang SC, Wernig M, Duncan ID *et al.* In vitro differentiation of transplantable neural precursors from human embryonic stem cells. *Nat Biotechnol.* 19(12):1129-33. 2001.
- Zhao S, Chai X, Frotscher M. Balance between neurogenesis and gliogenesis in the adult hippocampus: role for reelin. *Dev Neurosci.* 29(1-2):84-90. 2007.
- Zonta M, Angulo MC, Gobbo S *et al.* Neuron-to-astrocyte signaling is central to the dynamic control of brain microcirculation. *Nat Neurosci.* 6(1):43-50. 2003.
- Zou J, Wang YX, Dou FF *et al.* Glutamine synthetase down-regulation reduces astrocyte protection against glutamate excitotoxicity to neurons. *Neurochem Int.* 56(4):577-84. 2010.

6. Appendix

6.1 Abbreviations

Acsbg1	Acyl-CoA synthetase bubblegum family member 1
ALDH1L1	Aldehyde dehydrogenase 1 family, member L1
ANOVA	Analysis of variance
Apo E	Apolipoprotein E
APS	Ammonium Persulfate
Ara-C	Cytosine arabinoside
ATP	Adenosine triphosphate
BBB	Blood brain barrier
BDNF	Brain derived neurotrophic factor
bFGF	Fibroblast growth factor-basic
BLBP	Brain lipid-binding protein
BMP2	Bone morphogenetic protein 2
BSA	Bovine Serum Albumin
CD44	Cluster of differentiation protein 44
cDNA	Complementary deoxyribonucleic acid
Cx43	Connexin 43
ddH₂O	Double distilled water
DM	Dorsomorphin dihydrochloride
DMSO	Dimethyl sulfoxide
DPBS	Dulbecco's phosphate-buffered saline
DPBS^{-/-}	Dulbecco's phosphate-buffered saline minus Ca ²⁺ , Mg ²⁺
DSHB	Developmental studies hybridoma bank
EAAT1	Excitatory amino acid transporter 1
EAAT2	Excitatory amino acid transporter 2
EB	Embryoid body
ECL	Enhanced chemiluminescence
EDTA	Ethylenedinitrilotetraacetic acid
EEF1A1	Elongation factor 1-alpha 1
EGF	Epidermal growth factor

FACS	Fluorescence-activated cell sorting
FGFR3	Fibroblast growth factor receptor 3
GAPDH	Glyceraldehyde 3-phosphate dehydrogenase
GFAP	Glial fibrillary acidic protein
GS	Glutamine synthetase
HBSS	Hank's basal salt solution
HEPES	(4-(2-hydroxyethyl)-1-piperazineethanesulfonic acid)
iPSCs	Induced pluripotent stem cells
ITS	Insulin-Transferrin-Sodium selenite
Kd (Ca²⁺)	Dissociation constant for Ca ²⁺
LIF	Leukemia inhibitory factor
LPS	Lipopolysaccharide
lys	Lysine
mRNA	Messenger ribonucleic acid
NCAM	Neural cell adhesion molecule
NCoR	Nuclear Co-repressor
NF1A/B/C/X	Nuclear factor 1 A/B/C/X
NS21	Neuronal supplement 21
NSC	Neural stem cells
PCR	Polymerase chain reaction
PD	PD 0325901
PDC	L-trans-Pyrrolidine-2,4-dicarboxylic acid
PFA	Paraformaldehyde
pH	Power of Hydrogen
PIPES	Piperazine-N,N'-bis(2-ethanesulfonic acid)
pSTAT1/3	Phospho signal transducers and activators of transcription family of transcription factors 1/3
qPCR	quantitative PCR
ROI	Region of interest
s.e.m	Standard errors of the mean
SB	SB 431542
SDS	Sodium dodecyl sulphate
SDS-PAGE	SDS polyacrylamide gel electrophoresis

ser	Serine
Sox2	SRY (sex determining region Y)-box 2
Sox9	SRY (sex determining region Y)-box 9
TGFβ	Transforming growth factor- β
TNFα	Tumor necrosis factor alpha
tSTAT1/3	Total signal transducers and activators of transcription family of transcription factors 1/3
tyr	Tyrosine
λEm	Emission wavelength
λEx	Excitation wavelength

6.2 Units and prefixes

Units

s	second
min	minute
h	hour
d	day
wk	week

rpm	revolutions per minute
rcf	relative centrifugal force
Hz	Hertz

g	gram
m	meter
M	mol/litre (molarity)
l	litre

SI Prefixes

n	nano (10^9)
μ	micro (10^6)
m	milli (10^3)

6.3 List of plastic ware

Cell culture

Plastic ware/Glass ware	Supplier	Catalog no.
10 ml Steripipette	Corning	4488
0.2 μ filter	VWR	28145-477
0.2 μ , bottle top filter	Sarstedt	83.1822.101
10 ml Syringe	Brand	4606108V
100 mm petri dish	Sarstedt	83.1802
100 mm petri dish for panning	BD Falcon	351029
12 well plate	Sarstedt	83.3921
15 ml falcon tube	Greiner	188271
1500 μ l microfuge tubes	Sarstedt	72.706
20 ml Syringe	Brand	4606205V
2000 μ l microfuge tubes	Eppendorf	30120.094
24 well lumox dish	Sarstedt	94.6110.024
24 well plate	Sarstedt	83.1836
25 ml Steripipette	Corning	4489
35 mm lumox dish	Sarstedt	94.6077.331
35 mm petri dish	BD Falcon	353001
5 ml microfuge tubes	Eppendorf	30119.38
5 ml Steripipette	Corning	4487
50 ml falcon tube	Greiner	227261
500 μ l microfuge tubes	Eppendorf	30121.023
6 well plate	Sarstedt	83.392
60 mm petri dish	BD Falcon	353004
Cell scraper	TPP	99010
Cryovials	Thermo scientific	377267
Glass coverslip	Assistant	1001/12
Glass pasteur pipette	Brand	747715
T 25 flask	Sarstedt	83.1810.002

PCR

Plastic ware/Glass ware	Supplier	Catalog no.
Cell scaper	TPP	99002
96 well plate adaptor	Brand	781362
96-well plate for PCR	Sarstedt	72.1979.203
Adhesive film applicator	ABI	4333183
Adhesive PCR seal	Sarstedt	95.1993
Filter tips - 10 μ l	Starlabs	S1120-3810
Filter tips - 1000 μ l	Starlabs	S1120-1830
Filter tips - 200 μ l	Starlabs	S1120-8810
PCR tubes (0.2 ml)	Sigma	Z662585-1000EA

FACS

Plastic ware/Glass ware	Supplier	Catalog no.
FACS tubes	BD Falcon	352054

Western blot

Plastic ware/Glass ware	Supplier	Catalog no.
Cell scraper	TPP	99002
10 well comb 1mm	Biorad	1653359
15 well comb 1mm	Biorad	1653360
96 well plates for protein estimation	Greiner	655101
Gel loading tips	Biorad	2239915
Gel releaser	Biorad	1653320
Short glass plates	Biorad	1653308
Spacer glass plates 1 mm	Biorad	1653311
Western blot electrophoresis unit	Biorad	Mini-PROTEAN® Tetra Cell
Western Blot power pack	Biorad	PowerPac™ HC
Whatmann filter paper	Biorad	1703932

Glutamate uptake assay

Plastic ware/Glass ware	Supplier	Catalog no.
96 well plates	Greiner	655101

6.4 List of primary antibodies

S. no	Antibody	Supplier	Catalog no.	Stock	ICC	WB
1	A2B5	Miltenyi Biotec	130-093-394	0.1 mg/ml	1:100	n.a
2	Acsbg1	Abcam	ab118154	0.65 mg/ml	1:200	1:500
3	ALDH1L1	Abnova	H00010840-M01	0.2 mg/ml	1:200	n.a
4	ALDH1L1	Abcam	ab56777	0.2 mg/ml	n.a	1:500
5	CD44	Sigma	C7923	0.2 mg/ml	1:100	n.a
6	Cx43	Sigma	C6219	0.55 mg/ml	n.a	1:3000
7	EAAT1	Miltenyi Biotec	130-095-822	0.1 mg/ml	1:50	n.a
8	GAPDH	Sigma	G8795	1.2 mg/ml	n.a	1:10000
9	GFAP	Dako	Z0334	2.0 mg/ml	1:2000	1:5000
10	Glutamine Synthetase	Thermo Scientific	PA1-46165	n.d	1:200	n.a
11	HOXB4	DSHB	l12	n.d	1:100	n.a
12	Ki67	Novacastra	NCL-L-Ki67-MM1	0.072 mg/ml	1:500	n.a
13	LHX2	Millipore	AB10557	n.d	1:200	n.a
14	NCoR	Cell Signaling	5948	n.d	1:500	1:1000
15	Nestin	Millipore	AB5922	n.d	1:500	n.a
16	NF1A	Active Motif	39397	1.14 mg/ml	1:200	n.a
17	NKX2.1	Abcam	AB76013	n.d	1:200	n.a
18	Olig2	Millipore	AB9610	n.d	1:500	1:1000
19	OTX2	Millipore	AB9566	n.d	1:1000	n.a
20	pAkt1 (Thr 308)	Cell Signaling	13038	n.d	n.a	1:1000
21	pErk1,2 (Thr 202, Tyr 204)	Cell Signaling	4370	n.d	n.a	1:2000
22	pSMAD1/5 (Ser463/465)	Cell Signaling	9516	n.d	n.a	1:1000

23	pSTAT1 (Tyr701)	Cell Signaling	9171	n.d	n.a	1:1000
24	pSTAT3 (Tyr705)	Cell Signaling	9131	n.d	n.a	1:1000
25	S100 β	Sigma	S2532	9.9 mg/ml	1:2000	n.a
26	Sox2	Cell Signaling	3579	n.d	1:250	n.a
27	tSMAD	Cell Signaling	6944	n.d	n.a	1:1000
28	tSTAT1	Cell Signaling	9172	n.d	n.a	1:1000
29	tSTAT3	Cell Signaling	9139	n.d	n.a	1:1000

n.a = Not applicable

n.d = Not defined

ICC = Immunocytochemistry

WB = Western Blot

6.5 List of secondary antibodies

S.no	Antibody	Supplier	Catalog no.	Stock	Dilution
1	Goat anti mouse Alexa Fluor 488	Invitrogen	A11029	2.0 mg/ml	1:1000
2	Goat anti mouse Alexa Fluor 555	Invitrogen	A21424	2.0 mg/ml	1:1000
3	Goat anti rabbit Alexa Fluor 488	Invitrogen	A11034	2.0 mg/ml	1:1000
4	Goat anti rabbit Alexa Fluor 555	Invitrogen	A21429	2.0 mg/ml	1:1000
5	HRP conjugated anti mouse IgG	Santacruz	sc-2005	0.4 mg/ml	1:5000
6	HRP conjugated anti rabbit IgG	Cell Signaling	7074	n.d	1:5000

n.d = Not defined

Filter sets used for secondary antibodies

Dye	Zeiss filter set	λ_{Ex}	λ_{Em}
Alexa Fluor 488	38 (EGFP)	470 nm	525 nm
Alexa Fluor 555	43 (Cy3)	545 nm	605 nm
Calcein AM	17 (FITC)	485 nm	540 nm
Fluo-4 AM	17 (FITC)	485 nm	540 nm
Hoechst 33342	49 (DAPI)	365 nm	445 nm

6.6 List of primers for quantitative PCR

S.no	Gene	Primer Sequence	Amplicon Size (bp)
1	ALDOC	Forward: GCCAAATTGGGGTGGAAAACA Reverse: TGTTGAAACGCACAATGGTC	235
2	APO-E	Forward: GCGTTGCTGGTCACATTCC Reverse: TCAGTTGTTCTCCAGTTCCG	283
3	β -ACTIN	Forward: CTGAACCCCAAGGCCAAC Reverse: TAGCACAGCCTGGATAGCAA	93
4	CD44	Forward: TTTGCATTGCAGTCAACAGTC Reverse: GTTACACCCCAATCTTCATGTCCAC	234
5	CX43	Forward: TGCTGCGAACCTACATCATCAG Reverse: AGAGAGGAAACAGTCCACCTG	152
6	EAAT2	Forward: ATCTTGGCTCAGAGGAACCCA Reverse: CAGGATGACACCAAACACCG	104
7	EEF1A1	Forward: AGGTGATTATCCTGAACCATCC Reverse: AAAGGTGGATAGTCTGAGAAGC	235
8	EGFR	Forward: GTCCGCAAGTGTAAGAAGTGC Reverse: GAGTCACCCCTAAATGCCAC	173
9	GAPDH	Forward: TGCACCACCAACTGCTTAGC Reverse: GGCATGGACTGTGGTCATGAG	87
10	GFAP	Forward: CTGCGGCTCGATCAACTCA Reverse: TCCAGCGACTCAATCTTCCTC	209
11	MKI67 (Ki67)	Forward: ACGCCTGGTTACTATCAAAAGG Reverse: CAGACCCATTTACTTGTGTTGGA	209
12	LCN2	Forward: GAAGTGTGACTACTGGATCAGGA Reverse: ACCACTCGGACGAGGTAAC	111
13	NES (Nestin)	Forward: CTGCTACCCTTGAGACACCTG Reverse: GGGCTCTGATCTCTGCATCTAC	141
14	NF1A	Forward: TAATGTCAGCGTCACTTGGC Reverse: TAATCCAGGGCTCTGTGTCC	137
15	NF1B	Forward: AAAAAGCATGAGAAGCGAATGTC Reverse: ACTCCTGGCGAATATCTTTGC	136
16	NF1C	Forward: ACCTGGCATAACGACCTGAAC Reverse: TCCATCGAGCCCGATTGTG	100
17	NF1X	Forward: GTTTGATGTCCGCATCTCCT Reverse: GCCACATCACATTGGAGTCA	119
18	RPL13A	Forward: CATAGGAAGCTGGGAGCAAG Reverse: GCCCTCCAATCAGTCTTCTG	157

19	SERPINA3	Forward:TCGAGGGGACTATAACCTGAACG Reverse: TGTTGAAACGCACAATGGTC	235
20	SOX2	Forward: ATGGACAGTTACGCGCACA Reverse: TGCGAGTAGGACATGCTGTA	218
21	STAT3	Forward: CAGCAGCTTGACACACGGTA Reverse: AAACACCAAAGTGGCATGTGA	150

6.7 Reaction mixture and conditions for cDNA synthesis*

Master mix

Reagent	Amount (per reaction)
10X RT Buffer	2.0 μ l
10X Random Primers	2.0 μ l
25 X dNTP mix (100 mM)	0.8 μ l
Multiscribe Reverse Transcriptase (50 U/ μ l)	1.0 μ l
RNase Inhibitor	1.0 μ l
DEPC treated water	3.2 μ l
RNA	500 ng (in 10 μ l)
Total volume per reaction	20 μl

PCR conditions

Temperature ($^{\circ}$ C)	Time (min)
25	10
37	120
85	5
4	∞

* Make up volume of cDNA to 200 μ l using DEPC treated water.

6.8 Reaction mixture and conditions for quantitative PCR

Master mix

Reagent	Amount (per reaction)
2X SYBR Green master mix	12.5 µl
Forward Primer (5 µM)	1.0 µl
Reverse Primer (5 µM)	1.0 µl
cDNA (20 ng per reaction)	8.0 µl
DEPC treated water	2.5 µl
Total volume per reaction	25 µl

PCR conditions

Temperature (°C)	Time (min)
50	2
95	10
95	0.25
60	1
Cycles	40

PCR conditions for melting curve

Temperature (°C)	Time (sec)
95	15
60	60
95	15

6.9 Calculations for quantitative PCR

6.9.1 Determination of amplification efficiency

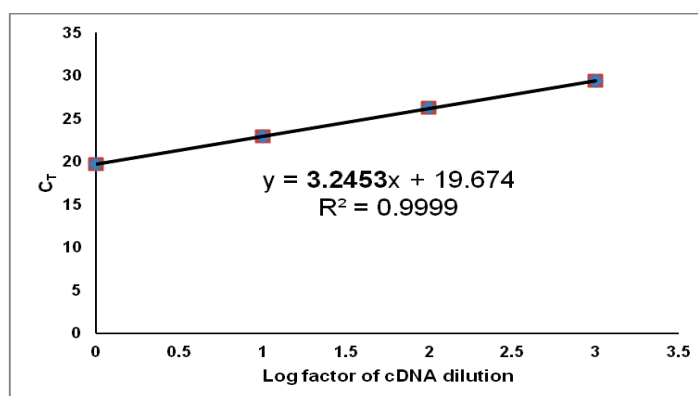
Every primer was first subjected to determination of amplification efficiency before it was used for qPCR. To follow the $2^{-(\Delta\Delta C_T)}$ method for relative quantification of PCR data, it is very important that the PCR amplicon doubles in quantity during the geometric phase of PCR amplification which in turn means a 100% efficiency for both the gene of interest and endogenous control. 100% efficient reaction results in a 10 fold increase in PCR amplicon every 3.32 cycles during the exponential phase ($\log_2 10 = 3.3219$).

In order to determine the primer efficiency, a 10 fold serial dilution of cDNA was prepared as shown below and qPCR was carried out.

cDNA conc. (ng)	Dilution	Log factor of dilution
10	1	0
1.0	10	1
0.1	100	2
0.01	1000	3

For calculations, a standard curve was made and its slope was used to estimate the PCR amplification efficiency. Standard curve was plotted as a semi log regression line plot of C_T value vs. log of input cDNA. Slope was determined from the value of 'm', using the equation of straight line:

$y = mx + c$ as shown in the graph below.



Efficiency was calculated with the following equation

$$E = (10^{-1/\text{slope}} - 1) * 100, \text{ where } E = \text{efficiency}$$

All the primers used for this study exhibited a slope ranging from 3.2-3.4 and were therefore considered to be 100 % efficient.

6.9.2 Relative quantification of qPCR data

The relative quantification of qPCR data represents the fold change in the treated group to untreated control after normalization to their respective endogenous controls (*Livak et al., 2001*). After taking the mean of the technical triplicates, the C_T values were used in the following equations.

$$\Delta C_T = (C_{T \cdot \text{GOI}} - C_{T \cdot \text{endogenous}}),$$

where, C_T = Threshold cycle, GOI = gene of interest

$$\Delta \Delta C_T = (\Delta C_{T \cdot \text{treated}} - \Delta C_{T \cdot \text{control}})$$

To further represent the data in terms of fold change, the log values were linearized by calculating $2^{(-(\Delta \Delta C_T))}$.

In case there was no untreated control condition to be compared to, data were represented as

$$2^{(-(\Delta C_T))}.$$

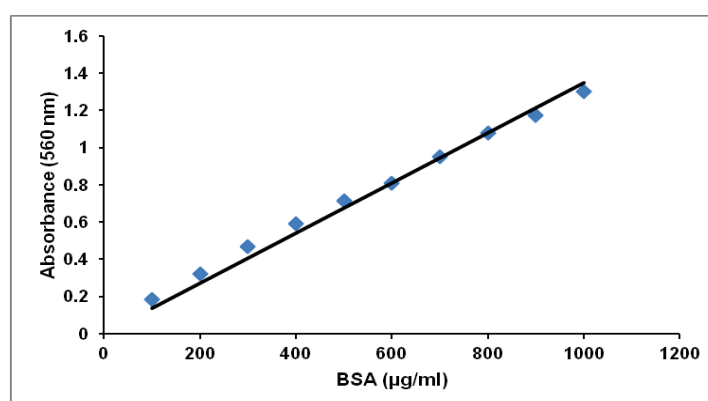
Intrasample variation was calculated using 2^{-C_T} .

6.10 Calculations for protein estimation

A serial dilution of BSA (as mentioned in the table below) was used to create a standard curve for protein estimation.

BSA concentration ($\mu\text{g/ml}$)	H ₂ O	BSA (1 mg/ml)
0.0	25.0 μl	0.0 μl
100	22.5 μl	2.5 μl
200	20.0 μl	5.0 μl
300	17.5 μl	7.5 μl
400	15.0 μl	10.0 μl
500	12.5 μl	12.5 μl
600	10.0 μl	15.0 μl
700	7.5 μl	17.5 μl
800	5.0 μl	20.0 μl
900	2.5 μl	22.5 μl
1000	0.0 μl	25.0 μl

The relation between absorbance and concentration was considered to be best described by a straight line, thereby following linear regression as shown in the example below. The thick black, straight line is the linear regression that best describes the entire set of standard points ($R^2 = 0.9862$).



The values of unknown protein samples were thus calculated using the equation for straight line:

$$y = mx + c$$

where, y = absorbance value; m = slope; c = 'y' intercept and x determines concentration of the sample.

$$\text{therefore, } x = y/m + c$$

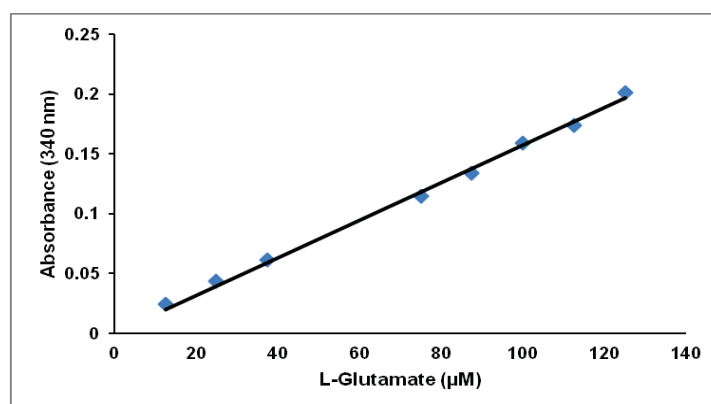
The x value thus obtained was multiplied with the dilution factor. This resulted in a concentration in terms of $\mu\text{g/ml}$. This value was then divided by a factor of 1000 to obtain the value in $\mu\text{g}/\mu\text{l}$. Subsequently, the amount of protein sample required for loading the gel was calculated.

6.11 Calculations for glutamate uptake assay

A serial dilution of L-Glutamate (as mentioned in the table below) was used to create a standard curve for the estimation of glutamate concentration.

L-Glutamate (μM)	H ₂ O	L-Glutamate (1 mM)
0.0	89.0 μl	0.0 μl
12.5	86.5 μl	2.5 μl
25.0	84.0 μl	5.0 μl
37.5	81.5 μl	7.5 μl
50.0	79.0 μl	10.0 μl
62.5	76.5 μl	12.5 μl
75.0	74.0 μl	15.0 μl
87.5	71.5 μl	17.5 μl
100.0	69.0 μl	20.0 μl
112.5	66.5 μl	22.5 μl
125.0	64.0 μl	25.0 μl

As for the protein estimation, the relation between absorbance and concentration was considered to be best described by a straight line, thereby following linear regression as shown in the example below. The thick black, straight line is the linear regression that best describes the entire set of standard points after background subtraction ($R^2 = 0.9966$).



After background subtraction, the values of unknown samples were thus calculated using the equation for straight line:

$$y = mx + c$$

where, y = absorbance value; m = slope; c = 'y' intercept and x determines concentration of the sample.

$$\text{therefore, } x = y/m + c$$

The 'x' value thus obtained was actually a measure of glutamate left in the extracellular solution. The 'x' value of each sample was therefore subtracted from a factor of 50, in order to determine

the amount of L-glutamate taken up by the cells. As cell density is a direct determinant of the amount of glutamate taken up by the system, therefore, the total L-Glutamate up taken was divided by total protein content of the culture in order to get an quantify $\mu\text{M}/\mu\text{g}$ of L-Glutamate uptake. Further, % inhibition in the presence of inhibitors was calculated with respect to glutamate alone condition.

6.12 List of figures

Figure 1	Generation of neural cell types during development.....	3
Figure 2	Transition from neurogenic to gliogenic state.....	6
Figure 3	Regulatory pathways for differentiation towards astrocytes.....	9
Figure 4	Astrocytic markers, their function and heterogeneity.....	10
Figure 5	Development and application of iPSCs.....	24
Figure 6	Generation of different neural lineage cells from iPSCs.....	25
Figure 7	Schematic representation of neural differentiation.....	39
Figure 8	Standardization of optimal concentration of PD.....	41
Figure 9	Standardization of optimal housekeeping gene for quantitative PCR.....	44
Figure 10	Dye loading and de-esterification.....	46
Figure 11	Diversity of Ca ²⁺ signaling in astrocytes.....	47
Figure 12	Experimental set up for glutamate uptake assay.....	48
Figure 13	Differential expression of neural stem cell and glial progenitor markers in human iPSCs derived neural stem cells.....	51
Figure 14	Determination of neurogenic and gliogenic lines based on differential expression of glial progenitor markers.....	52
Figure 15	Temporal increase in glial restricted progenitor markers in neural stem cells over passaging in culture.....	53
Figure 16	EGF dependent increase in astrocyte restricted precursor markers in early neural stem cells.....	55
Figure 17	Inefficient differentiation of NSCs into high GFAP expressing cells.....	57
Figure 18	Augmentation of GFAP positive cells with increasing passage of NSCs.....	59
Figure 19	High level of CD44 expression in low passage NSCs.....	60
Figure 20	FGF dependent induction of gliogenic switch augments differentiation of early neural stem cells into high GFAP expressing astrocytes upon exposure to CNTF..	61
Figure 21	Morphological differences upon PD treatment in neural stem cells.....	63
Figure 22	Decreased proliferation of neural stem cells after short term PD treatment.....	64
Figure 23	Reduction in NSCs and glial restricted progenitor markers in the presence of PD at mRNA level.....	65
Figure 24	Low level of GFAP expression in PD treated cells.....	66
Figure 25	Expression of pan astrocytic and functional astrocyte markers in PD differentiated astrocytes by immunostaining.....	67
Figure 26	Expression of pan astrocytic and functional astrocyte markers in PD differentiated astrocytes.....	68
Figure 27	Maintenance of low GFAP levels in astrocytes differentiated in NBNS21S.....	69
Figure 28	PD differentiated astrocytes exhibit cortical lineage.....	70

Figure 29	Absence of early phosphorylation of STAT1/3 and SMAD1 in the presence of PD..	72
Figure 30	Late phosphorylation of STAT1/3 in the presence of PD.....	74
Figure 31	Increased phosphorylation of Akt1 upon exposure to PD.....	75
Figure 32	PI3K-pAKT1 dependent phosphorylation of STAT1/3 upon PD treatment.....	76
Figure 33	Nuclear export of Olig2 upon PD treatment.....	78
Figure 34	Maintenance of NCoR in the nucleus upon PD treatment.....	79
Figure 35	Calcium oscillations in PD differentiated low GFAP astrocytes upon exposure to stimulatory agents.....	81
Figure 36	L-Glutamate uptake by PD differentiated low GFAP astrocytes.....	82
Figure 37	PD differentiated low GFAP astrocytes respond to inflammatory stimuli by augmenting markers for reactivity.....	84
Figure 38	PD differentiated cells exhibit increased GFAP expression under acidic conditions..	85

6.13 Curriculum vitae

Name: Pretty Garg

Date of birth: 26th May 1985

Place of birth: Panipat, Haryana, India

Marital status: Single

2012-2015 Ph.D, Heinrich-Heine-Universität Düsseldorf, Germany

2008-2012 Senior research fellow, National Brain Research Centre, Manesar, India

2006-2008 Masters of Biotechnology, Jamia Millia Islamia, Delhi, India

2003-2006 Bachelors of Microbiology, University of Delhi, Delhi, India

2001-2002 Senior Secondary School, D.A.V Public School, Panipat, Haryana, India

1999-2000 Secondary School, D.A.V Public School, Panipat, Haryana, India

6.14 Publications and conferences

6.14.1 Publications

Manuscript in preparation: Garg P, Gottmann K, Nieweg K. Efficient differentiation of low GFAP human astrocytes for disease modeling.

Book Chapter: Pant M*, **Garg P*** and Seth P (2012). Central nervous system infection by HIV-1: Special emphasis to NeuroAIDS in India. (*Both are equal authors). PNAS (India) 82 (1):81-94

6.14.2 Meetings and poster presentations

- XII European meeting on glial cell function in health and disease (07/2015)
Poster: Efficient Differentiation of Human Astrocytes for Disease Modeling
- 11th Göttingen Meeting of German Neuroscience Society, Göttingen, Germany (03/2015)
Poster: Chemically Defined Differentiation of Human Astrocytes for Disease Modeling
- SfN Neuroscience Meeting, San Diego (11/2013)
- Cell symposium - Using stem cells to model and treat human diseases, Los Angeles (11/2013)
- 7th International Stem cell meeting, Stem cell network, Köln, Germany (04/2013)

7. Acknowledgements

Even though words will not suffice, I take this opportunity to express my deepest gratitude to Prof. Dr. Kurt Gottmann, Institut für Neuro- und Sinnesphysiologie, Heinrich Heine University, Düsseldorf; for being my Ph.D project supervisor and providing me an opportunity to work in his laboratory. I would like to thank him for critically reviewing my research at every step and encouraging me to think and work independently.

Also, I owe my sincere thanks to Prof. Dr. Christine R. Rose, Institut für Neurobiology, Heinrich Heine University, Düsseldorf; for the co-supervision of my Ph.D project and her critical suggestions.

A special word of thanks is extended towards Jr. Prof. Dr. Katja Nieweg, Institut für Pharmakologie und Klinische Pharmazie, Philipps-Universität, Marburg; for her close mentorship, long but highly fruitful telephonic discussions throughout my Ph.D and for providing me with freedom to work in my way. Without her guidance and persistent support, this Ph.D thesis would not have been feasible.

Furthermore, I am grateful to Prof. Dr. N. Klöcker, Institut für Neuro- und Sinnesphysiologie and Prof. Dr. J. Scheller, Institut für Biochemie und Molekularbiologie II, Heinrich Heine University, Düsseldorf; for permitting me to use several instruments required for my Ph.D project. I am extremely thankful to Dr. Madhurendra Singh, Dr. Doreen M. Floß, Manuel Franke and Alexander Lang (Institut für Biochemie und Molekularbiologie II, Heinrich Heine University, Düsseldorf) for helping me with realtime PCR, FACS and confocal imaging set ups and being so generous to lend me several reagents.

Also, I am thankful to my laboratory and department colleagues for maintaining an open and healthy work atmosphere. Special appreciation is extended to Sabine Ueberschär-Sahlmann and Martina Bohndorf for providing the technical support.

I am highly obliged to iBrain, BMBF and DFG for supporting me financially throughout my Ph.D.

In the end, I would like to thank all my friends who always stood beside me and extended their thoughtful support which helped me to keep my motivation levels high during the difficult times.

Lastly, I am eternally grateful to all my family members for their immense love and support throughout my life.

8. Eidesstattliche Erklärung

Ich versichere hiermit an Eides Statt, dass die vorliegende Dissertation von mir selbstständig und ohne unzulässige fremde Hilfe unter Beachtung der „Grundsätze zur Sicherung guter wissenschaftlicher Praxis an der Heinrich-Heine-Universität Düsseldorf“ erstellt worden ist. Diese Dissertation wurde keiner anderen Fakultät vorgelegt und es gab bisher keine erfolglosen Promotionversuche.

Düsseldorf, den 14. Dezember 2015,

Pretty Garg